Reactivity of HO_2/O^-_2 Radicals in Aqueous Solution

Cite as: Journal of Physical and Chemical Reference Data **14**, 1041 (1985); https://doi.org/10.1063/1.555739
Published Online: 15 October 2009

Benon H. J. Bielski, Diane E. Cabelli, Ravindra L. Arudi, and Alberta B. Ross

Reactivity of HO_2/O_2^- Radicals in Aqueous Solution

Benon H. J. Bielski, Diane E. Cabelli, Ravindra L. Arudi,
Chemistry Department, Brookhaven National Laboratory, Upton, NY 11973

and

Alberta B. Ross
Radiation Chemistry Data Center, Radiation Laboratory, University of Notre Dame, Notre Dame, IN 46556

Kinetic data for the superoxide radical ($HO_2 \rightleftharpoons O_2^- + H^+$, $pK = 4.8$) in aqueous solution have been critically assessed. Rate constants for reactions of O_2^- and HO_2 with more than 300 organic and inorganic ions, molecules and other transient species have been tabulated.

Key words: aqueous solution; chemical kinetics; data compilation; perhydroxyl radical; rate constants; review; superoxide radical.

Contents

1. Introduction 1041
2. Generation of HO_2/O_2^- in Aqueous Solution 1042
   2.1. Radiolytic and Photolytic Generation of HO_2/O_2^- 1042
   2.2. Enzymatic Generation of O_2^- 1042
3. Spectral Characteristics of HO_2/O_2^- 1043
4. Detection of HO_2/O_2^- Radicals 1044
5. Kinetics of Disproportionation of HO_2/O_2^- . 1044
6. Reactions of HO_2/O_2^- 1044
   6.1 Kinetics 1044
   6.2 Criteria for Data Included in Table 3 . 1048
   6.3 Explanation of Table 3 1048
7. Abbreviations and Symbols 1049
8. References to Text 1050
9. References to Table 3 1086
10. Molecular Formula Index 1092
11. Compound Name Index 1096

List of Tables

1a. Effective extinction coefficient of the total radical concentration $[R\cdot] = [HO_2] + [O_2^-]$ for selected wavelength and pH values calculated by equation (III) at 23 °C 1043
1b. Effective extinction coefficient of the total radical concentration $[R\cdot] = [HO_2] + [O_2^-]$ corrected for the absorption of hydrogen peroxide formed during decay at 23 °C: $\epsilon_{decay} = (\epsilon_{R\cdot} - 0.5\,\epsilon_{H_2O_2})$ 1044
2. Properties of HO_2/O_2^- in aqueous solution .. 1046
3. Rate constants for reactions of HO_2/O_2^- in aqueous solution 1052

List of Figures

1. Absorption spectra of HO_2 and O_2^- 1043
2. Observed second-order rates as a function of pH for the spontaneous disproportionation of HO_2/O_2^- 1045

1. Introduction

The past decade has seen a renewed interest in the possible role the superoxide/perhydroxyl (O_2^-/HO_2) radicals play in biological systems, in radiation and UV-photolysis induced oxidations in the presence of oxygen, in the autoxidation of industrially important chemicals, in the oxidation of numerous compounds in the atmosphere, etc. This, in turn, has resulted in a substantial increase in the number of studies describing the reactions between HO_2/O_2^- radicals and specific compounds in an effort to unravel the kinetics and mechanisms of some of these systems [1–7].[a)]

In this introduction a brief discussion of the generation of HO_2/O_2^- radicals in aqueous solutions, the spectral characteristics and detection of these radicals and their kinetic properties will be presented. Finally, the acid-base dependent kinetic equations necessary for the description of HO_2/O_2^- reactions will be developed in detail as these kinetics are not well known. Although the kinetic

[a)] Figures in brackets indicate literature references at the end of the text.

descriptions are applicable to many systems, they do not consider a number of important complications, i.e. those systems in which reactions of product transients with oxygen or hydrogen peroxide occur, possible chain reactions, etc.

It should be noted that this entire review is applicable to aqueous solutions or systems that retain aqueous characteristics only.

2. Generation of HO_2/O_2^- in Aqueous Solutions

While there are numerous reactions in which HO_2/O_2^- can be generated in aqueous solutions, only the three most commonly used methods involving radiolysis, photolysis and the xanthine oxidase system will be discussed here. Because of the similarity of the mechanisms, the generation of HO_2/O_2^- by radiolysis and photolysis will be discussed together.

2.1. Radiolytic and Photolytic Generation of HO_2/O_2^-

The initial energy deposition processes and hence the primary radical distribution are different for high energy ionizing radiation, Eq. (I), and VUV-photolysis, Eq. (II):

$$H_2O\text{—}\wwwarrow H,\ e_{aq}^-,\ OH,\ H_2,\ H_2O_2,\ H_3O^+ \qquad (I)$$

$$H_2O \xrightarrow{h\nu} H,\ OH \qquad (II)$$

However extensive studies have shown that the subsequent reactions by which the primary radicals H, e_{aq}^- and OH are converted to HO_2/O_2^- in the presence of formate are similar:

$$e_{aq}^- + O_2 \rightarrow O_2^- \qquad (1)$$
$$k_1 = 2.0 \times 10^{10}\ \text{L mol}^{-1}\text{s}^{-1}\ [8a]$$

$$e_{aq}^- + H^+ \rightarrow H \qquad (2)$$
$$k_2 = 2.2 \times 10^{10}\ \text{L mol}^{-1}\text{s}^{-1}\ [8a,b]$$

$$H + O_2 \rightarrow HO_2 \qquad (3)$$
$$k_3 = 2 \times 10^{10}\ \text{L mol}^{-1}\text{s}^{-1}\ [9]$$

$$HCO_2^- + OH \rightarrow CO_2^- + H_2O \qquad (4)$$
$$k_4 = 3.5 \times 10^{9}\ \text{L mol}^{-1}\text{s}^{-1}\ [10]$$

$$HCO_2^- + H \rightarrow CO_2^- + H_2 \qquad (5)$$
$$k_5 = 1.3 \times 10^{8}\ \text{L mol}^{-1}\text{s}^{-1}\ [11]$$

$$CO_2^- + O_2 \rightarrow CO_2 + O_2^- \qquad (6)$$
$$k_6 = 2.4 \times 10^{9}\ \text{L mol}^{-1}\text{s}^{-1}\ [12]$$

where the O_2^- radical is always in equilibrium with its conjugate acid, the perhydroxyl radical

$$HO_2 \rightleftharpoons H^+ + O_2^- \qquad (7,-7)$$

$$K_{HO_2} = 1.6 \times 10^{-5}\ \text{mol L}^{-1}\ \text{(see Sec. 5)}$$

The formate system is particularily useful since the quantitative conversion of the primary radicals to HO_2/O_2^-, which occurs at near diffusion controlled rates, is independent of pH. Detailed methods for the preparation of aqueous HO_2/O_2^- solutions have been published [13,14].

Some alcohols (ethanol, methanol, 2-propanol) can be substituted for formate.

$$CH_3CH_2OH + OH \rightarrow CH_3\dot{C}HOH + H_2O \qquad (8)$$

$$CH_3CH_2OH + OH \rightarrow CH_3CH_2O\cdot + H_2O \qquad (9)$$

$$CH_3CH_2O\cdot + CH_3CH_2OH \rightarrow CH_3CH_2OH + CH_3\dot{C}HOH \qquad (10)$$

$$CH_3CH_2OH + H \rightarrow CH_3\dot{C}HOH + H_2 \qquad (11)$$

$$CH_3\dot{C}HOH + O_2 \rightarrow CH_3CH(\dot{O}_2)OH \qquad (12)$$

$$CH_3CH(\dot{O}_2)OH + OH^- \rightarrow CH_3CHO + H_2O + O_2^- \qquad (13)$$

The quantity of alcohol must be sufficiently small such that the solution retains its aqueous characteristics. It should be noted that aqueous alcoholic systems are efficient only in the alkaline range since reaction (13) is base catalyzed. The preparation of such solutions has been described elsewhere [14–16].

One of the oldest methods for generating HO_2/O_2^- involves the radiolysis/photolysis of aqueous hydrogen peroxide solutions [17]. Here, after the initial primary radical formation, Eqs. (I) and (II), both e_{aq}^- and H are converted to OH radicals by reaction with peroxide,

$$e_{aq}^- + H_2O_2 \rightarrow OH + OH^- \qquad (14)$$

$$H + H_2O_2 \rightarrow OH + H_2O \qquad (15)$$

while the photolysis of peroxide yields OH radicals directly,

$$H_2O_2 \rightarrow 2\ OH. \qquad (16)$$

The OH radicals then react with hydrogen peroxide to yield HO_2,

$$OH + H_2O_2 \rightarrow HO_2 + H_2O. \qquad (17)$$

As has been shown earlier, in this system HO_2/O_2^- can be generated anaerobically as well as aerobically [18].

2.2. Enzymatic Generation of O_2^-

Researchers in the biomedical fields preferentially use enzymatic methods for the generation of superoxide radicals as they are closest to *in vivo* situations. The most-frequently used enzyme for this purpose is xanthine oxidase [19,20]. The overall process is given by reactions (18) and (19):

$$\text{Enzyme-H}_2 + 2\ O_2 \rightarrow \text{Enzyme} + 2\ H^+ + 2\ O_2^- \quad (18)$$

$$\text{Enzyme-H}_2 + O_2 \rightarrow \text{Enzyme} + H_2O_2 \quad (19)$$

Preferred substrates for this enzyme are either xanthine or acetaldehyde which are oxidized to uric acid and acetic acid respectively while the enzyme is reduced by accepting two electrons. In the presence of molecular oxygen the reduced enzyme can lose these electrons by two different pathways, a univalent reaction step leading to O_2^- formation (reaction 18) and a divalent reaction step (reaction 19) leading to direct formation of hydrogen peroxide. The predominance of one reaction over the other is controlled by the pH of the medium, the oxygen concentration and the turnover rate of the enzyme. Although this method has been used successfully in competition kinetics, it is limited to the pH range in which xanthine oxidase is active.

There appears to be a general consensus that the successful use of any of the superoxide generating methods depends strongly upon the absence of catalytic impurities in the system. The presence of certain metallic impurities is known not only to accelerate the spontaneous disproportionation of the HO_2/O_2^- radicals (see Sec. 5) thus causing a rapid build-up of hydrogen peroxide, but also to initiate Fenton-type reactions ($Fe^{2+} + H_2O_2 \rightarrow Fe^{3+} + OH + OH^-$ [21]) that could obscure the reaction(s) under study.

3. Spectral Characteristics of HO_2/O_2^-

Both HO_2 and O_2^- have distinct absorption spectra in the low UV region with maxima at 225 and 245 nm respectively, Fig. 1. The molar extinction coefficients used in this review were determined by the stopped-flow radiolysis technique [21a] and are based on the molar extinction coefficients of nitroform ($\epsilon^{350nm} = 14{,}800 \pm 200$ L mol^{-1}cm^{-1}, [22-24]) and cytochrome C ($\Delta\epsilon^{550nm}$ [Fe(II) cyt C - Fe(III)cyt C] = 21,100 L mol^{-1}cm^{-1} [25]) without assuming G values [26]. At pH 1.5 $\epsilon_{HO_2}^{225nm} = 1400 \pm 80$ L mol^{-1}cm^{-1}; at pH 10.5 $\epsilon_{O_2^-}^{245nm} = 2350 \pm 120$ L mol^{-1}cm^{-1}. As HO_2 and O_2^- are in equilibrium (7,−7) the effective molar extinction coefficient varies with pH; see Table 1a.

$$\epsilon_{\text{effective}} = \left[\frac{[HO_2]}{[HO_2] + [O_2^-]}\right]\epsilon_{HO_2} + \left[\frac{[O_2^-]}{[O_2^-] + [HO_2]}\right]\epsilon_{O_2} \quad \text{(III)}$$

It should be noted that these effective extinction coefficients refer to the total radical concentration prior to spontaneous disproportionation and thus prior to peroxide formation. Any extinction coefficients must be corrected for the absorption of H_2O_2 (from reactions 23 and 24) if they are to be used for computation of decay rates. Since, as indicated in reactions (23) and (24), a mole of HO_2 or O_2^- produces a half mole of H_2O_2, the effective extinction coefficient has to be corrected for the absorbance of the latter:

$$\epsilon_{\text{effective (corrected)}} = (\epsilon_{HO_2/O_2^-} - 0.5\ \epsilon_{H_2O_2}) \quad \text{(IV)}$$

These corrected extinction coefficients are found in Table 1b; it should be noted that the correction is most significant at low wavelengths and high pH.

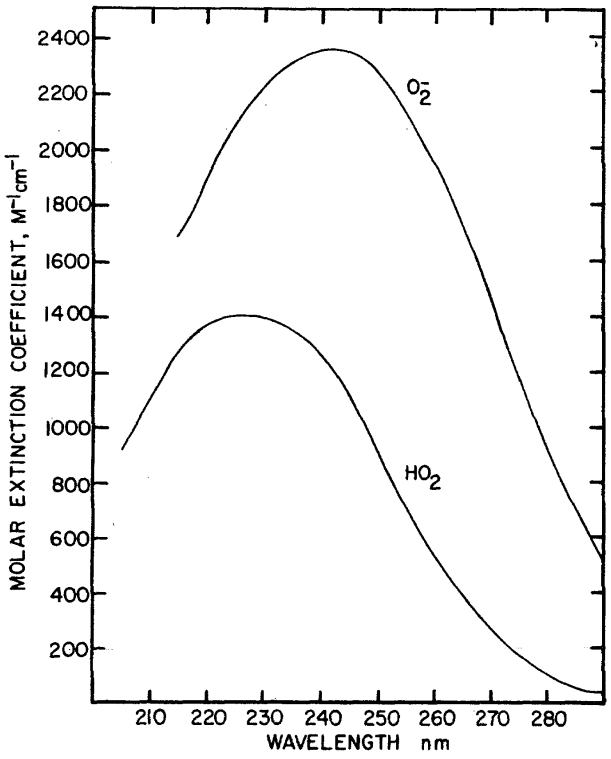

FIG. 1. Absorption spectra of HO_2 in air-saturated $HClO_4$ solution at pH 1.5 and O_2^- in air-saturated 0.01 mol L^{-1} sodium formate solution containing 1×10^{-4} mol L^{-1} EDTA at pH 10.5 [26].

TABLE 1a. Effective extinction coefficient ($\epsilon_{\text{effective}}^{\lambda}$, L mol^{-1} cm^{-1}) of the total radical concentration [R·] = [HO_2] + [O_2^-] for selected wavelength and pH values calculated by equation (III) at 23 °C

pH	ϵ^{230nm}	ϵ^{240nm}	ϵ^{250nm}	ϵ^{260nm}
0.5–1.5	1400	1260	915	540
2.0	1401	1261	917	542
2.5	1404	1265	922	547
3.0	1413	1277	936	562
3.5	1440	1312	979	699
4.0	1514	1410	1101	733
4.5	1679	1624	1366	1010
5.0	1911	1928	1745	1402
5.5	2093	2166	2038	1709
6.0	2181	2281	2181	1858
6.5	2214	2324	2234	1913
7.0	2225	2338	2252	1931
7.5	2228	2343	2257	1937
8.0–13.0	2230	2345	2260	1940

TABLE 1b. Effective extinction coefficient ($\epsilon^{\lambda}_{\text{effective(corrected)}}$, L mol^{-1} cm^{-1}) of the total radical concentration [R·] = [HO_2] + [O_2^-] corrected for the absorption of H_2O_2 formed during decay, $\epsilon_{\text{for decay}} = (\epsilon_{R\cdot} - 0.5\,\epsilon_{H_2O_2})$ at 23 °C[a]

pH	ϵ^{230nm}	ϵ^{240nm}	ϵ^{250nm}	ϵ^{260nm}
0.5–1.5	1368	1241	904	534
2.0	1369	1242	906	536
2.5	1372	1246	911	541
3.0	1381	1248	925	556
3.5	1408	1293	968	693
4.0	1482	1391	1090	727
4.5	1647	1423	1355	1004
5.0	1879	1909	1734	1396
5.5	2061	2147	1949	1703
6.0	2149	2262	2170	1852
6.5	2182	2305	2223	1907
7.0	2193	2319	2241	1925
7.5	2196	2324	2246	1931
8.0–9.0	2198	2326	2248	1933
9.5	2195	2324	2248	1932
10.0	2188	2319	2244	1929
10.5	2175	2307	2235	1923
11.0	2150	2287	2219	1913
11.5	2100	2245	2188	1893
12.0	2053	2205	2156	1869
12.5	2025	2183	2139	1856
13.0	2015	2173	2134	1850

[a] See [30] for the absorption spectrum of H_2O_2.

4. Detection of HO_2/O_2^- Radicals

A wide variety of methods has been used in the detection of HO_2/O_2^- radicals. The most direct of these is the optical detection of the low UV absorbances discussed in Sec. 3. In addition both HO_2 and O_2^- have characteristic electron spin resonance spectra with the former detectable at ambient temperatures in acidic solutions [27] while the latter can be detected only in ices at very low temperatures [28]. As a corollary to the esr technique, spin traps have also been used [29].

The most widely used method of detecting superoxide radicals is through the use of such chemical indicators as tetranitromethane, Nitro Blue Tetrazolium and cytochrome C which form products with intense optical absorbance:

$$C(NO_2)_4 + O_2^- \rightarrow C(NO_2)_3^- + NO_2 + O_2 \quad (20)$$

$$\text{Cyt C } (Fe^{3+}) + O_2^- \rightarrow \text{Cyt C } (Fe^{2+}) + O_2 \quad (21)$$

$$NBT^{2+} + O_2^- \rightarrow 1/2\ MF^+ + O_2 \quad (22)$$

The respective rate constants for reactions (20) to (22) are given in Table 3. All of these indicators are most advantageously used at pH near neutrality. Such indicators have been used competitively to determine relative reaction rates for other solutes with HO_2/O_2^-. Some of the compounds react by complicated mechanisms and should not be used in competition kinetics without consulting the original articles cited in Table 3.

5. Kinetics of Disproportionation of HO_2/O_2^-

Both HO_2 and O_2^- have been shown to disappear by second-order processes that vary with pH in aqueous solutions. Since HO_2 is always in equilibrium with O_2^-, reaction (7,–7), the spontaneous disproportionation can be described by the following reactions:

$$HO_2 + HO_2 \rightarrow H_2O_2 + O_2 \quad (23)$$

$$HO_2 + O_2^- + H_2O \rightarrow H_2O_2 + O_2 + OH^- \quad (24)$$

An equation can be derived that gives the experimentally observed rates (k_{obs}) in terms of the rate constants for reactions (23) and (24) and the equilibrium constant K_{HO_2}:

$$k_{obs} = \frac{k_{23} + k_{24}(K_{HO_2}/[H^+])}{(1 + K_{HO_2}/[H^+])^2} \quad (V)$$

A value for K_{HO_2} can be obtained independently from spectrophotometric measurements as well as from Eq. (V). As k_{obs} is invariant to pH in the range of 0.0 to 1.5, a value for k_{23} can be measured directly (i.e. $k_{obs} = k_{23}$ at pH 1.5). The rate constant k_{24}, however, must be calculated from Eq. (V), using k_{23} and K_{HO_2}. The results from a number of studies of the spontaneous disproportionation of HO_2/O_2^-, where the experimentally determined rates were all normalized by the molar extinction coefficients reported previously [26], yield the best average values of $k_{23} = (8.3 \pm 0.7) \times 10^5$ L mol^{-1}s^{-1} [26,30–33], $k_{24} = (9.7 \pm 0.6) \times 10^7$ L mol^{-1}s^{-1} [26,30,31,33] and $K_{HO_2} = 1.6 \times 10^{-5}$ mol L^{-1} [26,30,31,33–35,53] or $pK_a(HO_2) = 4.8 \pm 0.1$. Although other studies have shown that pK_a can vary with ionic strength [36], $pK_a(HO_2)$ was found to be invariant within experimental error over a formate concentration of 10^{-3}–10^{-1} mol L^{-1}. The curve shown in Figure 2 was calculated from these values and Eq. (V) and was found to be in very good agreement with the experimental data from a number of laboratories [30–33,37,38]

Two important features of Figure 2 should be noted. First, it is apparent that the curve has a slope of –1 above pH 6. At high pH, Eq. (V) reduces to

$$k_{obs} = k_{24}[H^+]/K_{HO_2} = 6 \times 10^{12}[H^+],\ \text{L mol}^{-1}\text{s}^{-1} \quad (VI)$$

giving a convenient method for calculating the spontaneous rate of disproportionation at a specific pH (pH > 6). Secondly, since the lowest reported $k_{obs} = 0.3$ L mol^{-1}s^{-1} at pH 13 is still on the straight line and hence represents reaction (24), one can conclude that the rate for a reaction between two O_2^- radicals (e.g. $O_2^- + O_2^-$) in aqueous solutions is for all practical purposes negligible.

The kinetic and spectral data for HO_2 and O_2^- discussed above are listed in Table 2 along with other properties for the radicals in aqueous solution.

6. Reactions of HO_2/O_2^- with Substrates

6.1. Kinetics

As mentioned previously, HO_2 is in a pH-dependent equilibrium with O_2^-. Further, many substrates can themselves ionize (equilibria (25,–25) and (26,–26)). Such

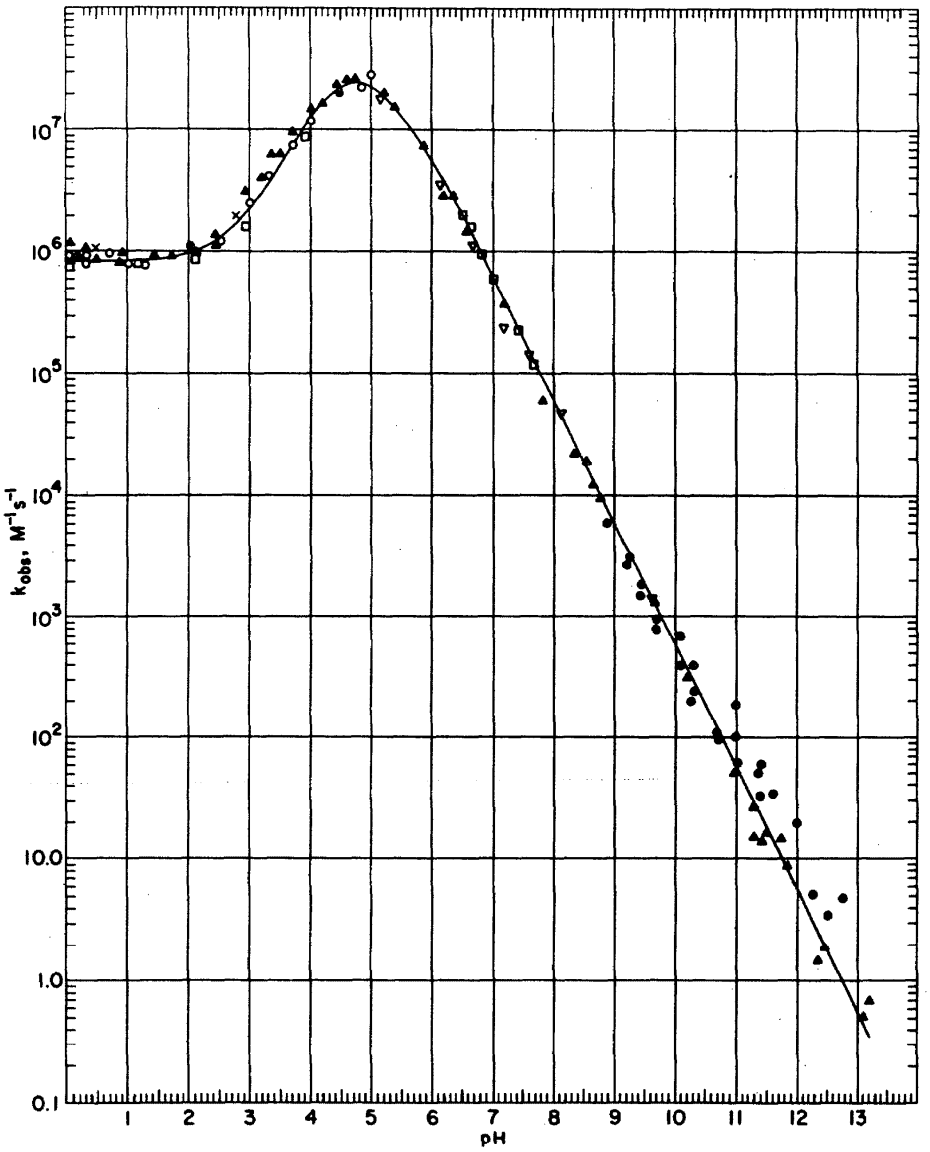

FIG. 2. Observed second-order rate constant, k_{obs} in Eq. (V), for the decay of HO_2/O_2^- plotted as a function of pH: ▲ Bielski and Allen [30], ●Marklund [37], × Sehested, et al. [38], ○ Bielski and Schwarz [32], □ Behar, et al. [31], ▽ Rabani and Nielsen [33].

dissociations not only influence the thermodynamics of the system but also the kinetics of reactions may be dramatically altered by protonation or dissociation. Hence, great care should be taken in extrapolating rate data reported at one pH in Table 3 to solutions of different pH. Ionization equilibria in substrates, including ionization of radical intermediates, are thus highly relevant to the chemistry of HO_2/O_2^- in aqueous media. A detailed kinetic treatment of such systems is given below, although it should be stressed that in many instances experimental conditions can be adjusted such that only one or two equilibria need be considered and the required kinetic treatment is then much simplified. A complete description of the interaction between HO_2/O_2^- and a species (QH_2) and its dissociation products (QH^-,Q^{2-}), with the assumption that the initial reaction produces a free radical that can in turn react with HO_2/O_2^- or disproportionate, involves four equilibria and thirteen reactions:

Equilibria: $HO_2 \rightleftharpoons O_2^- + H^+$, $pK_1 = 4.8$ (7,−7)

$QH_2 \rightleftharpoons QH^- + H^+$, pK_2 (25,−25)

$QH^- \rightleftharpoons Q^{2-} + H^+$, pK_3 (26,−26)

$QH\cdot \rightleftharpoons Q\cdot^- + H^+$, pK_4 (27,−27)

Reactions: $QH_2 + HO_2 \rightarrow QH\cdot + H_2O_2$ (28)

TABLE 2. Properties of HO_2/O_2^- in aqueous solution

Property	HO_2(aq)	O_2^-(aq)
Reduction potential[a] ($O_2 + e^- \rightarrow O_2^-$), pH 7		−0.33 V [45,54,55]
pK_a	4.8 [26,30,31,33,35,53]	
Diffusion constant ($cm^2\ s^{-1}$)		1.5 x 10^{-5} [b] [48]
$\Delta H_f°$(298 K) (kcal mol^{-1})	−8.6 ± 1 [47]	−5.9 ± 1 [47] −8 ± 2 [46]
$S°$(298 K) (cal $mol^{-1}\ K^{-1}$)	33 ± 1 [47]	19 [47]
Enthalpy of hydration (kcal mol^{-1})		−94 [46] −95 [47]
Free energy of hydration (kcal mol^{-1})		−85 [49]
Entropy of hydration (cal $K^{-1}\ mol^{-1}$)	−22 [49]	−29.6 [49]
Enthalpy of ionization (kcal mol^{-1})	0 [46] 2.7 ± 0.7 [18] 1.0 [49]	
Entropy of ionization (cal $K^{-1}\ mol^{-1}$)	−17.4 [49]	
Electron affinity (eV)	1.85 ± 0.12[c] [47]	
λ_{max} (nm)	225 [26]	245 [26]
ϵ_{max}(L $mol^{-1}\ cm^{-1}$)	1400 ± 80 [26]	2350 ± 120 [26]
$k(HO_2 + HO_2)$ = (8.3 ± 0.7) x 10^5 (L $mol^{-1}\ s^{-1}$) (See Sec. 5)		
$k(HO_2 + O_2^-)$ = (9.7 ± 0.6) x 10^7 (L $mol^{-1}\ s^{-1}$) (See Sec. 5)		
$E_a(HO_2 + HO_2)$ = 4.9–5.9 (kcal mol^{-1}) [32,46]		
$E_a(HO_2 + O_2^-)$ = 2.1 (kcal mol^{-1}) [32]		

[a] Standard state: 1 atm O_2.
[b] Soln. contg. 0.1 mol L^{-1} NaOH, 10 vol % PrOH.
[c] Gas phase.

$$QH_2 + O_2^- \rightarrow QH\cdot + HO_2^- \quad (29)$$

$$QH^- + HO_2 \rightarrow QH\cdot + HO_2^- \quad (30)$$

$$QH^- + O_2^- \rightarrow Q\cdot^- + HO_2^- \quad (31)$$

$$Q^{2-} + HO_2 \rightarrow Q\cdot^- + HO_2^- \quad (32)$$

$$Q^{2-} + O_2^- \rightarrow \text{(transient or product)} \quad (33)$$

$$QH\cdot + HO_2 \rightarrow Q + H_2O_2 \quad (34)$$

$$QH\cdot + O_2^- \rightarrow Q + HO_2^- \quad (35)$$

$$Q\cdot^- + HO_2 \rightarrow Q + HO_2^- \quad (36)$$

$$Q\cdot^- + O_2^- \rightarrow \text{(transient or product)} \quad (37)$$

$$QH\cdot + QH\cdot \rightarrow Q + QH_2 \quad (38)$$

$$QH\cdot + Q\cdot^- \rightarrow Q + QH^- \quad (39)$$

$$Q\cdot^- + Q\cdot^- \rightarrow Q + Q^{2-} \quad (40)$$

If all acid-base equilibria are ignored, this system reduces in principle to three second-order reactions that are in parallel and, in part, in series:

$$A + B \rightarrow C \quad (41)$$

$$B + C \rightarrow D \quad (42)$$

$$C + C \rightarrow D + A \quad (43)$$

Such a system has no simple solution; solutions for a mechanism involving only reactions (41) and (42) have been described in detail elsewhere [39–41] and are not trivial. However, experimental conditions can usually be adjusted such that two of the three reactions drop out, thus allowing for simple kinetic solutions. In the following kinetic development, reactions (41) through (43) will be discussed as independent systems and rate equations will be derived for the individual reactions in terms of their pH dependence.

A complete description of the initial step in the mechanism involves the equilibria (7,−7), (25,−25) and (26,−26) and reactions (28) to (33). The rate of disappearance of the radical ([R] = [HO_2] + [O_2^-]) is given by:

$$-\frac{d[R]}{dt} = k_{28}[QH_2][HO_2] + k_{29}[QH_2][O_2^-] + k_{30}[QH^-][HO_2] + k_{31}[QH^-][O_2^-] + k_{32}[Q^{2-}][HO_2] + k_{33}[Q^{2-}][O_2^-] \quad (VII)$$

Rearrangement of the equilibria (7,−7), (25,−25) and (26,−26) leads to the following relationships:

$$[O_2^-] = [HO_2](K_{HO_2}/[H^+]) = [HO_2]Y_1$$

$$[QH^-] = [QH_2](K_{25}/[H^+]) = [QH_2]Y_2$$

$$[Q^{2-}] = [QH_2](K_{25}K_{26}/[H^+]^2) = [QH_2]Y_2Y_3$$

Substituting these relationships into Eq. (VII) leads to:

$$-\frac{d[R]}{dt} = [HO_2][QH_2](k_{28} + k_{29}Y_1 + k_{30}Y_2 + k_{31}Y_1Y_2 + k_{32}Y_2Y_3 + k_{33}Y_1Y_2Y_3) \quad (VIII)$$

The total concentration of species S is given by [S] = [QH_2] + [QH^-] + [Q^{2-}] or [S] = [QH_2](1 + Y_2 + Y_2Y_3) and the total HO_2/O_2^- concentration is given by [R] = [HO_2](1 + Y_1). Substituting these relationships into Eq. (VIII) gives:

$$-\frac{d[R]}{dt} = \frac{[R][S](k_{28} + k_{29}Y_1 + k_{30}Y_2 + k_{31}Y_1Y_2 + k_{32}Y_2Y_3 + k_{33}Y_1Y_2Y_3)}{(1 + Y_1)(1 + Y_2 + Y_2Y_3)} \quad (IX)$$

Under first-order conditions where [S] is approximately constant, that is [S]≫[R], Eq. (IX) can be integrated to yield:

$$k = \frac{[S](k_{28} + k_{29}Y_1 + k_{30}Y_2 + k_{31}Y_1Y_2 + k_{32}Y_2Y_3 + k_{33}Y_1Y_2Y_3)}{(1 + Y_1)(1 + Y_2 + Y_2Y_3)} \quad (X)$$

where $k_{obs} = k/[S]$. Equation (X) describes the pH dependent kinetics of the reactions between HO_2/O_2^- and a compound with two pK's. This equation is simplified for compounds with one or no pK in the pH range studied. An example of this case can be found in the reaction between HO_2/O_2^- and tetranitromethane [23].

The model system becomes more complex if the reaction between QH_2 and HO_2/O_2^- produces a transient with an acid-base equilibrium (27,−27) that can also react with HO_2/O_2^- (reactions (34) to (37)). Following an analogous procedure to that used for the derivation of Eq. (V) and using the relationship

$$[Q\cdot^-] = [QH\cdot](K_{27}/[H^+]) = [QH\cdot]Y_4$$

one obtains (defining [S·] = [QH·] + [$Q\cdot^-$]):

$$-\frac{d[R]}{dt} = \frac{[R][S\cdot](k_{34} + k_{35}Y_1 + k_{36}Y_4 + k_{37}Y_1Y_4)}{(1 + Y_1)(1 + Y_4)} \quad (XI)$$

Detailed solutions for equations of this general form, where [R] ≠ [S·], are complex and will not be discussed here. Since radical-radical reactions of this nature generally occur on a very fast time scale, they can be measured only by fast kinetic techniques (flash photolysis or pulse radiolysis) where, with proper experimental design, equal amounts of [R] and [S·] are produced. Under these conditions Eq. (XI) can be integrated to yield:

$$k_{obs} = \frac{(k_{34} + k_{35}Y_1 + k_{36}Y_4 + k_{37}Y_1Y_4)}{(1 + Y_1)(1 + Y_4)} \quad (XII)$$

This equation describes a second-order reaction between two radicals, both having pKs, in which the radicals are generated independently and not from reactions (28) to (33). In fact, under the experimental conditions being considered, S· is generated from the reactions between HO_2/O_2^- and S (as in the generalized reactions (41) and (42)). If the rate of the HO_2/O_2^--radical reaction (42) is much slower than the rate at which the radical is generated (41), then reaction (42) will never occur since all of the HO_2 is consumed in reaction (41). On the other hand, if the rate of reaction (42) is much faster than reaction (41) steady state conditions prevail and the overall reaction becomes A + 2B → D. Therefore, the observed rate is now twice the true rate of reaction (41). This concept is introduced into Eq. (X) and (XII) by calculating the observed rates of reaction at a particular pH to determine which rate is faster at those specific experimental conditions and hence whether a factor of two must be included in Eq. (X). Such a situation has been described in the ascorbic acid system [42,43].

The final reaction in the model system involves the disproportionation of S· as described by reactions (38) and (40). The rates of disappearance of the radicals [QH·] and [$Q\cdot^-$] are given by:

$$-\frac{d[QH\cdot]}{dt} = 2k_{38}[QH\cdot]^2 + k_{39}[QH\cdot][Q\cdot^-] \quad \text{(XIII)}$$

$$-\frac{d[Q\cdot^-]}{dt} = k_{39}[QH\cdot][Q\cdot^-] + 2k_{40}[Q\cdot^-]^2 \quad \text{(XIV)}$$

and, substituting the relationship derived from equilibrium (27,−27), the rate of disappearance of the total radical concentration is given by the sum of Eqs. (XIII) and (XIV)

$$-\frac{d([QH\cdot] + [Q\cdot^-])}{dt} = \frac{2[S\cdot]^2(k_{38} + k_{39}Y_4 + k_{40}Y_4)^2}{(1 + Y_4)^2} \quad \text{(XV)}$$

and the observed second-order rate of disproportionation is merely

$$k_{obs} = \frac{2(k_{38} + k_{39}Y_4 + k_{40}Y_4)^2}{(1 + Y_4)^2} \quad \text{(XVI)}$$

The kinetics described by Eq. (XVI) gives the rate at which reaction (43) occurs as a function of pH when the radical S· has a pK. If reaction (43) occurs at a faster rate than reaction (42) then the system reduces to the formation of a transient which subsequently disappears by reaction with itself. In a system of this nature Eqs. (X) and (XVI) can be used independently to describe the kinetics of the entire system. As is apparent the kinetics that describe the spontaneous disproportionation of HO_2/O_2^-, Eq. (V), are merely a reduced form of Eq. (XVI) omitting the reaction of $(O_2^- + O_2^-)$ which is negligible as described in section 5.

6.2. Criteria for Assessment of the Kinetic Data

All of the data reported in Table 3 fall into two categories: (1) rate constants and (2) observed specific rates of reactions. An observed specific rate, $k(HO_2/O_2^- + X)$, is taken to represent a value valid under the specific experimental conditions reported by the authors whereas a rate constant, $k(HO_2 + X)$ or $k(O_2^- + X)$, is considered to be independent of pH (but not of temperature, ionic strength, etc.) and to represent the rate at which either HO_2 or O_2^- reacts with a given compound. A value of k_{obs} at a specific pH can be calculated by equation (X) if the rate constants for the reaction of HO_2 and O_2^- with that particular compound are known.

The following criteria were considered with regard to all of the rate studies listed in this table:

1. Whether, when pseudo first-order conditions were used, the rates were determined over a broad concentration range and corrected, if necessary, for the spontaneous disproportionation of HO_2/O_2^-.

2. Whether the reaction was studied either as a function of pH or under conditions such that only one of the two species reacted. Thus, $k_{obs} = 10^8$ L mol^{-1} s^{-1} at pH 8 must be for $k(O_2^- + X)$ and not $k(HO_2 + X)$, using equation (X), a limiting value for $k(HO_2 + X)$ of 10^{10} L mol^{-1} s^{-1} and assuming that the scavenger has no pK in this pH region.

3. Whether the reaction rate was found to be anomalous with respect to other studies of that particular reaction.

Comments relating to the above criteria are included in some entries in the table. In some studies it was impossible to ascertain details concerning either the experimental conditions or the kinetic analysis; such studies were nevertheless included in the table if they contained the only reported rates for these reactions.

Comments are also included when there are unexplained discrepancies in the data; the discrepancies may be due to differing experimental conditions or other reasons. It is hoped that further studies of some of these reactions will be carried out to resolve the conflicting data.

6.3. Explanation of Table 3

Table 3 contains rate constants for reactions of HO_2/O_2^- with various inorganic and organic solutes and other radical species in aqueous solution. The inorganic reactants are listed first, alphabetized by main element. Within the groupings by element the arrangement is in order of increasing oxidation state. Within a particular oxidation state for a metal, aquated ions are listed first followed by complexes with neutral ligands (amines), amino acids and other organic acids; polynuclear metal species are listed last. The metal ions are generally shown without ligated H_2O (and OH^- at high pH). The inorganic reactants are followed by the organic reactants, arranged alphabetically by name. Common names have been used in many cases and both a compound name index containing synonyms and a molecular formula index are provided as an aid to locating particular reactants.

The table entry number is followed by the name for the reactant. Reactions include products only when evidence for their identity has been reported. The radical has been given as either HO_2 or O_2^- when conditions were such that one species would predominate or when the study was carried out over a broad pH range with kinetic analysis as described above. Where studies were under conditions insufficient to determine the individual rate constants, the radical has been given as HO_2/O_2^- and the observed specific rate should be understood to be for an unspecified mixture of the two radical species. When the studies were carried out near the pK of a reactant and the contributions of the individual species were not determined, the pK [51] has been included in the table entry and the rate constant should be understood to be for a mixture of reactant species.

When the rate constants were corrected by the original authors for ionic strength it has been noted (cor. for I). The reviewers did not attempt to make such corrections because of uncertainties such as actual charge on the ions, concentrations, etc.

In some cases the reactant serves as a catalyst for the disproportionation of HO_2/O_2^-; for example, superoxide dismutase (SOD) and a number of copper complexes catalyze the formation of hydrogen peroxide and oxygen by a mechanism involving successive reduction and oxidation of the metal center [51,52]. Rate constants which are for the overall catalyzed reaction,

$$2\ O_2^- + 2\ H_2O \xrightarrow{\text{cat.}} H_2O_2 + O_2 + 2\ OH^-,$$

have been determined for various metal-centered species. Whenever the rate constants listed herein are for $k_{catalytic}$ the reaction is written accordingly or that information is given as a notation in the *Comments* column.

Error limits assigned by authors of the original papers have been included with the rate constants in column 3. Upper limits for rate constants for systems in which no reaction was observed have been included whenever they could be derived from the experimental conditions. Otherwise, the statement that no reaction was observed is included as a comment and the original paper should be consulted. In some cases the rate constants were calculated with reference to the rate constant for a competing reaction, which has been given in the *Comments* column.

The *Method* column includes the method of generation and detection of the radical; other details are given under *Comments*. The references to Table 3 are listed by serial number assigned by the Radiation Chemistry Data Center and included in the RCDC Bibliographic Data Base.

7. Abbreviations and Symbols

abs.	absorption
abstr.	abstraction
addn.	addition
alk.	alkaline
anal.	analysis
atm.	atmospheres (1.013×10^5 N m^{-2})
biol.	biological method, biological assay
bpy	2,2′-bipyridine
tert-BuOH	*tert*-butyl alcohol
CTAB	hexadecyltrimethylammonium bromide
calcd.	calculated
chem.	chemical
c.k.	competition kinetics
concn.	concentration
condy.	conductivity
contg.	containing
cor.	corrected
cyt C	cytochrome C
DCIP	dichloroindophenol
DMSO	dimethyl sulfoxide
DNA	deoxyribonucleic acid
detd.	determined
d.k.	decay kinetics (decay of radical absorption and bleaching of substrate absorption)
e-r.	electron radiolysis
ϵ	extinction coefficient (molar absorptivity)
E_a	activation energy
elec.	electrolysis, electrochemical method
EtOH	ethanol
esr	electron spin resonance
estd.	estimated
enz.	enzyme or enzymatic
FMN	flavin mononucleotide
f.p.	flash photolysis
formn.	formation
γ-r.	gamma radiolysis
G	radiation yield (molecules per 100 eV)
I	ionic strength
K	equilibrium constant
k	rate constant
$k_{catalytic}$	rate constant for the overall catalyzed reaction
meas.	measured
MF	monoformazan
NBT^{2+}	Nitro Blue Tetrazolium
obs.	observed
opt.	optical absorption
Pa	pascals (N m^{-2})
p.b.k.	product buildup kinetics
phot.	photolysis
pK_a	negative logarithm of the acid dissociation constant, e.g., where $AH + H_2O \rightleftharpoons A^- + H_3O^+$
p.r.	pulse radiolysis
2-PrOH	2-propanol
Q	1,4-benzoquinone (used in Table 3 as a competitor)
redn.	reduction
rel.	relative
satd.	saturated
SDS	sodium dodecylsulfate
s.f.	stopped flow
SOD	superoxide dismutase
soln.	solution
TMPO	trimethylpyrroline *N*-oxide
TNM	tetranitromethane
X-r.	X-radiolysis

Acknowledgments

This review was generated at Brookhaven National Laboratory under contract with the US Department of Energy, and supported by its Office of Basic Energy Sciences, and at the Radiation Laboratory at the University of Notre Dame, which is operated under Contract DE-AC02-76ER0038 with the Department of Energy. The Radiation Chemistry Data Center is supported jointly by the National Bureau of Standards, Office of Standard Reference Data and by the Office of Basic Energy Sciences and the Office of Health and Environmental Research of the Department of Energy. This is Radiation Laboratory Document No. NDRL-2542.

The authors would like to thank Dr. Peter Wardman for many helpful suggestions and comments concerning the introduction and Dr. W. Phillip Helman for assistance in preparation of the computer-readable files submitted for publication.

8. References to Text

[1] Bielski, B.H.J., Gebicki, J.M., Species in irradiated oxygenated water, Advan. Radiat. Chem. **2**: 177–279 (1970).

[2] Czapski, G., Radiation chemistry of oxygenated aqueous solutions, Annu. Rev. Phys. Chem. **22**: 171–208 (1971).

[3] Bors, W., Saran, M., Lengfelder, E., Spoettl, R., Michel, C., The relevance of the superoxide anion radical in biological systems, Curr. Top. Radiat. Res. Quart. **9**: 247–309 (1974).

[4] Fee, J.A., Valentine, J.S., Chemical and physical properties of superoxide, *Superoxide and Superoxide Dismutases*, p. 19–60, A.M. Michelson, J.M. McCord and I. Fridovich (eds), Academic Press, New York, (1977).

[5] Bors, W., Saran, M., Czapski, G., The nature of intermediates during biological oxygen activation, *Biological and Clinical Aspects of Superoxide and Superoxide Dismutase*, p.1–31, W.H. Bannister and J.V. Bannister (eds), Elsevier/North Holland, New York, (1980).

[6] Sawyer, D.T., Valentine, J.S., How super is superoxide? Acc. Chem. Res. **14**: 393–400 (1981).

[7] Allen, A.O., Bielski, B.H.J., Formation and disappearance of superoxide radicals in aqueous solution, *Superoxide Dismutase*, Vol. 1, p.125–41, L.W. Oberley (ed.), CRC Press, Boca Raton, FL (1982).

[8] a. Keene, J. P., The absorption spectrum and some reaction constants of the hydrated electron, Radiat. Res. **22**: 1–13 (1964); Gordon, S., Hart, E.J., Matheson, M.S., Rabani, J., Thomas, J.K., Reactions of the hydrated electron, Discuss. Faraday Soc. **36**: 193–205 (1963). b. Dorfman, L.M., Taub, I.A., Pulse radiolysis studies. III. Elementary reactions in aqueous ethanol solution, J. Am. Chem. Soc. **85**: 2370–4 (1963).

[9] Anbar, M., Farhataziz, and Ross, A.B., Selected specific rates of reactions of transients from water in aqueous solution. II. Hydrogen atom. NSRDS-NBS-51, U.S. Dept. of Commerce, National Bureau of Standards, Washington, DC, 1975, 56p.

[10] Willson, R.L., Greenstock, C.L., Adams, G.E., Wageman, R., Dorfman, L.M., The standardization of hydroxyl radical rate data from radiation chemistry., Int. J. Radiat. Phys. Chem. **3**: 211–20 (1971).

[11] Neta, P., Schuler, R.H., Effect of ionic dissociation of organic compounds on their rate of reaction with hydrogen atoms, J. Phys. Chem. **76**: 2673–9(1972).

[12] Adams, G.E., Willson, R.L., Pulse radiolysis studies on the oxidation of organic radicals in aqueous solution. Trans. Faraday Soc. **65**: 2981–7 (1969).

[13] Draganic, I.G., Draganic, Z.D., *The Radiation Chemistry of Water*, Academic Press, New York, 1971, 256p.

[14] Bielski, B.H.J., Arudi, R.L., Preparation and stabilization of aqueous ethanolic superoxide solutions, Anal. Biochem. **133**: 170–78 (1983).

[15] Bothe, E., Schuchmann, M.N., Schulte-Frohlinde, D., von Sonntag, C., Hydroxyl radical-induced oxidation of ethanol in oxygenated aqueous solutions. A pulse radiolysis and product study, Z. Naturforsch., Teil B **38B**: 212–9 (1983).

[16] McDowell, M.S., Bakac, A., Espenson, J.H., A convenient route to superoxide ion in aqueous solution, Inorg. Chem. **22**: 847–8 (1983).

[17] Baxendale, J.H., Wilson, J.A., The photolysis of hydrogen peroxide at high light intensities, Trans. Faraday Soc. **53**: 344–56 (1957).

[18] Nadezhdin, A., Dunford, H.B., Oxidation of nicotinamide adenine dinucleotide by hydroperoxyl radical. A flash photolysis study, J. Phys. Chem. **83**: 1957–61 (1979).

[19] McCord, J.M., Beauchamp, C.O., Goscin, S., Misra, H.P., Fridovich, I., *Superoxide and Superoxide Dismutase, Oxidases and Related Redox Systems*, Vol. I, T.E. King, S. Mason and M. Morrison (eds), University Press, Baltimore, MD, (1973)

[20] Olson, J.S., Ballou, D.P., Palmer, G., Massey, V., The mechanism of action of xanthine oxidase, J. Biol. Chem. **249**: 4363–82 (1974).

[21] Fenton, H.J.H., Jackson, H., The oxidation of polyhydric alcohols in presence of iron, J. Chem. Soc. (London) **75**: 1–11 (1899).

[21a] Bielski, B.H.J., Richter, H.W., A study of the superoxide radical chemistry by stopped-flow radiolysis and radiation induced oxygen consumption, J. Am. Chem. Soc. **99**: 3019–23 (1977).

[22] Henglein, A., Langhoff, J., Schmidt, G., Tetranitromethane as a radical scavenger in radiation chemical studies, J. Phys. Chem. **63**: 980 (1959).

[23] Rabani, J., Mulac, W.A., Matheson, M.S., The pulse radiolysis of aqueous tetranitromethane. I. Rate constants and the extinction coefficient of e_{aq}^-. II. Oxygenated solutions, J. Phys. Chem. **69**: 53–70 (1965).

[24] Bielski, B.H.J., Allen, A.O., Radiation chemistry of aqueous tetranitromethane solutions in the presence of air. J. Phys. Chem. **71**: 4544–9 (1967).

[25] Van Gelden, B.F., Slater, E.C., The extinction coefficient of cytochrome c, Biochim. Biophys. Acta **58**: 593–95 (1962).

[26] Bielski, B.H.J., Reevaluation of the spectral and kinetic properties of HO_2 and O_2^- free radicals, *Photochem. Photobiol.* **28**: 645–9 (1978).

[27] Saito, E., Bielski, B.H.J., The electron paramagnetic resonance spectrum of the HO_2 radical in aqueous solution, J. Am. Chem. Soc. **83**: 4467 (1961).

[28] Knowles, P.F., Gibson, J.F., Pick, F.M., Bray, R.C., Electron-spin-resonance evidence for enzymic reduction of oxygen to a free radical, the superoxide ion, Biochem. J. **111**: 53–8 (1969).

[29] Harbour, J.R., Chow, V., Bolton, J.R., An electron spin resonance study of the spin adducts of OH and HO_2 radicals with nitrones in the ultraviolet photolysis of aqueous hydrogen peroxide solutions, Can. J. Chem. **52**: 3549–53 (1974).

[30] Bielski, B.H.J., Allen, A.O., Mechanism of the disproportionation of superoxide radicals, J. Phys. Chem. **81**: 1048–50 (1977).

[31] Behar, D., Czapski, G., Rabani, J., Dorfman, L.M., Schwarz, H.A., The acid dissociation constant and decay kinetics of the perhydroxyl radical, J. Phys. Chem. **74**: 3209–13 (1970).

[32] Bielski, B.H.J., Schwarz, H.A., The absorption spectra and kinetics of hydrogen sesquioxide and the perhydroxyl radical. J. Phys. Chem. **72**: 3836–41 (1968).

[33] Rabani, J., Nielson, S.O., Absorption spectrum and decay kinetics of O_2^- and HO_2 in aqueous solutions by pulse radiolysis. J. Phys. Chem. **73**: 3736–44 (1969).

[34] Getoff, N., Prucha, M., Spectroscopic and kinetic characteristics of HO_2 and O_2^- species studied by pulse radiolysis, Z. Naturforsch., Teil A **38A**: 589–90 (1983).

[35] Barker, G.C., Fowles, P., Pulse radiolytic induced transient electrical conductance in liquid solutions. Part 3. Radiolysis of aqueous solutions of some inorganic systems, Trans. Faraday Soc. **66**: 1661–9 (1970).

[36] Perrin, D.D., Dempsey, B., Serjeant, E.P., *pK_a Prediction for Organic Acids and Bases*, p.5–7, Chapman and Hall, London, (1981).

[37] Marklund, S., Spectrophotometric study of spontaneous disproportionation of superoxide anion radical and sensitive direct assay for superoxide dismutase, J. Biol. Chem. **251**: 7504–7 (1976).

[38] Sehested, K., Bjergbakke, E., Rasmussen, O.L., Fricke, H., Reactions of H_2O_3 in the pulse-irradiated Fe(II)–O_2 system, *J. Chem. Phys.* **51**: 3159–66 (1969).

[39] Frost, A.A., Pearson, R.G., *Kinetics and Mechanisms*, p.165–71, John Wiley, New York, (1961).

[40] Benson, S.W., *The Foundations of Chemical Kinetics*, Chapter 2, McGraw-Hill, New York, (1960).

[41] Szabo, Z.G., Kinetic characterization of complex reaction systems, *Comprehensive Chemical Kinetics*, Vol. II, Chapter 1, C.H. Bamford and C.F.H. Tipper (eds), Elsevier, Amsterdam, (1969).

[42] Nadezhdin, A.D., Dunford, H.B., The oxidation of ascorbic acid and hydroquinone by perhydroxyl radicals. A flash photolysis study, Can. J. Chem. **57**: 3017–22 (1979).

[43] Cabelli, D.E., Bielski, B.H.J., Kinetics and mechanism for the oxidation of ascorbic acid/ascorbate by HO_2/O_2^- radicals. A pulse radiolysis and stopped-flow photolysis study, J. Phys. Chem. **87**: 1809–12 (1983).

[44] Bielski, B. H.J., Saito, E., The activation energy for the disproportionation of the HO_2 radical in acid solutions, J. Phys. Chem. **66**: 2266–8 (1962).

[45] Wood, P.M., The redox potential of the system oxygen-superoxide, FEBS Lett. **44**: 22–4 (1974).

[46] Baxendale, J.H., Ward, M.D., Wardman, P., Heats of ionization of HO_2 and OH in aqueous solution, Trans. Faraday Soc. **67**: 2532–7 (1971).

[47] Benson, S.W., Nangia, P.S., Electron affinity of HO_2 and HO_x radicals, J. Am. Chem. Soc. **102**: 2843–4 (1980).

[48] Divisek, J., Kastening, B., Electrochemical generation and reactivity of the superoxide ion in aqueous solutions. J. Electroanal. Chem. Interfacial Electrochem. **65**: 603–21 (1975).

[49] Koppenol, W.H., Solvation of the superoxide anion, *Oxy Radicals and their Scavenger Systems*, Vol. 1, p.274–7, G. Cohen and R.A. Greenwald (eds), Elsevier Biomedical, New York, (1983).

[50] p*K*s are taken from: *CRC Handbook of Chemistry and Physics*, R.C. Weast (ed.), 63rd ed., CRC Press, Boca Raton FL (1982); Kortum, G., Vogel, W. and Andrussow, K., *Dissociation Constants of Organic Acids in Aqueous Solution*, Butterworths, London, (1961); Serjeant, E.P., and Dempsey, B., *Ionisation Constants of Organic Acids in Aqueous Solution*, IUPAC Chemical Data Series No. 23, Pergamon Press, Oxford, (1979); Perrin, D.D., *Dissociation Constants of Organic Bases in Aqueous Solution*, Butterworths, London (1965), and Supplement (1972).

[51] Klug-Roth, D., Fridovich, I., Rabani, J., Pulse radiolytic investigations of superoxide catalyzed disproportionation. Mechanism for bovine superoxide dismutase, J. Am. Chem. Soc. **95**: 2786–90 (1973).

[52] Fielden, E.M., Roberts, P.B., Bray, R.C., Lowe, D.J., Mautner, G.N., Rotilio, G., Calabrese, L., The mechanism of action of superoxide dismutase from pulse radiolysis and electron paramagnetic resonance. Evidence that only half the active sites function in catalysis, Biochem. J. **139**: 49–60 (1974).

[53] Getoff, N., Prucha, M., Spectroscopic and kinetic characteristics of HO_2 and O_2^- species studied by pulse radiolysis, Z. Naturforsch., Teil A **38A**: 589–90 (1983).

[54] Ilan, Y.A., Meisel, D., Czapski, G., The redox potential of the $O_2-O_2^-$ system in aqueous media, Israel J. Chem. **12**: 891–5 (1974).

[55] Berdnikov, V.M., Zhuravleva, O.S., Thermodynamic characteristics of the hydroperoxy radical in aqueous solution, Russ. J. Phys. Chem. **46**: 1521–3 (1972), transl. from Zh. Fiz. Khim. **46**: 2658–60 (1972).

TABLE 3. Rate constants for reactions of HO_2/O_2^- in aqueous solutions

No.	Reaction	pH	k (L mol^{-1}s^{-1})	Method	Comment	Ref.
1	**Americium(IV) ion**					
	$HO_2 + Am^{4+} \rightarrow H^+ + Am^{3+} + O_2$	1	6.4×10^7	p.r., opt.	D.k. (Am^{IV}). k varies with pH due to different degrees of hydrolysis of Am(IV) at each pH.	771130
		2	5.2×10^7			
		3.2	5.0×10^7			77A243
		4.4	2.7×10^7			
2	**Borate ion**					
	$O_2^- + BO_3^{3-} \rightarrow$	10.0	<0.02	s.f., opt.	D.k. at 250 nm in air-satd. soln. contg. 0.2 mol L^{-1} formate and 2×10^{-4} mol L^{-1} EDTA and 0.01–0.1 mol L^{-1} borate; no reaction.	770046
3	**Tribromine ion**					
	$HO_2 + Br_3^- \rightarrow H^+ + Br_2^- + Br^- + O_2$	2–7	$< 10^7$	e–r., chem.	C.k. in formate-Br_2 soln.; rel. to $k(O_2^- + TNM) = 2 \times 10^9$.	720308
		2	$(1 \pm 0.5) \times 10^8$	p.r., opt.	C.k.; mechanistic anal.	650383
	$O_2^- + Br_3^- \rightarrow Br_2^- + Br^- + O_2$	7	$(3.8 \pm 0.7) \times 10^9$	e–r., chem.	C.k. in formate-Br_2 soln.; soln. contains 0.2 mol L^{-1} Br^-; rel. to $k(O_2^- + TNM) = 2 \times 10^9$.	720308
4	**Dibromine radical ion**					
	$HO_2 + Br_2^- \rightarrow HO_2^- + Br_2$	2	6.5×10^9	γ–r., chem.	C.k. in soln. contg. 10^{-4}–1 mol L^{-1} KBr; rel. to $HO_2 + Br_2$ and $Br_2^- + Br_2^-$.	650055
		2	$(4.6 \pm 1.2) \times 10^9$	p.r., opt.	D.k.; $k/\epsilon(Br_2^-) = (4.6 \pm 0.4) \times 10^5$ cm/s; more than one rate constant is involved in calcn. k cor. using ϵ(360 nm) = 9900 L mol^{-1} cm^{-1} for Br_2^-.	650382
		2	$(1.6 \pm 0.5) \times 10^9$	p.r., opt.	C.k.; obs. decay of Br_2^- at 360 nm (ϵ = 9600 L mol^{-1} cm^{-1}); data fitting.	650383
5	**Bromine**					
	$HO_2 + Br_2 \rightarrow Br + H^+ + Br^- + O_2$	2.1–2.9	$(1.1 \pm 0.5) \times 10^8$	e–r., chem.	C.k. in formate-Br_2 soln.; rel. to $k(O_2^- + TNM) = 2 \times 10^9$.	720308
		~1	1.5×10^8	p.r., opt.	C.k.; indirect estimation; more than one rate constant is involved; uncertainty is two-fold.	650382
	$O_2^- + Br_2 \rightarrow Br_2^- + O_2$	7	$(5.6 \pm 0.7) \times 10^9$	e–r., chem.	C.k. in formate-Br_2 soln.; rel. to $k(O_2^- + TNM) = 2 \times 10^9$.	720308
6	**Hypobromous acid**					
	$O_2^- + HOBr \rightarrow Br + OH^- + O_2$	7	$(9.5 \pm 0.8) \times 10^8$	e–r., chem.	C.k. in formate-Br_2 soln.; rel. to $k(O_2^- + TNM) = 2 \times 10^9$.	720308
7	**Carbonic acid, pK_a = 6.46, 10.3**					
	$HO_2/O_2^- + H_2CO_3/HCO_3^-/CO_3^{2-} \rightarrow HO_2^- + CO_3^-$	10.1	<0.04	s.f., opt.	D.k. at 250 nm in air-satd. soln. contg. 0.2 mol L^{-1} formate and 10^{-4} mol L^{-1} EDTA and (0.1–2.5) $\times 10^{-1}$ mol L^{-1} carbonate; no reaction.	770046
		5.5	$(1–2) \times 10^6$	p.r., condy.	D.k. (rotating sector); CO_2 soln.	720404
8	**Carbonate radical ion**[a]					
	$O_2^- + CO_3^- \rightarrow CO_3^{2-} + O_2$		$(4 \pm 1) \times 10^8$	f.p., opt.	D.k. in O_2-satd. soln. contg. 0.2 mol L^{-1} CO_3^{2-} at 260 nm and 600 nm; ϵ (CO_3^-) = 1860 at 600 nm and 200 at 260 nm and $\epsilon(O_2^-)$ = 1850 L mol^{-1}cm^{-1} at 260 nm.	700247
		12.8	1.3×10^8	f.p., opt.	D.k. at 260 and 600 nm; ϵ(260) for O_2^- = 900 and ϵ(600) for CO_3^- = 1830 L mol^{-1} cm^{-1}.	677012
		~13	1.5×10^9	p.r., opt.	D.k. at 600 as well as 260 nm; ϵ(600) for CO_3^- – 1.8×10^3, ϵ(260) for O_2^- – 1.22×10^3 L mol^{-1} cm^{-1}.	660001

[a]NOTE IN PROOF: A rate constant of $(3.0 \pm 0.5) \times 10^8$ has been determined by d.k. at 240 nm and 600 nm in carbonate solution at pH 10.1 (21 °C), with a small activation energy of 4.1 ± 0.7 kJ mol^{-1} [private communication: G.V. Buxton and S. Dyster, 26 Nov. 1984].

TABLE 3. Rate constants for reactions of HO_2/O_2^- in aqueous solutions — Continued

No.	Reaction	pH	k (L mol^{-1}s^{-1})	Method	Comment	Ref.
9	**Cerium(III) ion** $HO_2 + Ce^{3+} \rightarrow Ce^{4+} + H_2O_2$	0.4	$(2.1 \pm 0.2) \times 10^5$	p.r., opt.	P.b.k. at 320 nm, Ce(IV).	741107
10	**Cerium(IV) ion** $HO_2 + Ce^{4+} \rightarrow H^+ + Ce^{3+} + O_2$	0.4	$\sim 2.7 \times 10^6$	chem.	D.k.; flow technique; soln. cont. Ce(IV) + H_2O_2; calcd. rel. to HO_2 + Ce(III) using rate constant from [741107].	639017
11	**Chloride ion** $O_2^- + Cl^- \rightarrow$	11.02	<0.014	p.r., opt.	D.k. at 240 nm in O_2-satd. formate soln., cor. for O_2^- decay. Stopped-flow (γ-r. or vacuum uv photolysis) also used. Authors feel that no reaction occurs.	80A049
12	**Dichlorine radical ion** $HO_2 + Cl_2^- \rightarrow H^+ + Cl^- + Cl^- + O_2$	~ 1	$(1.0 \pm 0.1) \times 10^9$	p.r., opt.	Calcd. fit to d.k. at 340 nm in O_2-satd. soln. contg. 0.05 mol L^{-1} Cl^- and 0.15 mol L^{-1} $HClO_4$; assumed $2k(Cl_2^- + Cl_2^-) = 4 \times 10^9$.	80A378
13	**Chlorine** $HO_2 + Cl_2 \rightarrow H^+ + Cl_2^- + O_2$	2	1×10^9	p.r., opt.	D.k. at 260 nm (HO_2) as well as 340 nm (Cl_2^-) in oxygenated soln. contg. 0.19 mol L^{-1} NaCl and 0.01 mol L^{-1} $HClO_4$; $k(HO_2 + Cl_2^-)$ was taken to be identical to $k(HO_2 + Cl_2)$.	81A227
14	**Hypochlorous acid** $O_2^- + HOCl \rightarrow Cl^- + OH + O_2$	8.5–12.3	$(7.5 \pm 0.38) \times 10^6$	p.r., opt.	D.k. at 240 nm in O_2-satd. formate soln., k calcd. from k_{obs} vs pH study ($\sim 10^2 - 10^6$, see graph) and $K_{HClO} = 3.8 \times 10^8$ mol L^{-1}. Stopped-flow (γ-r. or vacuum uv photolysis) also used.	80A049
15	**Chlorite ion** $O_2^- + ClO_2^- \rightarrow$	7.4–11.3	<0.4	p.r., opt.	D.k. at 240 nm in O_2-satd. formate soln., cor. for O_2^- decay. Stopped-flow (γ-r. or vacuum uv photolysis) also used. Authors feel no reaction occurs.	80A049
16	**Chlorine dioxide** $O_2^- + ClO_2 \rightarrow ClO_2^- + O_2$	12	$(3.3 \pm 0.2) \times 10^9$	p.r., opt.	D.k. at 360 nm in soln. contg. 10^{-2} mol L^{-1} ClO_2^- and 1.3×10^{-2} mol L^{-1} H_2O_2.	81A242
17	**Chlorate ion** $O_2^- + ClO_3^- \rightarrow$	11.1	<0.003	p.r., opt.	D.k. at 240 nm O_2-satd. formate soln., cor. for O_2^- decay. Stopped-flow (γ-r. or vacuum uv photolysis) also used. Authors feel that no reaction occurs.	80A049
18	**Perchlorate ion** $O_2^- + ClO_4^- \rightarrow$	11.1		p.r., opt.	No reaction obs.; d.k. at 240 nm in O_2-satd. formate soln., cor. for O_2^- decay.	80A049
19	**Bis(2,2'-bipyridine)cobalt(II) ion** $O_2^- + Co(bpy)_2^{2+} \rightarrow O_2Co(bpy)_2^+$		1.9×10^6	p.r., opt.	P.b.k.; pH not given but probably 7–8.	771028
20	**(2,3,9,10-Tetramethyl-1,4,8,11-tetraazacyclotetradeca-1,3,8,10-tetraene)cobalt(II) ion** $O_2^- + Co(tetraeneN_4)_2^{2+} \rightarrow O_2Co(tetraeneN_4)^+$	7–8	1.6×10^9	p.r., opt.	P.b.k.	771028
21	**(5,7,7,12,14,14-Hexamethyl-1,4,8,11-tetraazacyclotetradeca-4,11-diene)cobalt(II) ion** $O_2^- + Co(4,11\text{-}dieneN_4)_2^{2+} \rightarrow O_2Co(4.11\text{-}dieneN_4)^+$	7–8	1.4×10^9	p.r., opt.	P.b.k. in soln. contg. 1.3×10^{-3} mol L^{-1} O_2 and 0.25 mol L^{-1} *tert*-BuOH.	771028

TABLE 3. Rate constants for reactions of HO_2/O_2^- in aqueous solutions — Continued

No.	Reaction	pH	k (L mol^{-1}s^{-1})	Method	Comment	Ref.
22	**1,3,6,8,10,13,16,19-Octaazabicyclo[6.6.6]eicosanecobalt(II) ion**					
	$O_2^- + Co(sepulchrate)^{2+} \rightarrow Co(sepulchrate)^{3+} + H_2O_2$	11.3–12.6	$(4.6 \pm 1.1) \times 10^7$	f.p., opt.	P.b.k. at 480 nm in soln. contg. 2 mol L^{-1} 2-PrOH, 5×10^{-6} mol L^{-1} benzophenone, 4×10^{-5} mol L^{-1} EDTA and 0.004–0.04 mol L^{-1} KOH.	83A304
23	**Nitrilotriacetatocobaltate(II) ion**					
	$O_2^- + CoNTA^- \rightarrow (CoNTAO_2)^{2-}$	7	$\leqslant 3 \times 10^8$	p.r.	Prod. reacted with another molecule of solute $\rightarrow [CoNTAO_2CoNTA]^{3-}$, $k = 1.4 \times 10^7$. ϵ(300 nm) $= 4.5 \times 10^3$ L mol^{-1} cm^{-1}.	79A255
	$HO_2/O_2^- + CoNTA^- \rightarrow (CoNTAO_2)^{2-}$	5.0	$(1.5 \pm 0.2) \times 10^8$	p.r., opt.	Inner-sphere mechanism; spectral data for product given.	78A436
24	**Ethylenediaminetetraacetatocobaltate(II) ion**					
	$HO_2/O_2^- + CoEDTA^{2-} \rightarrow$	5.0	$(2.0 \pm 0.3) \times 10^6$	p.r., opt.	Inner-sphere mechanism; spectral data for product given.	78A436
25	**(2,3,9,10-Tetramethyl-1,4,8,11-tetraazacyclotetradeca-1,3,8,10-tetraene)cobalt(III) ion**					
	$HO_2/O_2^- + Co(tetraeneN_4)_2^{3+} \rightarrow$		$<10^5$	p.r.	No reaction obs.; pH not given but probably 7–8.	771028
26	**Tetrakis(4-*N*-methylpyridyl)porphinecobalt(III) ion**					
	$HO_2/O_2^- + CoTMpyP^{5+} \rightarrow$	5.6	$(1.4 \pm 0.1) \times 10^7$	p.r., opt.	D.k. at 254 nm in soln. contg. 5×10^{-3} mol L^{-1} Na formate and 2×10^{-3} mol L^{-1} phosphate buffer.	82A319
		8.0	$(9.0 \pm 0.9) \times 10^5$			
		10.1	1×10^5	enz, opt.	C.k., rel. to $k(O_2^- + NBT^{2+}) = 6 \times 10^4$, in soln. contg. 0.05 mol L^{-1} carbonate buffer (pH 10.1) or borate buffer (pH 9.7). Obs. increase in absorbance at 560 nm ($NBT^{2+} \rightarrow$ formazan); O_2^- produced in xanthine/xanthine oxidase system contg. catalase.	79R111
		9.7	4×10^5			
27	**Tetrakis(*p*-sulfonatophenyl)porphinatocobaltate(III) ion**					
	$HO_2/O_2^- + CoTPPS^{3-} \rightarrow$	5.6	$\leqslant 6 \times 10^5$	p.r., opt.	D.k. at 254 nm in soln. contg. 5×10^{-3} mol L^{-1} Na formate and 2×10^{-3} mol L^{-1} phosphate buffer.	82A319
		8.0	$\leqslant 1 \times 10^5$			
28	**μ-Amido-μ-superoxidotetrakis(ethylenediamine)dicobalt(III) ion**					
	$HO_2 + O_2[Co(en)_2]_2NH_2^{4+} \rightarrow H^+ + O_2[Co(en)_2]_2NH_2^{3+} + O_2$	2.8–6.6	$(3.0 \pm 0.5) \times 10^6$	p.r., opt.	P.b.k. at 380 nm; calcd. from k_{obs} vs pH; product is peroxido complex.	80A139
	$O_2^- + O_2[Co(en)_2]_2NH_2^{4+} \rightarrow O_2[Co(en)_2]_2NH_2^{3+} + O_2$	2.8–6.6	$(5.8 \pm 0.3) \times 10^7$	p.r., opt.	P.b.k. at 380 nm, calcd. from k_{obs} vs pH; product is peroxido complex.	80A139
29	**Decakis(cyano)-μ-superoxidodicobaltate(III) ion**					
	$HO_2 + O_2[Co(CN)_5]_2^{5-} \rightarrow H^+ + O_2[Co(CN)_5]_2^{6-} + O_2$	2.8–6.6	$(4.7 \pm 0.3) \times 10^5$	p.r., opt.	D.k. at 310 nm in soln. contg. 0.1 mol L^{-1} formate ion studied as a function of pH; product is peroxido complex.	80A139
	$O_2^- + O_2[Co(CN)_5]_2^{5-} \rightarrow$	2.8–6.6		p.r., opt.	No reaction obs.; d.k. at 310 nm in solution contg. 0.1 mol L^{-1} formate.	80A139
30	**Cyanocob(III)alamin**					
	$O_2^- + B12 \rightarrow$			p.r.	No reaction obs.; pH not given but assumed to be 6–11.	730116
31	**Copper(I) ions**					
	$HO_2 + Cu^+ \rightarrow Cu^{2+} + H_2O_2$	2.3	2.3×10^9	phot., opt.	Sector method; assume $k(HO_2 + Cu^{2+}) = 3.4 \times 10^7$ and $k(H_2O_2 + Cu^+) = 4.7 \times 10^3$.	737514
		2.3	6×10^8	phot., opt.	Rotating sector; $k(HO_2 + Cu^+)/k(H_2O_2 + Cu^+) = 2.4$; soln. cont. Cu^{2+} and 4.5 mol L^{-1} H_2O_2; $I = 0.1$; see also [737514].	697082
	$O_2^- + Cu^+ \rightarrow OH + Cu^{2+} + H_2O_2$	~3–6.5	10^{10}	p.r., opt.	D.k. at 245 nm in Cu^{2+} soln.	730112
32	**Bis(1,10-phenanthroline)copper(I) ion**					
	$O_2^- + Cu(phen)_2^+ \rightarrow H_2O_2 + Cu(phen)_2^{2+}$	7.0	$(2.95 \pm 0.3) \times 10^8$	p.r., opt.	D.k. at 435 nm in soln. contg. 0.05 mol L^{-1} formate, 10^{-3} mol L^{-1} phosphate; 1,10-phenanthroline/Cu^{2+} concn. = 2.0–2.5.	83A299

TABLE 3. Rate constants for reactions of HO_2/O_2^- in aqueous solutions — Continued

No.	Reaction	pH	k (L mol^{-1}s^{-1})	Method	Comment	Ref.
33	**Copper(II) ions**					
	$HO_2 + Cu^{2+} \rightarrow H^+ + Cu^+ + O_2$	0.8–2	$\sim 10^8$	p.r., opt.	D.k. at 245 nm.	730112
	$HO_2/O_2^- + Cu^{2+} \rightarrow H^+ + Cu^+ + O_2$	2.3	3.4×10^7	phot., opt.	Sector method; $k(HO_2 + Cu^{2+})/k(O_2^- + Cu^{2+}) = 0.024$	737514
		2.3	1.5×10^7	f.p., opt.	D.k. at 254 nm. Rate may be too high by a factor of 2.	620050
	$O_2^- + Cu^{2+} \rightarrow Cu^+ + O_2$	8.0	$(4.81 \pm 0.27) \times 10^9$	p.r., opt.	D.k. at 245 nm (O_2^-); phosphate buffer.	82A448
		7.0	$(8.1 \pm 0.5) \times 10^9$	p.r., opt.	Observed rate; d.k. in soln. contg. 2×10^{-3} mol L^{-1} Na formate and 10^{-3} mol L^{-1} phosphate buffer and $Cu(ClO_4)_2$.	82A281
		7.8	$(2.7 \pm 0.2) \times 10^9$	p.r., opt.	D.k. at 245 nm in O_2-satd. soln. contg. 10^{-3} mol L^{-1} Na formate and 10^{-6} mol L^{-1} Cu^{2+}; k similar in presence of serum albumin. Observed rate.	741163
		~3–6.5	8×10^9	p.r., opt.	D.k. at 245 nm. Rate determined from a broad pH range.	730112
34	**Amminecopper(II) ion**					
	$O_2^- + CuNH_3^{2+} \rightarrow$	5.8–8.5	$(2.2 \pm 0.6) \times 10^9$	p.r., opt.	D.k. at 248 nm; $I = 1$	761021
35	**Bisamminecopper(II) ion**					
	$O_2^- + Cu(NH_3)_2^{2+} \rightarrow Cu(NH_3)_2^+ + O_2$	5.8–8.5	$(2.2 \pm 0.8) \times 10^9$	p.r., opt.	D.k. at 248 nm; $I = 1$.	761021
36	**Trisamminecopper(II) ion**					
	$O_2^- + Cu(NH_3)_3^{2+} \rightarrow$	5.8–8.5	$(1.0 \pm 0.5) \times 10^9$	p.r., opt.	D.k. at 248 nm; $I = 1$.	761021
37	**Tetraamminecopper(II) ion**					
	$O_2^- + Cu(NH_3)_4^{2+} \rightarrow$	5.8–8.5	$(2 \pm 0.8) \times 10^8$	p.r., opt.	D.k. at 248 nm; $I = 1$; authors feel value could be doubtful.	761021
38	**(5,7,7,12,12,14-Hexamethyl-1,4,8,11-tetraazacyclotetradeca-4,11-diene)copper(II) ion**					
	$HO_2/O_2^- + Cu(4,11\text{-dieneN}_4)_2^{2+} \rightarrow$		$< 10^5$	p.r.	No reaction. pH not given but probably 7–8. Limiting value.	771028
39	**Bis(1,10-phenanthroline)copper(II) ion**					
	$O_2^- + Cu(phen)_2^{2+} \rightarrow O_2 + Cu(phen)_2^+$	7.0	$(1.93 \pm 0.07) \times 10^9$	p.r., opt.	D.k. at 435 nm in soln. contg. 0.05 mol L^{-1} formate, 10^{-3} mol L^{-1} phosphate; 1,10-phenanthroline/Cu^{2+} concn. = 2.0–2.5. k(catalytic) = $(5.1 \pm 0.9) \times 10^8$.	83A299
40	**Tetrakis(4-*N*-methylpyridyl)porphinecopper(II) ion**					
	$HO_2/O_2^- + CuTMpyP^{4+} \rightarrow$	5.6	$\leqslant 6 \times 10^5$	p.r., opt.	D.k. at 254 nm in soln. contg. 5×10^{-3} mol L^{-1} Na formate and 2×10^{-3} mol L^{-1} phosphate buffer.	82A319
		8.0	$\leqslant 7 \times 10^4$			
41	**Tetrakis-4-(*N,N,N*-trimethylammonio)phenylporphinecopper(II) ion**					
	$HO_2/O_2^- + CuTAPP^{4+} \rightarrow$	5.6	$\leqslant 5 \times 10^6$	p.r., opt.	D.k. at 254 nm in soln. contg. 5×10^{-3} mol L^{-1} Na formate and 2×10^{-3} mol L^{-1} phosphate buffer.	82A319
		8.0	$\leqslant 1 \times 10^6$			
			$< 10^5$		Method (enz. or p.r.) and pH not given; k = k(catalytic); reaction in 0.5 mol L^{-1} carbonate buffer.	82R172
42	**Tetrakis(*p*-sulfonatophenyl)porphinatocuprate(II) ion**					
	$HO_2/O_2^- + CuTPPS^{4-} \rightarrow$	5.6	$\leqslant 8 \times 10^5$	p.r., opt.	D.k. at 254 nm in soln. contg. 5×10^{-3} mol L^{-1} Na formate and 2×10^{-3} mol L^{-1} phosphate buffer.	82A319
		8.0	$\leqslant 5 \times 10^4$			
43	**Formatocopper(II) ion**					
	$O_2^- + Cu(HCO_2)^+ \rightarrow O_2 + Cu(HCO_2)$		$(1.7 \pm 0.6) \times 10^9$	p.r., opt.	D.k. at 248 nm in soln. contg. 10^{-4} mol L^{-1} Cu(II) and $> 10^{-3}$ mol L^{-1} HCO_2^-; $I = 2$; pH not given but probably pH 6–7.	761021

TABLE 3. Rate constants for reactions of HO_2/O_2^- in aqueous solutions — Continued

No.	Reaction	pH	k (L mol^{-1}s^{-1})	Method	Comment	Ref.
44	**Copper(II) formate** $O_2^- + Cu(HCO_2)_2 \rightarrow$		3×10^8	p.r., opt.	D.k. at 248 nm; correct to a factor of 2; calculated using stability constants; $I = 2$; pH not given but probably pH 6–7.	761021
45	**Trisformatocuprate(II) ion** $O_2^- + Cu(HCO_2)_3^- \rightarrow$		8.0×10^8	p.r., opt.	D.k. at 248 nm; correct to a factor of 2; calculated using stability constants; $I = 2$; pH not given but probably pH 6–7.	761021
46	**Tetrakisformatocuprate(II) ion** $O_2^- + Cu(HCO_2)_4^{2-} \rightarrow$		$(4.0 \pm 1.5) \times 10^8$	p.r., opt.	D.k. at 248 nm; calcd. using stability constants; $I = 2$; pH not given but probably pH 6–7.	761021
47	**Bis(2-pyridinecarboxylato)copper(II)** $HO_2/O_2^- + Cu(2\text{-}pyCO_2)_2 \rightarrow$		2×10^6	enz., opt.	D.k. at 250 nm (p.r.) in N_2O/O_2 (4:1) satd. soln. contg. 0.1 mol L^{-1} formate gave k(catalytic) $= 1.4 \times 10^8$; pH not given, probably 8.5.	83A209
48	**DL-Alaninatocopper(II) ion** $HO_2/O_2^- + Cu(Ala)^+ \rightarrow$	7.4	$(2.8\text{–}3.5) \times 10^6$	p.r., opt.	D.k. at 280 nm in soln. contg. 10^{-2} mol L^{-1} alanine, 5×10^{-3} mol L^{-1} formate and $(1\text{–}3) \times 10^{-4}$ mol L^{-1} Cu^{2+}.	761021
49	**Alanylhistidinatocopper(II)** $O_2^- + Cu(AlaHis) \rightarrow$	8.0	$(8.75 \pm 0.41) \times 10^7$	p.r., opt.	D.k. at 245 nm (O_2^-); phosphate buffer.	82A448
50	**Glutamatocopper(II) ion** $HO_2/O_2^- + Cu(Glu)^+ \rightarrow$	7.1	$(1\text{–}2) \times 10^6$	p.r., opt.	D.k. at 280 nm in soln. contg. (1 or 3) $\times$ 10^{-4} mol L^{-1} Cu^{2+} and 0.1 mol L^{-1} glutamate.	761021
51	**Glycinatocopper(II) ion** $O_2^- + Cu(Gly)^+ \rightarrow$	7.9	2.1×10^6	p.r., opt.	D.k. at 280 nm in soln. contg. 5×10^{-3} mol L^{-1} formate and 2×10^{-3} mol L^{-1} glycine; $k = \sim 1 \times 10^6$ with 1 mol L^{-1} glycine at pH 6 (d.k. at 248 nm).	761021
		8.0	$(4.1 \pm 0.6) \times 10^6$	p.r., opt.	D.k. at 275 nm in N_2O–O_2–satd. soln. contg. 5×10^{-2} mol L^{-1} glycine and 10^{-4} mol L^{-1} $Cu(ClO_4)_2$; same when formate was added.	761082
52	**Glycylglycinatocopper(II) ion** $HO_2/O_2^- + Cu(GlyGly)^+ \rightarrow$	6.7	$(1.9\text{–}2.0) \times 10^7$	p.r., opt.	D.k. at 280 nm in soln. contg. $1\text{–}2 \times 10^{-4}$ mol L^{-1} Cu^{2+} and 10^{-2} mol L^{-1} glycylglycine.	761021
53	**Bis(glycylhistidinato)cuprate(II) ion** $O_2^- + Cu(GlyHis)_2^{2-} \rightarrow$	7.8	$(3.0 \pm 0.2) \times 10^8$	p.r., opt.	D.k. at 245 nm in O_2–satd. soln. contg. 10^{-3} mol L^{-1} Na formate and 10^{-5}–10^{-6} mol L^{-1} Cu^{2+}; k similar in presence of serum albumin.	741163
54	**Bis(glycylhistidylleucinato)cuprate(II) ion** $O_2^- + Cu(GlyHisLeu)_2^{2-} \rightarrow$	7.8	$(2.1 \pm 0.2) \times 10^8$	p.r., opt.	D.k. at 245 nm in O_2–satd. soln. contg. formate ion and $\sim 10^{-6}$ mol L^{-1} complex; k $= 1 \times 10^8$ in presence of bovine serum albumin. Concn. varied giving true pseudo first-order conditions.	75A243 741163

TABLE 3. Rate constants for reactions of HO_2/O_2^- in aqueous solutions — Continued

No.	Reaction	pH	k (L mol^{-1}s^{-1})	Method	Comment	Ref.
55	**Bis(histidinato)copper(II) ion, conjugate monoacid** $HO_2/O_2^- + Cu(His)_2H^+ \rightarrow$	2–7	$(3.4 + 0.9) \times 10^8$	p.r., opt.	D.k. at 250 nm in soln. contg. 0.1 mol L^{-1} formate, 4×10^{-4} mol L^{-1} histidine and $1\text{–}100 \times 10^{-6}$ mol L^{-1} Cu(II) acetate; $k = k_{catalytic}$.	80A175
56	**Histidylalaninatocopper(II)** $O_2^- + Cu(HisAla) \rightarrow$	8.0	$(4.52 \pm 0.34) \times 10^9$	p.r., opt.	D.k. at 245 nm (O_2^-); phosphate buffer.	82A448
57	**Histidylphenylalaninatocopper(II)** $O_2^- + Cu(HisPhe) \rightarrow$	8.0	$(3.57 \pm 0.38) \times 10^9$	p.r., opt.	D.k. at 245 nm (O_2^-); phosphate buffer.	82A448
58	**Histidyltyrosinatocopper(II)** $O_2^- + Cu(HisTyr) \rightarrow$	8.0	$(2.42 \pm 0.23) \times 10^9$	p.r., opt.	D.k. at 245 nm (O_2^-); phosphate buffer.	82A448
59	**Histidylvalinatocopper(II)** $O_2^- + Cu(HisVal) \rightarrow$	8.0	$(2.22 \pm 0.27) \times 10^9$	p.r., opt.	D.k. at 245 nm (O_2^-); phosphate buffer.	82A448
60	**L-Hydroxyprolinecopper(II) ion** $HO_2/O_2^- + Cu(Hyp)^+ \rightarrow$	8.1	1.2×10^6	p.r., opt.	D.k. at 270 nm in soln. contg. 5×10^{-3} mol L^{-1} formate, 2×10^{-3} mol L^{-1} hydroxyproline and 5×10^{-5} mol L^{-1} Cu^{2+}; $k = 1.0 \times 10^6$ with 10^{-4} mol L^{-1} Cu^{2+} and 9.0×10^5 with 10^{-4} mol L^{-1} Cu^{2+} and 10^{-2} mol L^{-1} hydroxyproline at pH 7.7.	761021
61	**Bis(lysinato)copper(II)** $O_2^- + Cu(Lys)_2 \rightarrow$	7.8	$(5.6 \pm 1) \times 10^8$	p.r., opt.	D.k. at 245 nm in O_2-satd. soln. contg. 10^{-3} mol L^{-1} Na formate and 10^{-5}–10^{-6} mol L^{-1} Cu^{2+}; k similar in presence of serum albumin.	741163
62	**L-Methioninatocopper(II) ion** $HO_2/O_2^- + Cu(Met)^+ \rightarrow$	7.1 7.8	5.6×10^6 6.8×10^6	p.r., opt.	D.k. at 280 nm in soln. contg. 5×10^{-2} mol L^{-1} methionine and 10^{-4} mol L^{-1} Cu^{2+}; at pH 7.8 $k = 8 \times 10^6$ with $[Cu^{2+}] = 2 \times 10^{-4}$ and at pH 7.1 $k = 4.8 \times 10^6$ with $[Cu^{2+}] = 3 \times 10^{-4}$ mol L^{-1}.	761021
63	**Phenylalanylhistidinatocopper(II)** $HO_2/O_2^- + Cu(PheHis) \rightarrow$	8.0	$(9.90 \pm 1.20) \times 10^4$	p.r., opt.	D.k. at 245 nm (O_2^-); phosphate buffer.	82A448
64	**L–Prolinatocopper(II) ion** $HO_2/O_2^- + Cu(Pro)^+ \rightarrow$	7.5	5×10^5	p.r., opt.	D.k. at 270 nm in soln. contg. 10^{-4} mol L^{-1} Cu^{2+} and 10^{-3} mol L^{-1} proline.	761021
65	**Bis(tyrosinato)copper(II)** $O_2^- + Cu(Tyr)_2 \rightarrow$	7.4–7.8	$(1.0 \pm 0.1) \times 10^9$	p.r., opt.	D.k. at 245 nm in O_2-satd. soln. contg. formate ion and $\sim 10^{-6}$ mol L^{-1} complex; same result in presence of 0.11 g L^{-1} bovine serum albumin.	75A243
66	**L-Valinatocopper(II) ion** $HO_2/O_2^- + Cu(Val)^+ \rightarrow$	6.2 8.1	2.4×10^8 1.7×10^6	p.r., opt.	D.k. at 280 nm in soln. contg. 10^{-4} mol L^{-1} Cu^{2+} and 0.5×10^{-3} (pH 8.1) or 10^{-2} mol L^{-1} (pH 6.2) valine.	761021
67	**Valylhistidinatocopper(II)** $HO_2/O_2^- + Cu(ValHis) \rightarrow$	8.0	$(1.01 \pm 0.16) \times 10^5$	p.r., opt.	D.k. at 245 nm (O_2^-); phosphate buffer.	82A448

TABLE 3. Rate constants for reactions of HO_2/O_2 in aqueous solutions — Continued

No.	Reaction	pH	k (L mol^{-1}s^{-1})	Method	Comment	Ref.
68	**Ethylenediaminetetraacetatocuprate(II) ion**					
	$O_2^- + CuEDTA^{2-} \rightarrow$	6.8–9.8	$<10^5$	p.r., opt.	Soln. cont. 2×10^{-8} mol L^{-1} Cu^{2+}, 10^{-6} mol L^{-1} EDTA.	82A281
69	**Bis(salicylato)copper(II)**					
	$O_2^- + Cu(Sal)_2 \rightarrow$	7.5	$(1.64 \pm 0.15) \times 10^9$	p.r., opt.	D.k. at 250 nm in O_2-satd. soln. contg. formate and $1–5 \times 10^{-6}$ mol L^{-1} Cu^{II}.	78A309
70	**Bis(diisopropylsalicylato)copper(II)**					
	$O_2^- + Cu(2\text{-}PrSal)_2 \rightarrow$	7.5	$(2.4 \pm 0.12) \times 10^9$	p.r., opt.	D.k. at 250 nm in O_2-satd. soln. contg. formate and $2.2–5.4 \times 10^{-6}$ mol L^{-1} Cu^{II}.	78A309
71	**Bis(acetylsalicylato)copper(II)**					
	$O_2^- + Cu(AcSal)_2 \rightarrow$	7.5	$(0.96 \pm 0.20) \times 10^9$	p.r., opt.	D.k. at 250 nm in O_2—satd. soln. contg. formate and $1.1–8.4 \times 10^{-6}$ mol L^{-1} Cu^{II}.	78A309
72	**Bis(*p*-aminosalicylato)copper(II)**					
	$O_2^- + Cu(NH_2Sal)_2 \rightarrow$	7.5	$(0.79 \pm 0.16) \times 10^9$	p.r., opt.	D.k. at 250 nm in O_2-satd. soln. contg. formate and $2–10 \times 10^{-6}$ mol L^{-1} Cu^{II}.	78A309
73	**Bis[copper(2-[2-(pyridyl)ethyliminomethyl]pyridine)]imidazole bridged complex**					
	$O_2^- + Cu(pip)ImCu(pip)^{3+} \rightarrow$	~8	$(1.7 \pm 1) \times 10^8$	p.r., opt.	D.k. at 250 nm in soln. contg. 10^{-2} mol L^{-1} formate.	81A430
74	**Copper(2-[2-(pyridyl)ethyliminomethyl]pyridine) zinc(2-[2-(pyridyl)ethyliminomethyl]pyridine) imidazole bridged complex**					
	$O_2^- + Cu(pip)ImZn(pip)^{3+} \rightarrow$	~8	$(5.9 \pm 1.0) \times 10^8$	p.r., opt.	D.k. at 250 nm in soln. contg. 10^{-2} mol L^{-1} formate	81A430
75	**Penicillaminecopper complex**					
	$HO_2/O_2^- + Cu_{14}(Pen)_{12}Cl^{5-} \rightarrow$	7.0	$(4.5 \pm 0.5) \times 10^8$	p.r., opt.	D.k. at 250 nm in O_2-satd. soln. contg. 10^{-2} mol L^{-1} formate and 10^{-6}–10^{-5} mol L^{-1} penicillamine.	79A072
		3.1	$(9.2 \pm 1.5) \times 10^8$	p.r., opt.	D.k. in soln. contg. 0.05 mol L^{-1} formate and 0.91–9.1 $\times 10^{-6}$ mol L^{-1} Cu penicillamine.	79A455
		5.0	$(3.15 \pm 0.82) \times 10^9$			
		7.0	$(6.8 \pm 1.5) \times 10^8$			
		8.9	$(5.1 \pm 0.6) \times 10^8$			
			4.2×10^8		1:1 in EDTA ($k = 1.1 \times 10^8$ in 1:10 EDTA, ten-fold excess of EDTA); $k = 7.8 \times 10^8$ in 1:1 KCN ($k = 8.2 \times 10^7$ in 1:10 KCN, ten-fold excess of KCN); conditions and pH not given.	81R192
			See comment.		$[Cu^I_8Cu^{II}_6(D\text{-penicillamine})_{12}Cl]^{5-}$ does not catalyze O_2^- dismutation but rather decomposes to simpler Cu complexes which are active.	80R189
	$O_2^- + Cu_{14}(Pen)_{12}Cl^{5-} \rightarrow$	3–9	2.0×10^8	p.r., opt.	D.k. (see 79A072, 79R055) in presence of 10^{-8}–10^{-6} mol L^{-1} Cu complex; reaction thought to involve sulfur: $Cu(I)\dot{S}R + O_2^- \rightarrow Cu(I)^-SR + O_2$ and $Cu(I)^-SR + O_2^- \rightarrow Cu(II)\dot{S}R + O_2^{2-}$. Slight variation in k_{obs} with pH.	80Z241
			$(1.54 \pm 0.5) \times 10^9$	p.r., opt.	D.k. Refer to [79A072] for experimental details.	79R055
76	**Copper indomethacin**		3.2×10^9		1:1 in EDTA ($k < 10^7$ in 1:10 EDTA, ten-fold excess of EDTA); $k = 4.1 \times 10^9$ in 1:1 KCN ($k < 10^7$ in 1:10 KCN, ten-fold excess of KCN); conditions and pH not given.	81R192
	$HO_2/O_2^- + Cu_2I_4 \rightarrow$					
	$O_2^- + Cu_2I_4 \rightarrow$	7.0	$(6.0 \pm 0.3) \times 10^9$	p.r., opt.	D.k. at 250 nm in soln. contg. 10^{-2} mol L^{-1} formate; in 50/50 (v/v) acetonitrile-water $k = (1.1 \pm 0.4) \times 10^9$.	80A201
		6.6	6×10^9	p.r., opt.	D.k. in soln. contg. 0.05 mol L^{-1} formate and 9.8–83 $\times 10^{-8}$ mol L^{-1} Cu indomethacin.	79A455

TABLE 3. Rate constants for reactions of HO_2/O_2^- in aqueous solutions — Continued

No.	Reaction	pH	k (L mol^{-1}s^{-1})	Method	Comment	Ref.
77	**Iron(II) ion**					
	$HO_2 + Fe^{2+} \rightarrow Fe^{3+}\cdot HO_2^-$	1	$(1.2 \pm 0.5) \times 10^6$	p.r., opt.	P.b.k. at 250 nm at 25°C; $I = 1.0$; $k = 9.1 \times 10^5$ at 20°C; $E_a = 10.0 \pm 1.0$ kcal/mol (42 kJ/mol); supercedes [640090] and [690434].	730038
78	**Tris(1,10-phenanthroline)iron(II) ion**					
	$O_2^- + Fe(phen)_3^{3+} \rightarrow$	10.1	1×10^5	enz., opt.	C.k.; rel. to $k(O_2^- + NBT^{2+}) = 6 \times 10^4$.	79A018
79	**Bis(4,7-diphenyl-1,10-phenanthroline)iron(II) ion** *(Bathophenanthroline)*					
	$O_2^- + Fe(Ph_2phen)_2^{2+} \rightarrow$	7.0	$<2.8 \times 10^5$	p.r., opt.	D.k. at 310 nm in 0.1 mol L^{-1} Na formate contg. 10^{-1} mol L^{-1} phosphate buffer.	82A449
80	**Dicyanotetrakis(4-*N*-methylpyridyl)porphineiron(II) ion**					
	$O_2^- + FeTMpyP(CN)_2^{3+} \rightarrow O_2 + FeTMpyP(CN)_2^{3+}$	10.2	$(3.1 \pm 0.6) \times 10^6$	p.r., opt.	Calcd. from equil. concn. formed in O_2-satd. soln. of Fe^{III} complex and reduced (Fe^{II}) complex; $k_{obs} = (1.7 \pm 0.3) \times 10^6$ in presence of formate.	82A119
81	**Tetrakis(4-*N*-methylpyridyl)porphineiron(II)-diimidazole complex**					
	$HO_2/O_2^- + FeTMpyP(Im)_2^{4+} \rightarrow OH^- + H_2O_2 + FeTMpyP(Im)_2^{5+}$		$(3.8 \pm 0.7) \times 10^6$	p.r., opt.	P.b.k. Measured in absence of formate. k in presence of formate = $(1.3 \pm 0.6) \times 10^6$. Probably pH 8.0.	82A119
82	**Tetrakis(4-*N*-methylpyridyl)porphineiron(II)-dihistidine complex**					
	$HO_2/O_2^- + FeTMpyP(His)_2^{4+} \rightarrow OH^- + H_2O_2 + FeTMpyP(His)_2^{5+}$		$(3.1 \pm 0.5) \times 10^6$	p.r., opt.	P.b.k. Measured in absence of formate. k in presence of formate = $(1.7 \pm 0.3) \times 10^6$. Probably pH 8.0.	82A119
83	**Ferrocyanide ion**					
	$HO_2 + Fe(CN)_6^{4-} \rightarrow Fe(CN)_6^{3-} + HO_2^-$	0.46–4.37	$(3.0 \pm 1.5) \times 10^4$	p.r., opt.	P.b.k. at 420–460 nm; pH effects obs.	720431
		~2	1.64×10^5	p.r., opt.	P.b.k. at 420 nm (ferricyanide). Soln. cont. 5×10^{-3} mol L^{-1} ferrocyanide.	650007
84	**Potassium hexacyanoferrate(II) ion**					
	$HO_2 + KFe(CN)_6^{3-} \rightarrow$	0–6.5	$(3.0 \pm 1.5) \times 10^4$	p.r., opt.	P.b.k. at 420 nm.	720431
85	**Hydrogen hexacyanoferrate(II) ion**					
	$HO_2 + HFe(CN)_6^{3-} \rightarrow$	0.46–4.37	$(1.4 \pm 0.1) \times 10^5$	p.r., opt.	P.b.k. at 420–460 nm.	720431
86	**Dihydrogen hexacyanoferrate(II) ion**					
	$HO_2 + H_2Fe(CN)_6^{2-} \rightarrow$	0.46–4.37	$(1.0 \pm 0.3) \times 10^4$	p.r., opt.	P.b.k. at 420–460 nm.	720431
87	**Ethylenediaminetetraacetatoferrate(II) ion**					
	$O_2^- + FeEDTA^{2-} \rightarrow Fe(O_2)EDTA^{3-}$	10.4	$\sim 8 \times 10^6$	s.f., opt.	P.b.k. at 520 nm; soln. cont. 10^{-6} mol L^{-1} complex; $I = 1$.	83A163
		10.4	$(3 \pm 0.3) \times 10^6$	p.r., opt.	P.b.k. at 310–350 nm in soln. contg. 0.1 mol L^{-1} Na formate.	82A449
		7.8	2×10^6	p.r., opt.	D.k. at 250 nm.	82A446
		10.1	3×10^5	enz., opt.	C.k.; rel. to $k(O_2^- + NBT^{2+}) = 6 \times 10^4$.	79A018
		9.7	4×10^5	enz, opt.	C.k.; rel. to $k(O_2^- + NBT^{2+}) = 6 \times 10^4$, in 0.05 mol L^{-1} borate buffer. Obs. increase in absorbance at 560 nm ($NBT^{2+} \rightarrow$ formazan); O_2^- produced in xanthine/xanthine oxidase system contg. catalase.	79R111
		9–10	$(2 \pm 0.3) \times 10^6$	p.r., opt.	P.b.k. at 300 nm in air-satd. soln. contg. 10^{-2} mol L^{-1} Na formate and 0.5–2 $\times 10^{-3}$ mol L^{-1} carbonate buffer; at pH 11–12 k is 50% higher; above pH 9 the substrate is a hydroxo complex.	771088

TABLE 3. Rate constants for reactions of HO_2/O_2^- in aqueous solutions — Continued

No.	Reaction	pH	k (L mol^{-1}s^{-1})	Method	Comment	Ref.
88	**Diethylenetriaminepentaacetatoferrate(II) ion** *(Detapac Fe^{2+})*					
	$O_2^- + FeDTPA^{3-} \rightarrow$	7.0	$(2 \pm 0.5) \times 10^7$	p.r., opt.	P.b.k. at 310 nm in 0.1 mol L^{-1} Na formate contg. 10^{-1} mol L^{-1} phosphate buffer.	82A449
		10.1	1×10^5	enz., opt.	C.k.; rel. to $k(O_2^- + NBT^{2+}) = 6 \times 10^4$.	79A018
89	**Adenosine triphosphate-iron(II) complex**					
	$O_2^- + Fe^{II}ATP \rightarrow$	7.0	$(1.1 \pm 0.1) \times 10^6$	p.r., opt.	P.b.k. at 310 nm in 0.1 mol L^{-1} Na formate contg. 10^{-1} mol L^{-1} phosphate buffer.	82A449
90	**Iron(III) ions**					
	$HO_2 + Fe^{3+} \rightarrow H^+ + Fe^{2+} + O_2$	1.51	2×10^4	p.r., opt.	In H_2SO_4 soln.; calcd. rel. to $k(HO_2 + Fe^{2+}) = 1 \times 10^6$; in $HClO_4$ soln. $k = 2.1 \times 10^5$ and 1.0×10^6, resp. at pH 1.51 and 2.74.	690413
		2.74	3.1×10^5			
		1	$\sim 4 \times 10^5$	γ-r., chem.	C.k. using $k(HO_2 + Fe^{2+})/k(HO_2 + Fe^{3+}) = 30[H^+]$ from data in [730038].	690642
			6.6×10^3	γ-r., chem.	C.k.; calcd. using data from [730038]; rel. to $HO_2 + Fe^{2+} = 1.2 \times 10^6$; 0.25 mol L^{-1} H_2SO_4.	600102
		2.1	1.2×10^5	γ-r., chem.	C.k.; calcd. using data from [730038]; rel. to $HO_2 + Fe^{2+} = 1.2 \times 10^6$.	580004
		0.4	$< 1.2 \times 10^4$			
		2.7	3.6×10^5	γ-r., chem.	C.k.; calcd. using data from [730038]; rel. to $HO_2 + Fe^{2+} = 1.2 \times 10^6$.	570010
		2.0	1.32×10^5			
91	**Bis(4,7-diphenyl-1,10-phenanthrolineiron(III) ion**					
	$O_2^- + Fe(Ph_2phen)_2^{3+} \rightarrow$	7.0	$< 4 \times 10^4$	p.r., opt.	D.k. at 300–320 nm in 0.1 mol L^{-1} Na formate contg. 10^{-1} mol L^{-1} phosphate buffer.	82A449
92	**Tetrakis(4-*N*-methylpyridyl)porphineiron(III) ion**					
	$O_2^- + FeTMpyP^{5+} \rightarrow$ $[FeTMpyP\text{-}O_2]^{4+}$	5.6	$(1.7 \pm 0.2) \times 10^9$	p.r., opt.	D.k. at 420 as well as p.b.k. at 445 nm in O_2-satd. soln. contg. 0.1 mol L^{-1} *tert*-BuOH; $k_{obs} = 3.8 \times 10^8$ at pH 8.0 and 3.1×10^8 at pH 5.6 in the presence of 0.1 mol L^{-1} formate; at pH 10.1 in soln. contg. 0.05 mol L^{-1} carbonate $k = (3.9 \pm 0.4) \times 10^8$.	82A119
		8.0	$(2 \pm 0.2) \times 10^9$ (cor. for I)			
		5.6	$(2.2 \pm 0.2) \times 10^8$	p.r., opt.	D.k. at 254 nm in soln. contg. 5×10^{-3} mol L^{-1} Na formate and 2×10^{-3} mol L^{-1} phosphate buffer.	82A319
		8.0	$(3.0 \pm 0.3) \times 10^8$			
		7.8	$\sim (7 \pm 2) \times 10^8$	p.r., opt.	D.k. at 350 nm (also obs. at 580 nm) indicated different product from e_{aq}^- or CO_2^- reaction, interpreted as adduct formn.; obs. rate includes aggregates of Fe complex.	81A207
		7.8	$\sim 3 \times 10^7$	p.r., opt.	D.k. at 280 and 296 nm in O_2-satd. soln. contg. 10^{-3} mol L^{-1} phosphate buffer, 5×10^{-3} mol L^{-1} formate and 2×10^{-4} mol L^{-1} EDTA.	81A207
		10.1	3×10^7	enz., opt.	C.k.; rel. to $k(O_2^- + NBT^{2+}) = 6 \times 10^4$; obs. decrease in redn. of nitro blue tetrazolium to formazan at 560 nm; biphasic, $k = 2 \times 10^6$ in phase II.	79A018
		9.7	1×10^7	enz, opt.	C.k.; rel. to $k(O_2^- + NBT^{2+}) = 6 \times 10^4$, in 0.05 mol L^{-1} borate buffer at pH 9.7 (0.05 mol L^{-1} carbonate buffer at pH 10.1). Obs. increase in absorbance at 560 nm ($NBT^{2+} \rightarrow$ formazan); O_2^- produced in xanthine/xanthine oxidase system contg. catalase; imidazole complex had similar reactivity.	79R111
		10.1	3×10^7			
93	**Tetrakis(4-*N*-methylpyridyl)porphineiron(III)-superoxide complex**					
	$O_2^- + [FeTMpyP\text{-}O_2]^{4+} \rightarrow OH^- + OH^- + FeTMpyP^{5+} + H_2O_2$	8.1	$(2.3 \pm 0.3) \times 10^9$	p.r., opt.	Calcd. from equil. concn. formed in O_2-satd. soln. of Fe^{III} complex and O_2^- adduct ($I = 10^{-3}$); in presence of formate $k = (7.6 \pm 1.0) \times 10^8$.	82A119

TABLE 3. Rate constants for reactions of HO_2/O_2^- in aqueous solutions — Continued

No.	Reaction	pH	k (L mol^{-1}s^{-1})	Method	Comment	Ref.
94	**Dicyanotetrakis(4-*N*-methylpyridyl)porphineiron(III) ion**					
	$O_2^- + FeTMpyP(CN)_2^{3+} \rightarrow FeTMpyP(CN)_2^{2+} + O_2$	10.2	$(2.0 \pm 0.2) \times 10^6$	p.r., opt.	D.k. as 435 as well as p.b.k. at 470 nm in soln. contg. 2.0×10^{-3} mol L^{-1} KCN and $1\text{–}5 \times 10^{-5}$ mol L^{-1} Fe^{III} complex.	82A119
95	**Tetraakis(4-*N*-methylpyridyl)porphineiron(III)-diimidazole complex**					
	$O_2^- + FeTMpyP(Im)_2^{5+} \rightarrow FeTMpyP(Im)_2^{4+} + O_2$	8.0	$(1.0 \pm 0.1) \times 10^6$	p.r., opt.	P.b.k at 450 nm in O_2-satd. soln. contg. $1\text{–}2.5 \times 10^{-5}$ mol L^{-1} Fe^{III} TMpyP and 4×10^{-2} mol L^{-1} imidazole and 0.5 mol L^{-1} formate.	82A119
		9.7	9×10^5	enz., opt.	C.k. in 0.05 mol L^{-1} borate buffer; rel. to $k(O_2^- + NBT^{2+}) = 6 \times 10^4$.	79R111
96	**Tetrakis(4-*N*-methylpyridyl)porphineiron(III)-dihistidine complex**					
	$HO_2/O_2^- + FeTMpyP(His)_2^{5+} \rightarrow FeTMpyP(His)_2^{4+} + O_2$	8.0	$(1.2 \pm 0.1) \times 10^6$	p.r., opt.	P.b.k.	82A119
97	**Tetrakis-4-(*N,N,N*-trimethylammonio)phenylporphineiron(III) ion**					
	$HO_2/O_2^- + FeTAPP^{5+} \rightarrow$		See comment		Method (enz. or p.r.) or pH not given; k(catalytic) $= 5 \times 10^5$; reaction in 0.5 mol L^{-1} carbonate buffer.	82R172
98	**Tetrakis(*p*-sulfonatophenyl)porphineferrate(III) ion**					
	$HO_2/O_2^- + FeTPPS^{3-} \rightarrow$	5.6	$(8 \pm 0.8) \times 10^6$	p.r., opt.	D.k. at 254 nm in soln. contg. 5×10^{-3} mol L^{-1} Na formate and 2×10^{-3} mol L^{-1} phosphate buffer and 0.1 mol L^{-1} NaCl.	82A319
		8.0	$(1.2 \pm 0.1) \times 10^6$			
	$O_2^- + FeTPPS^{3-} \rightarrow$	9.7	4×10^5	enz, opt.	C.k.; rel. to $k(O_2^- + NBT^{2+}) = 6 \times 10^4$, in 0.05 mol L^{-1} borate buffer at pH 9.7 (0.05 mol L^{-1} carbonate buffer at pH 10.1). Obs. increase in absorbance at 560 nm ($NBT^{2+} \rightarrow$ formazan); O_2^- produced in xanthine/xanthine oxidase system contg. catalase; BSA and imidazole complexes had similar reactivity.	79R111
		10.1	6×10^5			
99	**Tetrakis(*p*-sulfonatophenyl)porphineferrate(III)-diimidazole complex**					
	$O_2^- + FeTPPS(Im)_2^{3-} \rightarrow$	9.7	3×10^5	enz.	C.k. in 0.05 mol L^{-1} borate buffer; rel. to $k(O_2^- + NBT^{2+}) = 6 \times 10^4$.	79R111
100	**Tetrakis(*p*-sulfonatophenyl)porphineferrate(III)-bovine serum albumin complex**					
	$O_2^- + FeTPPS(BSA)^{5-} \rightarrow$	9.7	5×10^5	enz.	C.k. in 0.05 mol L^{-1} borate buffer (in carbonate buffer at pH 10.1); rel. to $k(O_2^- + NDT^{2+}) = 6 \times 10^4$	79R111
		10.1	6×10^5			
101	**Ferricyanide ion**					
	$O_2^- + Fe(CN)_6^{3-} \rightarrow O_2 + Fe(CN)_6^{4-}$	9.5–9.7	$(2.7 \pm 0.9) \times 10^2$ (cor. for I)	p.r., opt.	P.b.k. at 420–440 nm.	720431
102	**Potassium hexacyanoferrate(III) ion**					
	$O_2^- + KFe(CN)_6^{2-} \rightarrow KFe(CN)_6^{3-} + O_2$	9.5–9.7	$(6.2 \pm 0.6) \times 10^3$ (cor. for I)	p.r., opt.	P.b.k. at 420–440 nm.	720431
103	**Hydroxybis(2-pyridinecarboxylato)iron(III)**					
	$HO_2/O_2^- + Fe(2\text{-}pyCO_2)_2OH \rightarrow$	8.5	See comment	p.r., opt.	D.k. at 250 nm in N_2O/O_2 (4:1) satd. soln. contg. 0.1 mol L^{-1} formate; k(catalytic) $= 9.3 \times 10^4$.	83A209
104	***N*-Hydroxyethylenediaminetriacetatoferrate(III)**					
	$HO_2/O_2^- + FeHETA \rightarrow$	6.0	3.8×10^6	p.r., opt.	D.k. at 250 nm (O_2^-) as well as 280–300 nm (Fe^{III}) in O_2-satd. soln. contg. 0.02 mol L^{-1} formate ion, 5×10^{-3} mol L^{-1} phosphate buffer and 10^{-4} mol L^{-1} complex.	83A158
		7.0	7.6×10^5			

TABLE 3. Rate constants for reactions of HO_2/O_2^- in aqueous solutions — Continued

No.	Reaction	pH	k (L mol^{-1}s^{-1})	Method	Comment	Ref.
105	**Ethylenediaminetetraacetatoferrate(III) ion**					
	$O_2^- + FeEDTA^- \rightarrow$ $FeEDTA^{2-} + O_2$		2×10^6	s.f., opt.	P.b.k at 520 nm, data taken above pH 9.5 and compared with earlier data at a variety of ionic strengths and pH to give $k = 2 \times 10^6[H^+]/[H^+] + K_a$ assuming that $FeEDTA(OH)^{3-}$ is unreactive (pK_a for $FeEDTA(H_2O)^{2-} = 7.6$). Velocity increases with ionic strength. At pH 10.4 and $I = 1$ $k \approx 8 \times 10^6$.	83A163
		6.0	3.1×10^6	p.r., opt.	D.k. at 250 nm (O_2^-) as well as 280–300 nm (Fe^{III}) in O_2-satd. soln. contg. 0.02 mol L^{-1} formate ion, 5×10^{-3} mol L^{-1} phosphate buffer and 10^{-4} mol L^{-1} complex.	83A158
		7.0	1.9×10^6			
		8.0	5.0×10^5			
		5.65	$(6.2 \pm 1.0) \times 10^6$	p.r., opt.	D.k. at 310–340 nm in O_2-satd. soln. contg. 0.1 mol L^{-1} Na formate and 1–20 $\times 10^{-4}$ mol L^{-1} chelate.	82A449
		6.0	$(3.6 \pm 0.3) \times 10^6$			
		6.5	$(1.8 \pm 0.2) \times 10^6$			
		6.75	$(1.5 \pm 0.12) \times 10^6$			
		7.0	$(1.3 \pm 0.15) \times 10^6$			
		7.5	$(8 \pm 1) \times 10^5$			
		7.6	$(7 \pm 0.8) \times 10^5$			
		7.75	$(5 \pm 0.05) \times 10^5$			
		8.0	$(3 \pm 0.5) \times 10^5$			
		8.5	$(2 \pm 0.5) \times 10^5$			
		9.0	<0.1			
		9.5	<0.1			
		10.0	<0.1			
		8.4	1.5×10^5	p.r., opt.	D.k. at 250 nm (O_2^-) in O_2-satd. soln. contg. 0.1 mol L^{-1} EtOH, 1×10^{-4} mol L^{-1} EDTA.	82A446
		10.1	2×10^5	enz., opt.	C.k.; rel. to $k(O_2^- + NBT^{2+}) = 6 \times 10^4$.	79A018
		10.1	3×10^5	enz., opt.	C.k.; rel. to $k(O_2^- + NBT^{2+}) = 6 \times 10^4$; $k = 4 \times 10^5$ in borate buffer at pH 9.7.	79R111
		5.8	5×10^6	p.r., opt.	D.k. at 300 nm in O_2-satd. soln. contg. 10^{-4} mol L^{-1} complex, 10^{-2} mol L^{-1} Na formate and 2×10^{-3} mol L^{-1} phosphate buffer at pH 5.8–7.2. 10^{-3} mol L^{-1} borax buffer at pH 8.1 and 0.5–1 $\times 10^{-3}$ mol L^{-1} carbonate buffer at pH 9; above the pK at 7.6 the substrate is a hydroxo complex.	771088
		7	1.8×10^6			
		8.1	4.6×10^5			
		9	$\sim 10^5$			
106	**Diethylenetriaminepentaacetatoferrate(III) ion**					
	$HO_2/O_2^- + FeDTPA^{2-} \rightarrow$	6.0	$<10^4$	p.r., opt.	D.k. at 250 nm (O_2^-) as well as 280–300 nm (Fe^{III}) in O_2-satd. soln. contg. 0.02 mol L^{-1} formate ion, 5×10^{-3} mol L^{-1} phosphate buffer and 10^{-4} mol L^{-1} complex.	83A158
		7.0	$<10^4$			
		8.0	$<10^4$			
		7.0	$<10^5$	p.r., opt.	D.k. at 300–320 nm in 0.1 mol L^{-1} Na formate contg. 10^{-1} mol L^{-1} phosphate buffer.	82A449
	$O_5^- + FeDTPA^{2-} \rightarrow$	10.1	0.8×10^5	enz., opt.	C.k.; rel. to $k(O_2^- + NBT^{2+}) = 6 \times 10^4$.	79A018
107	**Adenosine triphosphate-iron(III) complex**					
	$HO_2/O_2^- + Fe^{III}ATP \rightarrow$	7.0	$<10^5$	p.r., opt.	D.k. at 300–320 nm in 0.1 mol L^{-1} Na formate contg. 10^{-1} mol L^{-1} phosphate buffer.	82A449
108	**Desferrioxamine B**					
	$HO_2/O_2^- + DB \rightarrow$	7.0	$<2 \times 10^5$	p.r., opt.	D.k. at 450–550 nm in 0.1 mol L^{-1} Na formate contg. 10^{-1} mol L^{-1} phosphate buffer.	82A449
109	**Hemin**					
	$HO_2/O_2^- + Fe^{3+}$ heme $\rightarrow$	9.7	$\sim 1 \times 10^4$	enz, opt.	C.k.; rel. to $k(O_2^- + NBT^{2+}) = 6 \times 10^4$, in 0.05 mol L^{-1} borate buffer. Obs. increase in absorbance at 560 nm ($NBT^{2+} \rightarrow$ formazan); O_2^- produced in xanthine/xanthine oxidase system contg. catalase; imidazole complex had similar reactivity.	79R111

TABLE 3. Rate constants for reactions of HO_2/O_2^- in aqueous solutions — Continued

No.	Reaction	pH	k (L mol^{-1}s^{-1})	Method	Comment	Ref.
110	**Hemin-diimidazole complex**					
	$O_2^- + Hemin(Im)_2 \rightarrow$	9.7	$\sim 3 \times 10^4$		C.k. in soln. contg. 0.05 mol L^{-1} borate buffer; rel. to $k(O_2^- + NBT^{2+}) = 6 \times 10^4$.	79R111
111	**Hydroxyprotoferrihaem dimer**					
	$HO_2/O_2^- +$ $H_2OFe^{III}porOFe^{III}porOH^{n-} \rightarrow$	9.2	$< 1.7 \times 10^3$	p.r., opt.	No reaction in soln. contg. 0.1 mol L^{-1} formate and O_2; $I = 0.1$. Limiting rate.	761071
112	**Hydrogen**					
	$HO_2/O_2^- + H_2 \rightarrow H + H_2O_2$	~ 2	< 1	phot.	Data fitting; soln. under 10–100 atm H_2.	767025
113	**Hydrogen ion**					
	$O_2^- + H^+ \rightarrow HO_2$	4	$(5 \pm 1) \times 10^{10}$	p.r., opt.	P.b.k. (and d.k.) at 270 nm in O_2-satd. soln. contg. 10^{-4} $HClO_4$; protonation reaction.	761132
		~ 2	7.2×10^{10}	phot.	Data fitting.	767025
			4.8×10^{10}	elec., pol.	D.k.	759347
114	**Iodine**					
	$HO_2/O_2^- + I_2 \rightarrow I_2^- + H^+ + O_2$	3.9	$\leqslant 1 \times 10^8$	p.r., opt.	P.b.k. at 410 nm, in air-satd. soln. contg. 0.4–1 $\times 10^{-4}$ mol L^{-1} I_2 and 0.3–2 $\times 10^{-2}$ mol L^{-1} formate ion.	83A901
	$O_2^- + I_2 \rightarrow I_2^- + O_2$	3.9–5.5	5.5×10^9	p.r., opt.	P.b.k. at 410 nm in air-satd. soln. contg. 0.4–1 $\times 10^{-4}$ mol L^{-1} I_2 and 0.3–2 $\times 10^{-2}$ mol L^{-1} formate ion.	83A901
115	**Triiodine ion**					
	$O_2^- + I_3^- \rightarrow I_2^- + I^- + O_2$	3.9–5.5	8×10^8	p.r., opt.	P.b.k. at 700 nm in air-satd. soln. contg. 5 $\times 10^{-3}$ mol L^{-1} I^-, 0.4–1 $\times 10^{-4}$ mol L^{-1} I_2 and 0.3–2 $\times 10^{-2}$ formate ion.	83A901
116	**Manganese(II) ions**					
	$HO_2/O_2^- + Mn^{2+} \rightarrow MnO_2^+$		$(1.1 \pm 0.2) \times 10^8$	p.r., opt.	P.b.k. at 275 nm in soln. contg. 0.01 mol L^{-1} formate and oxygen; $k = 7.0 \times 10^7$ at $I = 0.5$ ($NaClO_4$) and 3.2×10^7 in 0.5 mol L^{-1} formate, pH probably 6.7.	761109
117	**Manganese(II) pyrophosphate complex**					
	$HO_2/O_2^- + Mn(II) \rightarrow Mn(III) + H_2O_2$	1.1	1.31×10^6	p.r., opt.	P.b.k. at 260 nm in soln. contg. 10^{-2} mol L^{-1} Na pyrophosphate, 10^{-2} mol L^{-1} formate, 1.5–5 $\times 10^{-4}$ mol L^{-1} Mn(II); k varies from 3×10^5 to 4.4×10^7 with pH 0.14–7.18.	84A910
		6.5	2.6×10^7			
	$O_2^- + Mn(II) \rightarrow Mn(III) + H_2O_2$	7.3	1.3×10^7	p.r., opt.	10^{-4} mol L^{-1} $MnSO_4$, 10^{-4} mol L^{-1} pyrophosphate, 0.1 mol L^{-1} formate.	82A455
		7.8	$\sim 6 \times 10^6$	enz., opt.	P.b.k. at 258 nm; $\epsilon(Mn^{3+}) = 6 \times 10^3$ mol L^{-1} cm^{-1}; xanthine-xanthine oxidase system contg. 10^{-5} mol L^{-1} $MnCl_2$, 5×10^{-2} mol L^{-1} Na pyrophosphate and SOD, assuming $k(O_2^- + SOD) = 2.3 \times 10^9$.	76R190
118	**Manganese(II) sulfate**					
	$HO_2 + MnSO_4 \rightarrow Mn(O_2)SO_4^-$	2.7–3.4	$\sim 6 \times 10^6$	p.r., opt.	P.b.k. at 230–270 nm in soln. contg. 1–2 $\times 10^{-2}$ mol L^{-1} Mn^{2+}, 0.1 mol L^{-1} Na sulfate and 5–20 $\times 10^{-3}$ mol L^{-1} formate. Complex mechanism.	84A910
	$O_2^- + MnSO_4 \rightarrow Mn(O_2)SO_4^-$	5.1–5.6	5.2×10^7	p.r., opt.	P.b.k. at 270 nm in soln. contg. 1–5 $\times 10^{-3}$ mol L^{-1} Mn^{2+}, 0.1 mol L^{-1} Na sulfate and 1–2 $\times 10^{-3}$ mol L^{-1} formate.	84A910

TABLE 3. Rate constants for reactions of HO_2/O_2^- in aqueous solutions — Continued

No.	Reaction	pH	k (L mol^{-1}s^{-1})	Method	Comment	Ref.
119	**Manganese(II) formate**					
	$HO_2 + Mn(HCO_2)_2 \rightarrow Mn(O_2)(HCO_2)_2^-$	2.2–3.0	$\sim 6 \times 10^6$	p.r., opt.	P.b.k. at 260 nm, 3–18 $\times$ 10^{-3} mol L^{-1} Mn^{2+}, and 0.4 mol L^{-1} formate. Complex mechanism.	84A910
	$O_2^- + Mn(HCO_2)_2 \rightarrow Mn(O_2)(HCO_2)_2^-$	5.7–7.1	4.3×10^7	p.r., opt.	P.b.k. at 270 nm in soln. contg. 4.15 $\times$ 10^{-3} mol L^{-1} Mn^{2+} and 0.4 mol L^{-1} formate.	84A910
120	**Nitrilotriacetatomanganate(II) ion**					
	$HO_2/O_2^- + MnNTA^- \rightarrow$	4.5	4.0×10^8	p.r., opt.	P.b.k. at 350 and 470 nm.	78A436
		5.5	1.2×10^8			
121	**Ethylenediaminetetraacetatomanganate(II) ion**					
	$HO_2/O_2^- + MnEDTA^{2-} \rightarrow$	4.5	3.0×10^7	p.r., opt.	P.b.k. at 350 and 475 nm.	78A436
		5.5	7.5×10^6			
122	**Tetrakis(4-*N*-methylpyridyl)porphinemanganese(III) ion**					
	$O_2^- + MnTMpyP^{5+} \rightarrow$	5.6	$(5.1 \pm 0.5) \times 10^7$	p.r., opt.	D.k. at 254 nm in soln. contg. 5 $\times$ 10^{-3} mol L^{-1} Na formate and 2 $\times$ 10^{-3} mol L^{-1} phosphate buffer.	82A319
		8.0	$(4.0 \pm 0.4) \times 10^7$			
		10.1	2.2×10^7	enz	Beauchamp-Fridovich assay; rel. to Nitro Blue Tetrazolium conversion to formazan (NBT^{2+} rate not given).	81R125
123	**Tetrakis-4-(*N,N,N*-trimethylammonio)phenylporphinemanganese(III) ion**					
	$HO_2/O_2^- + MnTAPP^{5+} \rightarrow$	5.6	$(1.3 \pm 0.1) \times 10^7$	p.r., opt.	D.k. at 254 nm in soln. contg. 5 $\times$ 10^{-3} mol L^{-1} Na formate and 2 $\times$ 10^{-3} mol L^{-1} phosphate buffer.	82A319
		8.0	$(2.9 \pm 0.3) \times 10^6$			
	$O_2^- + MnTAPP^{5+} \rightarrow$		See comment		Method not given (enz. or p.r.), k(catalytic) = 3 $\times$ 10^6; pH not given, reaction in 0.5 mol L^{-1} carbonate buffer. Probably pH 8–10.	82R172
124	**Tetrakis(*p*-sulfonatophenyl)porphinatomanganate(III) ion**					
	$HO_2/O_2^- + MnTPPS^{3-} \rightarrow$	5.6	$\leqslant 6 \times 10^5$	p.r., opt.	D.k. at 254 nm in soln. contg. 5 $\times$ 10^{-3} mol L^{-1} Na formate and 2 $\times$ 10^{-3} mol L^{-1} phosphate buffer.	82A319
		8.0	$\leqslant 7 \times 10^4$			
125	**Ethylenediaminetetraacetatomanganate(III) ion**					
	$O_2^- + MnEDTA^- \rightarrow MnEDTA^{2-} + O_2$	10.0	$\sim (5 \pm 1) \times 10^4$	KO_2, s.f., opt.	D.k. at 500 nm (Mn^{III}); soln. contains $KMn^{III}EDTA$ which is probably a hydroxo species.	79A329
126	**1,2-Cyclohexanediaminetetraacetatomanganate(III) ion**					
	$HO_2/O_2^- + MnCyDTA^- \rightarrow O_2 + MnCyDTA^{2-}$		$\sim 1 \times 10^6$	KO_2, opt., s.f.	D.k. at 500 nm; pH not given explicitly.	79A329
127	**Permanganate ion**					
	$HO_2/O_2^- + MnO_4^- \rightarrow H^+ + MnO_4^{2-} + O_2$	2	8×10^6	p.r., opt.	D.k.	650385
128	**Octacyanomolybdate(IV) ion**					
	$HO_2/O_2^- + Mo(CN)_8^{4-} \rightarrow Mo(CN)_8^{3-} + H_2O_2$	2.0	$(5.7 \pm 0.6) \times 10^4$	p.r., opt.	P.b.k. at 385 nm in soln. contg. 0.3 mol L^{-1} formate and $HClO_4$ and O_2.	761140
129	**Octacyanomolybdate(V) ion**					
	$O_2^- + Mo(CN)_8^{3-} \rightarrow Mo(CN)_8^{4-} + O_2$	8.3–10.4	$(3.0 \pm 0.3) \times 10^5$	p.r., opt.	D.k. at 385 nm in soln. contg. O_2 and Mo(IV), Mo(V), and 5 $\times$ 10^{-3} mol L^{-1} $NaClO_4$.	761140
130	**Azide radical**					
	$O_2^- + \cdot N_3 \rightarrow N_3^- + O_2$		$(1.2 \pm 0.2) \times 10^{10}$	p.r., opt.	D.k. in O_2-satd. soln at 278 nm; cor. for $k(\cdot N_3 + \cdot N_3)$; pH not given explicitly, probably 8.5–10.8.	81A216

TABLE 3. Rate constants for reactions of HO_2/O_2^- in aqueous solutions — Continued

No.	Reaction	pH	k (L mol^{-1}s^{-1})	Method	Comment	Ref.
131	**Hydroxylamine, pK_a = 6**					
	$HO_2 + NH_2OH_2^+/NH_2OH \rightarrow$	1.1–10.5	<44	p.r., s.f., opt.	D.k. at 250–270 nm in soln. contg. 0.01–0.2 mol L^{-1} NH_2OH, 0.001–1 mol L^{-1} formate and EDTA; studied as a function of pH. See paper for limiting rates at all pH. Authors feel there is negligible reaction.	84A908
	$O_2^- + NH_2OH_2^+/NH_2OH \rightarrow$	1.1–10.5	<35	p.r., s.f., opt.	D.k. at 250–270 nm, 0.01–0.2 mol L^{-1} NH_2OH, 0.001–1 mol L^{-1} formate, EDTA; studied as a function of pH. See paper for limiting rates at all pH. Authors feel there is negligible reaction.	84A908
132	**Nitrogen dioxide**					
	$HO_2 + NO_2 \rightarrow HO_2NO_2$	1.85	4×10^9	p.r., opt.	Deduced from p.b.k. at 350 nm and d.k. of transient (nitroform) in soln. contg. oxygen, formic acid and tetranitromethane; reverse reaction is interpreted to have k = 0.014 ± 0.002 s^{-1}.	750347
133	**Nitrite ion**					
	$HO_2/O_2^- + NO_2^- \rightarrow NO_2^{2-} + O_2$		5×10^6	γ-r.	Obs. $G(NF^-)$ in soln. contg. tetranitromethane.	750403
134	**5,7,7,12,12,14-Hexamethyl-1,4,8,11-tetraazacyclotetradecanenickel(II) ion**					
	$HO_2 + Ni(aneN_4)^{2+} \rightarrow H^+ + O_2 + Ni(aneN_4)^{3+}$	0.3	$(1.1 \pm 0.2) \times 10^7$	p.r., opt.	P.b.k. in soln. contg. H_2O_2 and 0.5 mol L^{-1} acid; acid catalyzed.	79A038
135	**Tetrakis(4-*N*-methylpyridyl)porphinenickel(II) ion**					
	$HO_2/O_2^- + NiTMpyP^{4+} \rightarrow$	5.6	$\leqslant 6 \times 10^5$	p.r., opt.	D.k. at 254 nm in soln. contg. 5×10^{-3} mol L^{-1} Na formate and 2×10^{-3} mol L^{-1} phosphate buffer.	82A319
		8.0	$\leqslant 8 \times 10^4$			
136	**Tetrakis-4-(*N,N,N*-trimethylammonio)phenylporphinenickel(II) ion**					
	$HO_2/O_2^- + NiTAPP^{4+} \rightarrow$	5.6	$\leqslant 8 \times 10^5$	p.r., opt.	D.k. at 254 nm in soln. contg. 5×10^{-3} mol L^{-1} Na formate and 2×10^{-3} mol L^{-1} phosphate buffer.	82A319
		8.0	$\leqslant 7 \times 10^4$			
137	**Tetrakis(*p*-sulfonatophenyl)porphinatonickelate(II) ion**					
	$HO_2/O_2^- + NiTPPS^{4-} \rightarrow$	5.6	$\leqslant 6 \times 10^5$	p.r., opt.	D.k. at 254 nm in soln. contg. 5×10^{-3} mol L^{-1} Na formate and 2×10^{-3} mol L^{-1} phosphate buffer.	82A319
		8.0	$\leqslant 7 \times 10^4$			
138	**5,7,7,12,12,14-Hexamethyl-1,4,8,11-tetraazacyclotetradecanenickel(III) ion**					
	$HO_2/O_2^- + Ni(aneN_4)^{3+} \rightarrow Ni(aneN_4)^{2+} + O_2$	2.0	$(1.0 \pm 0.2) \times 10^5$	p.r., opt.	D.k.	79A038
	$O_2^- + Ni(aneN_4)^{3+} \rightarrow Ni(aneN_4)^{2+} + O_2$	6.2	$(2.1 \pm 0.4) \times 10^9$	p.r., opt.	D.k.	79A038
139	**5,7,7,12,12,14-Hexamethyl-1,4,8,11-tetraazacyclotetradeca-4,11-dienenickel(III) ion**					
	$HO_2/O_2^- + Ni(4,11\text{-dieneN}_4)^{3+} \rightarrow Ni(4,11\text{-dieneN}_4)^{2+} + O_2$	2.0	$(1.6 \pm 0.3) \times 10^5$	p.r., opt.	D.k.	79A038
	$O_2^- + Ni(4,11\text{-dieneN}_4)^{3+} \rightarrow Ni(4,11\text{-dieneN}_4)^{2+} + O_2$	6.2	$(1.6 \pm 0.4) \times 10^9$	p.r., opt.	D.k.	79A038
140	**5,7,7,12,12,14-Hexamethyl-1,4,8,11-tetraazacyclotetradeca-1,4,8,11-tetraenenickel(III) ion**					
	$HO_2/O_2^- + Ni(1,4,8,11\text{-tetraeneN}_4)^{3+} \rightarrow O_2 + Ni(1,4,8,11\text{-tetraeneN}_4)^{2+}$	2.0	$(8.5 \pm 1.0) \times 10^5$	p.r., opt.	D.k.	79A038
	$O_2^- + Ni(1,4,8,11\text{-tetraeneN}_4)^{3+} \rightarrow O_2 + Ni(1,4,8,11\text{-tetraeneN}_4)^{2+}$	6.2	$(1.0 \pm 0.2) \times 10^9$	p.r., opt.	D.k.	79A038

TABLE 3. Rate constants for reactions of HO_2/O_2^- in aqueous solutions — Continued

No.	Reaction	pH	k (L mol^{-1}s^{-1})	Method	Comment	Ref.
141	**Hydroxyl**					
	$HO_2 + OH \rightarrow H_2O_3$	0.46–6.76	0.71×10^{10}	p.r., opt.	Calcd. from G values for oxygenated aqueous H_2O_2 with sulfuric and perchloric acid; product detn. in [630075].	680014
	$O_2^- + OH \rightarrow OH^- + O_2$	0.46–6.76	1.01×10^{10}	p.r., opt.	Calcd. from G values for oxygenated aqueous H_2O_2 with sulfuric and perchloric acid.	680014
142	**Oxygen ion(1−)**					
	$O_2^- + O^- \rightarrow OH^- + OH^- + O_2$	13–14	$(6.0 \pm 1.0) \times 10^8$	p.r., opt.	D.k. at 430 nm (O_3^-) as well simultaneous buildup at 250 nm (O_2^-) and decay, in soln. satd. with 4 MPa N_2O and 0–1 MPa O_2; computer simulation.	82A133
143	**Hydrogen peroxide**					
	$HO_2 + H_2O_2 \rightarrow OH + H_2O + O_2$	0.5–3.5	0.50 ± 0.09	γ-r., chem.	Obs. oxygen yield in 0.08–1.5 mol L^{-1} H_2O_2 soln.; pH independent rate.	79A001
		2.3	3.0 ± 0.6	γ-r., chem.	Calcd. from obs. decrease in $[H_2O_2]$ under 2 atm N_2 or O_2.	78A362
		~2	<5	phot.	Data fitting; soln. under 10–100 atm. H_2.	767025
		0.8–1.5	0.20 ± 0.01	γ-r., chem.	C.k.; obs. $G(-H_2O_2)$; includes $k(H_2O_2 + H_2O_2 \rightarrow H_3O^+ + O_2 + OH)$; rel. to $k(HO_2 + HO_2) = 1.1 \times 10^6$.	690643
		1	1×10^{-2}	γ-r., chem.	Mechanistic fit; k at 10°C; $[H_2O_2] \sim 1$–35 mol L^{-1}.	650046
	$HO_2/O_2^- + H_2O_2 \rightarrow OH + H_2O + O_2$	nat.	1.1	γ-r., chem.	k at O°C. no pH effects considered.	530014
		nat.	3.7 ± 1.6	phot., chem.	Propagation step in chain reaction; k at 25°C; no pH effects considered.	530014
	$O_2^- + H_2O_2 \rightarrow OH^- + OH + O_2$	7.0–9.9	0.13 ± 0.07	γ-r., chem.	Obs. O_2 yield as function of $[H_2O_2]$ in soln. contg. 0.08–1.5 mol L^{-1} H_2O_2; assumed values of radical combination rates and pK; pH independent rate.	79A001
		5.4–7.85	2.25 ± 0.20	γ-r., chem.	Obs. $G(-H_2O_2)$ vs dose rate or $[H_2O_2]$.	78A364
		9.6	$<0.23 \pm 0.09$	γ-r.	Anal. for hydroxylated products in soln. contg. 5×10^{-4} mol L^{-1} benzoate and H_2O_2.	78A389
		5.4–9.4	$<10^{-4}$	KO_2	No redn. of 7×10^{-3} mol L^{-1} p-nitrosodimethylaniline obs. (by OH formed in reaction). Limiting value.	779154
144	**Hydroperoxide ion**					
	$O_2^- + HO_2^- \rightarrow H_2O_2 + O_2$	8.9–12.7	<2	KO_2, opt.	D.k at ~250 nm.	769352
145	**Ozone**					
	$O_2^- + O_3 \rightarrow O_3^- + O_2$	8.4–10.3	$(1.52 \pm 0.05) \times 10^9$	p.r., opt.	P.b.k. at 430 nm in soln. contg. 0.025–0.1 mol L^{-1} HCO_3^-/CO_3^{2-} and $(0.41–1.71) \times 10^{-4}$ mol L^{-1} ozone.	83A117
146	**Osmium tetroxide**					
	$HO_2 + OsO_4 \rightarrow H^+ + O_2 + OsO_4^-$	<1	5.7×10^5	γ-r., chem.	C.k.; obs. $G(H_2O_2)$; dose rate 9.7×10^{18} eV cm^{-3}h^{-1}; rel. to $k(HO_2 + HO_2) = 2.35 \times 10^6$.	640050
147	**Pentaammine(isonicotinamide)ruthenium(II) ion**					
	$HO_2/O_2^- + Ru(NH_3)_5isn^{2+} \rightarrow HO_2^- + Ru(NH_3)_5isn^{3+}$	2.35	$(9.07 \pm 0.54) \times 10^6$	p.r., opt.	P.b.k. in soln. contg. 0.1 mol L^{-1} formic acid, k for third-order H^+ catalyzed reaction $<5.7 \times 10^6$ L^2 mol^{-2} s^{-1}.	80A317
148	**Pentaammine(isonicotinamide)ruthenium(III) ion**					
	$HO_2 + Ru(NH_3)_5isn^{3+} \rightarrow H^+ + Ru(NH_3)_5isn^{2+} + O_2$	3.3–4.9	$<2.0 \times 10^6$	p.r., opt.	P.b.k.; $I = 0.1$.	80A317
	$O_2^- + Ru(NH_3)_5isn^{3+} \rightarrow Ru(NH_3)_5isn^{2+} + O_2$	3.86–4.91	$(2.18 \pm 0.19) \times 10^8$	p.r., opt.	P.b.k. in O_2-satd. soln. contg. formate; $I = 0.1$	80A317

TABLE 3. Rate constants for reactions of HO_2/O_2^- in aqueous solutions — Continued

No.	Reaction	pH	k (L mol^{-1}s^{-1})	Method	Comment	Ref.
149	**Tris(2,2'-bipyridine)ruthenium(III) ion**					
	$HO_2 + Ru(bpy)_3^{3+} \rightarrow H^+ + Ru(bpy)_3^{3+} + O_2$	~1	$(1.25 \pm 0.1) \times 10^7$	f.p., opt.	D.k. at 450 nm in air-satd. soln. contg. 0.5 mol L^{-1} H_2SO_4.	82A198
150	**Sulfide ion**					
	$HO_2/O_2^- + S^{2-} \rightarrow$	7.8	1.5×10^6	enz., opt.	Xanthine-xanthine oxidase system; c.k., rel. to $k(HO_2/O_2^- + \text{adrenaline}) = 4 \times 10^4$.	76R183
151	**Sulfite ion**					
	$HO_2/O_2^- + SO_3^{2-} \rightarrow SO_3^- + OH^- + H_2O_2$	9.8	82	p.r., opt.	D.k. at 245 nm in aerated soln. contg. 3×10^{-3} mol L^{-1} sulfite ion and 0.3 mol L^{-1} formate ion; data fitting with $2k(O_2^- + O_2^-) = 2500$ and $\epsilon(O_2^-) = 2000$ L mol^{-1} cm^{-1}.	81G067
152	**Thiocyanogen**					
	$HO_2 + SCN \rightarrow H^+ + SCN^- + O_2$	1	1.6×10^9	p.r., opt.	C.k.; pH effect on decay $SCN + SCN \rightarrow (SCN)_2$.	650386
153	**Tellurate(IV) ion**					
	$HO_2 + TeO_3^{2-} \rightarrow TeO_3 + OH$	0.4	1.9×10^2	γ-r., chem.	C.k.; more than one rate involved in calcn.; rel. to $k(HO_2 + HO_2) = 2.5 \times 10^6$.	680356
154	**Thorium(IV) ion**					
	$HO_2 + Th^{4+} \rightarrow$ Th(IV)-HO_2	1	$(1.8 \pm 0.2) \times 10^6$	p.r., opt.	P.b.k.	741107
		~1	$\geqslant 5 \times 10^6$	esr	D.k. as well as p.b.k.; radical from Ce(IV)-H_2O_2.	739071
155	**Thorium(IV)-hydroperoxy complex**					
	$HO_2 +$ Th(IV)-$HO_2 \rightarrow Th^{4+} + H_2O_2 + O_2$	1	$(8.0 \pm 2.0) \times 10^5$	esr	Radical from Ce(IV)-H_2O_2; $k(\text{Th(IV)-}HO_2 \rightarrow \text{Th(IV)} + H_2O_2 + O_2) = (5 \pm 2) \times 10^2$.	739071
156	**Thallium(II) ion**					
	$HO_2 + Tl^{2+} \rightarrow H^+ + Tl^+ + O_2$	1	$(2.5 \pm 1) \times 10^9$	p.r., opt.	D.k. (Tl^{2+}); rel. to $k(Tl^{2+} + Tl^{2+}) = 2.3 \times 10^9$.	660097
157	**Uranyl(VI) ion**					
	$HO_2 + UO_2^{2+} \rightarrow$ UO_2-HO_2^{2+}	1	$(1.5 \pm 0.1) \times 10^5$	p.r., opt.	P.b.k. and d.k.	741107
		~1	$\geqslant 1 \times 10^5$	esr	D.k. as well as p.b.k.; radical from Ce(IV)-H_2O_2.	739071
158	**Dioxouranium(VI)-hydroperoxy complex**					
	$HO_2 +$ UO_2-$HO_2^{2+} \rightarrow UO_2^{2+} + H_2O_2 + O_2$		$(5 \pm 1) \times 10^5$	p.r., opt.	P.b.k. and d.k.; $k(UO_2^{2+}\text{-}HO_2 \rightarrow UO_2^{2+} + H_2O_2 + O_2) = (8 \pm 2) \times 10^4$.	741107
		~1	$(9.0 \pm 1.5) \times 10^5$	esr.	P.b.k. as well as d.k.	739071
159	**Oxoperoxyvanadium(IV) ion**					
	$HO_2/O_2^- + VO(O_2)^+ \rightarrow$		$(9.4 \pm 1) \times 10^4$	esr	Radical from Ce(IV)-H_2O_2; flow technique; 0.1 mol L^{-1} $HClO_4$ soln.; rel. to $k(HO_2 + HO_2) = 9 \times 10^5$.	709058
160	**Tetrakis(4-*N*-methylpyridyl)porphinatezinc(II) ion**					
	$HO_2/O_2^- + ZnTMpyP^{4+} \rightarrow$	5.6	$\leqslant 8 \times 10^5$	p.r., opt.	D.k. at 254 nm in soln. contg. 5×10^{-3} mol L^{-1} Na formate and 2×10^{-3} mol L^{-1} phosphate buffer.	82A319
		8.0	$\leqslant 7 \times 10^4$			
	$O_2^- + ZnTMpyP^{4+} \rightarrow$		See comment		Method not given (enz. or p.r.), k(catalytic) $\leqslant 10^5$; pH not given, reaction in 0.5 mol L^{-1} carbonate buffer.	82R172
161	**Tetrakis-4-(*N,N,N*-trimethylammonio)phenylporphinezinc(II) ion**					
	$HO_2/O_2^- + ZnTAPP^{4+} \rightarrow$	5.6	$\leqslant 8 \times 10^5$	p.r., opt.	D.k. at 254 nm in soln. contg. 5×10^{-3} mol L^{-1} Na formate and 2×10^{-3} mol L^{-1} phosphate buffer.	82A319
		8.0	$\leqslant 1 \times 10^5$			

TABLE 3. Rate constants for reactions of HO_2/O_2^- in aqueous solutions — Continued

No.	Reaction	pH	k (L mol^{-1}s^{-1})	Method	Comment	Ref.
162	**Tetrakis(*p*-sulfonatophenyl)porphinatozincate(II) ion**					
	$HO_2/O_2^- + ZnTPPS^{4-} \rightarrow$	5.6	$\leqslant 6 \times 10^5$	p.r., opt.	D.k. at 254 nm in soln. contg. 5×10^{-3} mol L^{-1} Na formate and 2×10^{-3} mol L^{-1} phosphate buffer.	82A319
		8.0	$\leqslant 7 \times 10^4$			
163	**Bis(2-pyridinecarboxylato)zinc(II)**					
	$HO_2/O_2^- + Zn(2\text{-}pyCO_2)_2 \rightarrow$			p.r., opt.	D.k. at 250 nm in N_2O/O_2 (4:1) satd. soln. contg. 0.1 mol L^{-1} formate; pH not given, probably 8.5; no reaction obs.	83A209
164	**Acetate ion**					
	$O_2^- + CH_3CO_2^- \rightarrow$	10.1	<0.06	*e*-r., s.f., opt.	D.k. at 250 nm in air-satd. soln. contg. 0.2 mol L^{-1} formate and 10^{-4} mol L^{-1} EDTA and 0.01–0.1 mol L^{-1} acetate; no reaction.	770046
165	**2-Acetylaminofluorene**					
	$HO_2/O_2^- +$ $C_{13}H_9NHCOCH_3 \rightarrow$		$\sim 3.5 \times 10^7$	p.r.	C.k. in soln. contg. 0.01 mol L^{-1} CTAB; rel. to $k(O_2^- + Q) = 9.5 \times 10^6$. pH not given.	78A367
166	**Acetyl peroxide**					
	$HO_2/O_2^- + (CH_3CO)_2O_2 \rightarrow$		2×10^7	p.r., opt.	C.k. with benzoquinone; pH not given.	81A374
167	**Adrenaline**					
	HO_2/O_2^- + Adr $\rightarrow$	7.8	5.4×10^4	enz., opt.	P.b.k. at 485 nm (buildup of adrenochrome); xanthine-xanthine oxidase system, no buffers.	78A483
	AdrO· + H_3O^+	9.5	2.5×10^4			
		7.8	4.0×10^4	enz., opt.	Xanthine-xanthine oxidase system; c.k. with Cu,Zn-SOD from spinach, $k(O_2^- + SOD) = 2.3 \times 10^9$.	76R183
168	**Adrenalone**					
	$HO_2/O_2^- +$ Adr $\rightarrow$ AdrO·	7.0	$(2.34 \pm 0.31) \times 10^7$	p.r.	C.k.; rel. to $k(O_2^- + DCIP) = 2.14 \times 10^8$.	79A240
169	**DL-Alanine, pK_a = 2.3, 9.8**					
	HO_2 + Ala $\rightarrow$	1.6	$<44 \pm 11.0$	γ-r., s.f., opt.	D.k. in O_2-satd. soln. contg. formate and 5×10^{-5} mol L^{-1} EDTA and 0.1 mol L^{-1} alanine; upper limit.	79A358
	O_2^- + Ala $\rightarrow$	10.0	$<0.06 \pm 0.02$	γ-r., s.f., opt.	D.k. in O_2-satd. soln. contg. formate and 5×10^{-5} mol L^{-1} EDTA and 0.1 mol L^{-1} alanine, no reaction.	79A358
170	**Alloxan**					
	HO_2/O_2^- + Al $\rightarrow O_2$ + ·AlH	5.7	$(5 \pm 1) \times 10^5$	p.r., opt.	Buildup and decay of dialuric acid (275 nm) and semiquinone at 310 and 370 nm in soln contg. 0.1 mol L^{-1} formate ion, 1.46×10^{-4} mol L^{-1} O_2, 5×10^{-3} mol L^{-1} alloxan; assumed mechanism, ϵ(·AlH) = 4000(275), 4900(310) and 1900(370 nm), ϵ(Al) = 16000(275) and 160(310 nm).	81A271
171	**Alloxan semiquinone**					
	HO_2/O_2^- + ·AlH $\rightarrow$ Al + H_2O_2	5.7	$(2.5 \pm 0.5) \times 10^8$	p.r., opt.	Buildup and decay of dialuric acid (275 nm) and semiquinone at 310 and 370 nm in soln contg. 0.1 mol L^{-1} formate ion, 1.46×10^{-4} mol L^{-1} O_2, 5×10^{-3} mol L^{-1} alloxan; assumed mechanism, ϵ(·AlH) = 4000(275), 4900(310) and 1900(370 nm), ϵ(Al) = 16000(275) and 160(310 nm).	81A271
172	**Arachidonate ion**					
	O_2^- + A^- $\rightarrow$	alk.	10^{-2}–10^{-1}	s.f., opt.	Anaerobic conditions; 85% v/v EtOH in 0.001–0.01 mol L^{-1} KOH/H_2O. D.k. at 240–270 nm. Reaction negligible.	83A087
		11.0	<1	p.r., opt.	D.k. in soln. contg. 0.6 mol L^{-1} formate, 0.01 mol L^{-1} arachidonate.	78A365

TABLE 3. Rate constants for reactions of HO_2/O_2^- in aqueous solutions — Continued

No.	Reaction	pH	k (L mol^{-1}s^{-1})	Method	Comment	Ref.
173	**Arachidonic acid**					
	$HO_2 + AH \rightarrow$	acid	$(3.05 \pm 0.29) \times 10^3$	s.f., opt.	85% v/v ethanolic soln.; d.k. at 240–270 nm; 0.05 mol L^{-1} H_2SO_4.	83A087
174	**L-Arginine, pK_a = 1.82, 9, 12.5**					
	$HO_2 + Arg \rightarrow$	1.6	$<63.0 \pm 14.0$	γ-r., s.f., opt.	D.k. in O_2—satd. soln. contg. formate and 5×10^{-5} mol L^{-1} EDTA and 0.1 mol L^{-1} arginine; upper limit.	79A358
	$O_2^- + Arg \rightarrow$	10.1	$<0.13 \pm 0.03$	γ-r., s.f., opt.	D.k. in O_2-satd. soln. contg. formate and 5×10^{-5} mol L^{-1} EDTA and 0.15 mol L^{-1} arginine; no reaction.	79A358
175	**Ascorbate oxidase**					
	$HO_2/O_2^- + AAO \rightarrow$	7.5		p.r., opt.	D.k. at 250 and 610 nm in oxygenated soln. contg. 2×10^{-6} mol L^{-1} AAO and 0.1 mol L^{-1} formate ion; no bleaching at 610 nm; no reaction obs.	83A147
176	**Ascorbate radical anion**					
	$HO_2 + \cdot A^- \rightarrow HO_2^- + A$	1.42–2.72	$(5.0 \pm 0.5) \times 10^9$	p.r., opt.	D.k. at 360 nm ($A\cdot^-$) in O_2-satd. soln. contg. (0.1 1) $\times 10^{-3}$ mol L^{-1} AH_2.	83A103
	$O_2^- + \cdot A^- \rightarrow OH^- + HO_2^- + A$	7.8, 8.0	$(2.6 \pm 0.4) \times 10^8$	p.r., opt.	D.k. at 360 nm ($A\cdot^-$) in O_2-satd. soln. contg. (0.1–1) $\times 10^{-3}$ mol L^{-1} AH_2.	83A103
		7.4	$<2.3 \times 10^8$	chem., opt.	Estd. from $k(AH^- + O_2^-)[AH^-]/k(\cdot A^- + O_2^-)[\cdot AH] = 22$ s^{-1} detd. in soln. contg. ascorbate, catalase, FeEDTA$^-$ and SOD, followed at 265 nm.	83R034
177	**Ascorbic acid, pK_a = 4.1**					
	$HO_2 + AH_2 \rightarrow \cdot A^- + H_2O_2$	0.3–1.0	1.6×10^4	s.f., opt.	D.k. in soln. contg. 0.1 mol L^{-1} formate ion.	83A103
	$HO_2 + AH^- \rightarrow \cdot A^- + H_2O_2$	3–8		s.f., opt.	Fitting process gave $k + 0.356k(O_2^- + AH_2) = 1.22 \times 10^7$.	83A103
	$HO_2/O_2^- + AH_2/AH^- \rightarrow \cdot A^- + H_2O_2$	~3	$(1.25 \pm 0.15) \times 10^6$	f.p., opt.	P.b.k. at 360 nm; cor. for $\cdot A^-$ decay; detd. from pH dependence (3–8); I = 0.02.	79A340
	$HO_2/O_2^- + AH_2/AH^- \rightarrow \cdot A^- + H_2O_2$	7.4	2.7×10^5	enz., opt.	D.k. at 249.6 nm in soln. contg. 0.1 mol L^{-1} phosphate buffer and xanthine-xanthine oxidase. Observed rate. Rel. to $k(O_2^- + SOD) = 1.9 \times 10^9$.	751031
	$O_2^- + AH^- \rightarrow HO_2^- + \cdot A^-$	3–8	$(5.75 \pm 0.35) \times 10^4$	f.p., opt.	P.b.k. at 360 nm; cor. for $\cdot A^-$ decay; detd. from pH dependence (3–8); I = 0.02.	79A340
		9.9	$(1.52 \pm 0.1) \times 10^5$	s.f., opt.	D.k. at 270 nm in air-satd. soln. contg. 0.2 mol L^{-1} formate and 2×10^{-4} mol L^{-1} EDTA; cor. for O_2^- decay. Factor of 2 should be considered to recalculate rate.	770046
	$O_2^- + AH^- \rightarrow$ unidentified product	8.2–11.0	5×10^4	s.f., opt.	D.k. in soln. contg. 0.1 mol L^{-1} formate ion. Rate taken from pH vs k_{obs} study. Products not determined.	83A103
178	**DL-Asparagine, pK_a = 2.213, 8.85**					
	$HO_2 + Asn \rightarrow$	1.4	$<53.8 \pm 10.0$	γ-r., s.f., opt.	D.k. in O_2-satd. formate soln. contg. 5×10^{-5} mol L^{-1} EDTA and 0.1 mol L^{-1} asparagine; upper limit.	79A358
	$O_2^- + Asn \rightarrow$	10.1	$<0.16 \pm 0.02$	γ-r., s.f., opt.	D.k. in O_2-satd. formate soln. contg. 5×10^{-5} mol L^{-1} EDTA and 0.1 mol L^{-1} asparagine; no reaction.	79A358
179	**DL-Aspartic acid, pK_a = 2.1, 4.0, 9.82**					
	$HO_2 + Asp \rightarrow$	1.5	$<12.0 \pm 4.0$	γ-r., s.f., opt.	D.k. in O_2—satd. formate soln. contg. 5×10^{-5} mol L^{-1} EDTA and 0.1 mol L^{-1} aspartic acid; upper limit.	79A358
	$O_2^- + Asp \rightarrow$	10.0	$<0.18 \pm 0.04$	γ-r., s.f., opt.	D.k. in O_2-satd. formate soln. contg. 5×10^{-5} mol L^{-1} EDTA and 0.1 mol L^{-1} aspartic acid; no reaction.	79A358

TABLE 3. Rate constants for reactions of HO_2/O_2^- in aqueous solutions — Continued

No.	Reaction	pH	k (L mol^{-1}s^{-1})	Method	Comment	Ref.
180	**Benzidine**					
	$HO_2/O_2^- + H_2NC_6H_4C_6H_4NH_2 \rightarrow$		$>25 \times 10^7$	p.r.	C.k.; rel. to $k(O_2^- + Q) = 9.5 \times 10^8$; pH not given	78A367
181	**Benzo[a]pyrene**					
	$HO_2/O_2^- + C_{20}H_{12} \rightarrow$		$<1 \times 10^7$	p.r.	C.k.; rel. to $k(O_2^- + Q) = 9.5 \times 10^8$; pH not given.	78A367
182	**1,4-Benzoquinone**					
	$O_2^- + Q \rightarrow Q^{\cdot -} + O_2$	~7	$(9 \pm 1) \times 10^8$	p.r., opt.	P.b.k. at 410 nm in O_2-satd. soln. contg. 0.5 mol L^{-1} *tert*-BuOH.	761056
		6.9	9.0×10^8 (±10%)	p.r., opt.	P.b.k. at 430 nm in soln. contg. 0.1 mol L^{-1} formate, 2×10^{-5} mol L^{-1} Q and 7×10^{-4} mol L^{-1} O_2.	730049
		7.0	9.8×10^8	p.r., opt.	P.b.k. at 430 nm in soln. contg. 5×10^{-5} mol L^{-1} Q.	730068
		~7	9.6×10^8	p.r., opt.	P.b.k. at 430 nm in O_2—satd. soln. contg. 10^{-4} mol L^{-1} Q and 1.0 mol L^{-1} *tert*-BuOH.	710619
183	**Bilirubin**					
	$HO_2/O_2^- + C_{33}H_{36}N_4O_6 \rightarrow$	8.3	2.3×10^4	enz., opt.	D.k. at 446 nm; xanthine-xanthine oxidase system.	82R164
184	**Biliverdin**					
	$HO_2/O_2^- + C_{33}H_{34}N_4O_6 \rightarrow$	8.3	7×10^3	enz., opt.	D.k. at 377 or 650 nm; xanthine-xanthine oxidase system.	82R164
185	**1,1'-Bis(2-hydroxyethyl)-4,4'-bipyridinium radical ion(1+)**					
	$O_2^- + BP^{\cdot +} \rightarrow$	6.8	$(12.0 \pm 1) \times 10^8$	p.r.	Ar-satd. soln. contg. 10^{-3} mol L^{-1} BP^{2+} $2Cl^-$, 0.1 mol L^{-1} Na formate and ~0.3% O_2.	78A321
186	***N*-Bromo-2,2,6,6-tetramethylpiperidine**					
	$HO_2/O_2^- + (CH_3)_4C_5H_6NBr \rightarrow Br^- + (CH_3)_4C_5H_6N\cdot + O_2$	9.2	1.1×10^3	KO_2, esr	Estd. from formn of nitroxide radical by subsequent reaction. DMSO/H_2O system contg. 18-crown-6.	79A184
187	***tert*-Butyl allyl peroxide**					
	$O_2^- + ROOR' \rightarrow$			s.f., opt.	D.k. at 250–270 nm in 80% EtOH soln. with 10^{-2} mol L^{-1} KOH, 1×10^{-5} mol L^{-1} EDTA, 1.2×10^{-3} mol L^{-1} O_2; peroxide concn. 3×10^{-3} mol L^{-1}; no reaction obs.	84A909
	$HO_2 + ROOR' \rightarrow$			s.f., opt.	D.k. at 250–270 nm in 80% EtOH soln. with 5×10^{-2} mol L^{-1} H_2SO_4, 1×10^{-5} mol L^{-1} EDTA, 1.2×10^{-3} mol L^{-1} O_2; peroxide concn. 3.8×10^{-2} mol L^{-1}; no reaction obs.	84A909
188	***tert*-Butylhydroquinone**					
	$HO_2 + (CH_3)_3CC_6H_3$-1,4-$(OH)_2 \rightarrow$	0.5–1.0	1.2×10^4	s.f., opt.	D.k. at 240–250 nm in soln. contg. 10^{-2} mol L^{-1} formate, EDTA, and substrate from 10^{-4}–2×10^{-3} mol L^{-1}.	83A902
	$O_2^- + (CH_3)_3CC_6H_3$-1,4-$(OH)_2 \rightarrow$	5.0–7.0	5×10^4	s.f., opt.	D.k. at 240–250 nm in soln. contg. 10^{-2} mol L^{-1} formate, EDTA, and substrate from 10^{-4}–2×10^{-3} mol L^{-1}.	83A902
189	**Catechol**					
	$HO_2 + 1,2\text{-}C_6H_4(OH)_2 \rightarrow$	0.5–9	$(4.7 \pm 0.5) \times 10^4$	s.f., opt.	D.k. at 245 nm; soln. prepd. as in [83G122].	82Z254
	$O_2^- + 1,2\text{-}C_6H_4(OH)_2 \rightarrow$	0.5–9	$(2.7 \pm 0.3) \times 10^5$	s.f., opt.	D.k. at 245 nm; soln. prepd. as in [83G122].	82Z254

TABLE 3. Rate constants for reactions of HO_2/O_2^- in aqueous solutions — Continued

No.	Reaction	pH	k (L mol^{-1}s^{-1})	Method	Comment	Ref.
190	**Ceruloplasmin**					
	HO_2/O_2^- + Ceruloplasmin →	7.8	1.8×10^6	p.r., opt.	D.k. at 610 nm in air-satd. soln. contg. formate (type 1 Cu^{II}). No change in absorption at 330 nm and no marked increase in O_2^- decay at 250 nm. Authors note that this rate may be due to CO_2^- radicals and not O_2^-.	80A220
191	**Citrate ion**					
	O_2^- + $R(CO_2^-)_3$ →	10.1	<0.14	e-r., s.f., opt.	D.k. at 250 nm in air-satd. soln. contg. 0.2 mol L^{-1} formate and 10^{-4} mol L^{-1} EDTA and 0.01–0.1 mol L^{-1} citrate; no reaction	770046
192	**Crocin**					
	O_2^- + crocin →	5.9		X-r.	No bleaching in oxygenated soln. contg. Na formate; at low pH bleaching occurs indicating HO_2 reactivity.	82R027
193	**4-Cyanophenyl-*N*-*tert*-butylnitrone**					
	HO_2/O_2^- + 4-CN-PBN → OH^- + 4-CN-PBN(OOH)		<6×10^6	p.r., opt.	C.k. in O_2-satd. soln. contg. *tert*-BuOH or formate; obs. $Q^{\cdot-}$ at 420 nm; rel. to $k(O_2^- + Q) = 1.0 \times 10^9$; Cf. [80A176], this value seems high.	82A184
194	**Cyclohexylperoxy**					
	HO_2 + c-$C_6H_{11}O_2\cdot$ → c-$C_6H_{11}O_2H$ + O_2	1.85	2.26×10^6	γ-r., chem.	Detd. H_2O_2 and RO_2H yields; assume $k(RO_2 + RO_2) = 2.7 \times 10^6$; pH not given.	670737
	O_2^- + c-$C_6H_{11}O_2\cdot$ → c-$C_6H_{11}O_2H$ + O_2	6–8	2.54×10^8	γ-r., chem.	Detd. from pH dependence of H_2O_2 and RO_2H yields; assume $k(RO_2 + RO_2) = 2.7 \times 10^6$.	670737
195	**Cysteine, pK_a = —2, 8.14, 10.34**					
	HO_2 + $CysH^+$ →	1.4	<601.0 ± 85.0	γ-r., s.f., opt.	D.k. in O_2-satd. soln. contg. formate and 5 × 10^{-5} mol L^{-1} EDTA and 0.1 mol L^{-1} cysteine; also detd. by O_2-consumption. upper limit.	79A358
	HO_2/O_2^- + Cys →	3–5.1	~1.8×10^4	γ-r., chem.	Obs. increase in $G(H_2O_2)$ with pH.	740188
		7	>5×10^4	γ-r., chem.	Obs. $G(H_2O_2)$ as function of dose.	700882
	O_2^- + Cys →	10.9	<15 ± 2.0	γ-r., s.f., opt.	D.k. in O_2-satd. soln. contg. formate and 5 × 10^{-5} mol L^{-1} EDTA and 0.05 mol L^{-1} cysteine; no reaction.	79A358
196	**L-Cystine, pK_a = 7.85, 9.85, 11.8, 12.4**					
	O_2^- + Cyt →	10.0	<0.40 ± 0.07	γ-r., s.f., opt.	D.k. in O_2-satd. soln. contg. formate and 5 × 10^{-5} mol L^{-1} EDTA and 5 × 10^{-4} mol L^{-1} cystine; no reaction.	79A358
197	**Cytochrome C (ferri), pK_a = 7.45, 9.2**					
	HO_2 + Cyt C (Fe^{3+}) → O_2 + Cyt C (Fe^{2+})	1.2–6.2		p.r., opt.	No reaction obs.	753093
		1.84		p.r., opt.	No reaction obs. (550 nm); c.k.	710327
	O_2^- + Cyt C (Fe^{3+}) → O_2 + Cyt C (Fe^{2+})		~6×10^4	phot., s.f., opt.	D.k. at 550 nm in soln. contg. 10.2 mol L^{-1} EtOH. pH not certain in EtOH/H_2O mixture.	82A021
		7.8	6×10^5	p.r., opt.	D.k. at 250 nm.	82A446
		7.3	5.84×10^5	f.p., opt.	D.k. in soln. contg. 2 × 10^{-2} mol L^{-1} tetramethylenediamine, 10^{-5} mol L^{-1} EDTA, 6 × 10^{-5} mol L^{-1} FMN and 1–4 × 10^{-5} mol L^{-1} cyt C.	82A269
		7.8	(2.6 ± 0.1) × 10^5	p.r., opt.	P.b.k. at 550 nm in soln. contg. 5 × 10^{-2} mol L^{-1} phosphate, 1 × 10^{-4} mol L^{-1} EDTA; pH dependence and effect of added Cu^{2+}, see FIGURE 2.	82A281

TABLE 3. Rate constants for reactions of HO_2/O_2^- in aqueous solutions — Continued

No.	Reaction	pH	k (L mol^{-1}s^{-1})	Method	Comment	Ref.
		7.2	8.0×10^5	p.r., opt.	D.k. at 550 nm in soln. contg. *tert*-BuOH or glycerol as OH scavenger; k decreases with added detergent; $k = 5 \times 10^4$ extrapolated to infinite SDS concn.	82N062
		~7	8.0×10^5	p.r., opt.	D.k. at 550 nm in soln. contg. 0.1 mol L^{-1} formate and 2×10^{-3} mol L^{-1} phosphate; observed rate.	79A312
		9.0	$(2.6 \pm 0.2) \times 10^5$	p.r., opt.	P.b.k. at 550 nm in air-satd. soln. contg. 0.01 mol L^{-1} formate and 10^{-4} mol L^{-1} EDTA.	78A361
		9.0	$(2.6 \pm 0.2) \times 10^5$	e-r., s.f., opt.	P.b.k. at 550 nm in air-satd. soln. contg. 0.2 mol L^{-1} formate and 2×10^{-4} mol L^{-1} EDTA and 5–20 $\times 10^{-5}$ mol L^{-1} cyt C; cor. for O_2^- decay.	770046
		7.4 8.5	$(5 \pm 0.3) \times 10^5$ $(2 \pm 0.2) \times 10^5$	p.r., opt.	D.k. at 550 nm in O_2-satd. soln. contg. 0.1 mol L^{-1} Na formate; also in D_2O (no isotope effect).	771096
		6.6 7.3 8.7 9.2	6.2×10^5 5.0×10^5 2.6×10^5 2.0×10^5	p.r., opt.	D.k. at 450 and 550 nm in soln. contg. Na formate and O_2; $I = 0.1$; E_a, $\Delta S^\ddagger$, $\Delta H^\ddagger$ and I discussed.	761127
		7.1	$(3.1 \pm 0.1) \times 10^6$ (cor. for I)	p.r., opt.	P.b.k. at 550 nm in soln. contg. 10^{-3} mol L^{-1} phosphate buffer, 2×10^{-3} mol L^{-1} formate and 2×10^{-5} mol L^{-1} EDTA and 2×10^{-3} mol L^{-1} O_2; $I = 0.1$; observed rate.	761163
		7 9.3	2.4×10^6 1.5×10^5	p.r., opt.	P.b.k. k_{obs} vs pH given for pH 6.0–10.5.	751012
		4.7–6.7	$(1.4 \pm 0.15) \times 10^9$	p.r., opt.	P.b.k. at 550 nm; from pH effect $k = 3.0 \times 10^4$ for the form present above pH 7.45 (pK_a cyt C = 7.45, 9.2). The form present above pH 9.2 does not react.	753093
		8.5	1.1×10^5	p.r., opt.	P.b.k. at 550 nm; at pH 10.4 $k = 8 \times 10^3$.	710327
		8.4	1.6×10^5	esr	D.k.; O_2^- from tetraacetylriboflavin + O_2. Observed rate.	699128
198	**Cytochrome C, acetylated** HO_2/O_2^- + Ac-cyt C →	~7	3.5×10^5	p.r., opt.	D.k. at 550 nm in soln. contg. 0.1 mol L^{-1} formate; $I = 0.1$.	79A312
199	**Cytochrome C, carboxymethylated** O_2^- + Cxm-cyt C →			p.r.	No reaction obs.	79A312
200	**Cytochrome C, succinylated** O_2^- + Succ-cyt C →			p.r.	No reaction obs.	79A312
201	**Cytochrome C (ferro)** HO_2/O_2^- + Cyt C (Fe^{2+}) → H_2O_2 + Cyt C (Fe^{3+})	5.3	5×10^5 to 5×10^6	p.r., opt.	D.k. at 550 nm; estimated value studied at a single pH.	753093
202	**Cytochrome P-450** O_2^- + cyt P-450 →			p.r.	No reaction obs.	79A036
203	**Cytochrome f (Fe^{3+})** O_2^- + Cyt f (Fe^{3+}) → Cyt f (Fe^{2+})	7.8	6.1×10^6	enz., opt.	Xanthine-xanthine oxidase system; soln. cont. phosphate (5×10^{-2} mol L^{-1}) and EDTA (10^{-4} mol L^{-1}).	77R240
204	**Dialuric acid** HO_2/O_2^- + AlH_2 → H_2O_2 + ·AlH	5.7	$\leqslant 10^3$	p.r., opt.	Buildup and decay of dialuric acid (275 nm) and semiquinone at 310 and 370 nm in soln contg. 0.1 mol L^{-1} formate ion, 1.46×10^{-4} mol L^{-1} O_2, 5×10^{-3} mol L^{-1} alloxan; assumed mechanism, ϵ(·AlH) = 4000(275), 4900(310) and 1900(370 nm), ϵ(Al) = 16000(275) and 160(310 nm).	81A271

TABLE 3. Rate constants for reactions of HO_2/O_2^- in aqueous solutions — Continued

No.	Reaction	pH	k (L mol^{-1}s^{-1})	Method	Comment	Ref.
205	**Diamide** *(Diazenedicarboxylic acid bisdimethylamide)*					
	$HO_2/O_2^- + ((CH_3)_2NCON=)_2 \rightarrow$	~7	$<10^6$	p.r., opt.	P.b.k. at 400 nm in soln. contg. 0.1 mol L^{-1} formate and 10^{-4} mol L^{-1} substrate; <3% electron transfer.	751194
206	**1,4-Diazabicyclo[2.2.2]octane**					
	$O_2^- +$ DABCO $\rightarrow$	7.2		p.r.	D.k. at 270 nm; no reaction obs.	78R103
207	**2,5-Dichloro-*p*-benzoquinone**					
	$O_2^- + 2,5\text{-}Cl_2Q \rightarrow$	7.0	1.1×10^9	p.r., opt.	P.b.k. at 430 nm in soln. contg. 5×10^{-5} mol L^{-1} quinone.	730068
208	**2,5-Dichlorohydroquinone**					
	$O_2^- + Cl_2C_6H_2(OH)_2 \rightarrow$ $2,5\text{-}Cl_2Q\cdot^- + H_2O_2$	7.0	1.3×10^7	p.r., opt.	P.b.k. in O_2-satd. soln. contg. 10^{-3} mol L^{-1} quinone, 0.1 mol L^{-1} formate.	751011
209	**2,6-Dichloroindophenolate ion**					
	$O_2^- +$ DCIP$^- \rightarrow$ $O_2 +$ DCIP$^{\cdot 2-}$	7.0	$(2.14 \pm 0.05) \times 10^8$	p.r., opt.	C.k., rel. to $k(O_2^- + SOD) = 3.7 \times 10^9$.	79A240
		~7	$\sim 1.5 \times 10^8$	p.r., opt.	D.k. at 600 nm (oxidized DCIP) in O_2-satd. soln. contg. *tert*-BuOH and $(1\text{-}6) \times 10^{-4}$ mol L^{-1} DCIP.	761056
		~7	$(1.7 \pm 0.3) \times 10^8$	p.r., opt.	D.k. at 430 nm in soln. contg. 5×10^{-5} mol L^{-1} substrate; rel. to $k(O_2^- + Q) = 9 \times 10^8$.	761056
210	**3,4-Dihydroxyacetophenone**					
	$O_2^- + (HO)_2C_6H_3COCH_3 \rightarrow$	7	$(2.94 \pm 0.22) \times 10^7$	p.r.	C.k.; rel. to $k(O_2^- +$ DCIP$^-) = 2.14 \times 10^8$.	79A303
211	**3,4-Dihydroxybenzaldehyde**					
	$O_2^- + (HO)_2C_6H_3CHO \rightarrow$	7	$(1.40 \pm 0.03) \times 10^7$	p.r.	C.k.; rel. to $k(O_2^- +$ DCIP$^-) = 2.14 \times 10^8$.	79A303
212	**4,5-Dihydroxy-*m*-benzenedisulfonate ion**					
	$HO_2/O_2^- + (HO)_2C_6H_2(SO_3)_2^{2-} \rightarrow$		1.0×10^7	p.r.	Neutral pH assumed; no buffer; rel. to $k(O_2^- +$ DCIP$^-) = 2.1 \times 10^8$.	79A014
	$O_2^- + (HO)_2C_6H_2(SO_3)_2^{2-} \rightarrow$	7	1.5×10^8	p.r, opt.	C.k.; rel. to $k(O_2^- + Q) = 9 \times 10^8$.	751087
		7	5×10^8	p.r., opt.	P.b.k. at 400 nm.	751087
213	**2,5-Dihydroxybenzoic acid**					
	$HO_2 + (HO)_2C_6H_3CO_2H \rightarrow$	0.5–1.5	$(3.9 \pm 0.3) \times 10^4$	s.f., opt.	D.k. at 245–255 nm; soln. prepd. as in [83G122].	82Z254
214	**5,8-Dihydroxy-1,4-naphthoquinone**					
	$HO_2/O_2^- + NQ(OH)_2 \rightarrow O_2 +$ $\cdot NQ(OH)_2^-$	5.2	$(5.8 \pm 0.5) \times 10^8$	p.r., opt.	P.b.k. at 380 nm in air-satd. soln. contg. 0.1 mol L^{-1} formate and phosphate buffer; from equilibrium constant = 5.6, $k_{reverse} = (1.1 \pm 0.2) \times 10^8$.	83A039
215	**2,3-Dimethyl-1,4-benzoquinone**					
	$O_2^- + 2,3\text{-}(CH_3)_2Q \rightarrow$ $2,3\text{-}(CH_3)_2Q\cdot^- + O_2$	7	$(4.5 \pm 1) \times 10^8$	p.r., opt.	P.b.k.	730125
216	**2,5-Dimethyl-1,4-benzoquinone**					
	$O_2^- + 2,5\text{-}(CH_3)_2Q \rightarrow$ $[2,5\text{-}(CH_3)_2Q]\cdot^- + O_2$	7.2	1.7×10^8	p.r., opt.	P.b.k. (semiquinone) in soln. contg. 0.1 mol L^{-1} Na formate and 1.25–12.5 $\times 10^{-4}$ mol L^{-1} O_2.	761063
		7.0	7.5×10^8	p.r., opt.	P.b.k. at 430 nm in soln. contg. 5×10^{-5} mol L^{-1} quinone.	730068
		7	$(3.6 \pm 1) \times 10^8$	p.r., opt.	P.b.k.	730125

TABLE 3. Rate constants for reactions of HO_2/O_2^- in aqueous solutions — Continued

No.	Reaction	pH	k (L mol^{-1}s^{-1})	Method	Comment	Ref.
217	**2,6-Dimethylbenzoquinone**					
	$O_2^- + 2,6\text{-}(CH_3)_2Q \rightarrow [2,6\text{-}(CH_3)_2Q]^{\cdot -} + O_2$	7	$(5.8 \pm 1) \times 10^8$	p.r., opt.	P.b.k.	730125
218	**1,1'-Dimethyl-4,4'-bipyridinium radical ion (1+)**					
	$HO_2 + MV^{\cdot +} \rightarrow$	3.5	2.1×10^9	p.r., opt.	D.k. in soln. contg. 4–16 $\times 10^{-2}$ mol L^{-1} H_2O_2; $G(HO_2) = 5.98$, 6.51 assumed from $OH + H_2O_2 \rightarrow HO_2$.	83A043
	$O_2^- + MV^{\cdot +} \rightarrow$	7	2.8×10^9	p.r., opt.	D.k. in soln. contg. 4–16 $\times 10^{-2}$ mol L^{-1} H_2O_2; $G(HO_2) = 6.15$ assumed from $OH + H_2O_2 \rightarrow HO_2$.	83A043
		6.8	$(9.2 \pm 1.1) \times 10^8$	p.r.	Ar-satd. soln. contg. 10^{-3} mol L^{-1} MV^{2+} $2Cl^-$ and 0.1 mol L^{-1} Na formate and ~0.3% O_2.	78A321
			6.5×10^8	p.r., opt.	Calcd. from d.k.; $k(O_2 + MV^{\cdot +}) = 7.7 \times 10^8$.	731074
219	**2,3-Dimethylnaphthoquinone**					
	$O_2^- + 2,3\text{-}(CH_3)_2NQ \rightarrow 2,3\text{-}(CH_3)_2NQ^{\cdot -} + O_2$	7	4×10^6	p.r., opt.	Detd. from equil. const. and d.k. of semiquinone in soln. contg. 10^{-3} mol L^{-1} quinone, 5 mol L^{-1} 2-PrOH and 1 mol L^{-1} acetone.	730125
220	**5,5-Dimethyl-1-pyrroline-*N*-oxide**					
	$HO_2/O_2^- + DMPO \rightarrow$		6.6×10^3	esr	Calcd. from effect of pH (5–9) on k_{obs}; c.k. with SOD; rel. to $k(O_2^- + Fe^{3+}$ cyt C) = 6×10^5.	80A176
	$O_2^- + DMPO \rightarrow$	7.8	10	enz., esr	Spin trapping; rel. to $k(O_2^- + TMPO) = 7$.	80A176
		8.0	15.7	phot., esr	Spin trapping; c.k. with SOD; rel. to $k(O_2^- + Fe^{3+}$ cyt C) = 6×10^5. Studied from pH 5–9.	80A176
221	**Diphenoquinone**					
	$O_2^- + O{=}C_6H_4C_6H_4{=}O \rightarrow {\cdot}OC_6H_4C_6H_4O^- + O_2$	7.0	1.4×10^9 (±10%)	p.r., opt.	P.b.k. at 400 nm in soln. contg. 5×10^{-5} mol L^{-1} quinone.	730068
222	**1,1'-Diphenyl-4,4'-bipyridinium radical ion (1+)**					
	$O_2^- + BP^{\cdot +} \rightarrow$		$(6.2 \pm 2.0) \times 10^9$	p.r.	Ar-satd. soln. contg. 10^{-3} mol L^{-1} BP^{2+} $2Cl^-$ and 0.1 mol L^{-1} formate and ~0.3% O_2; pH not given.	78A321
223	**Dithiothreitol**					
	$HO_2/O_2^- + DTT \rightarrow$	7.8	1.0×10^6	enz., opt.	Xanthine-xanthine oxidase system; c.k., rel. to $k(HO_2/O_2^- +$ adrenaline) = 4×10^4.	76R183
224	**Duroquinone**					
	$O_2^- + DQ \rightarrow DQ^{\cdot -} + O_2$	7	1.0×10^7	p.r., opt.	D.k. (semiquinone) in soln. contg. Na formate and O_2.	751090
		7	$(4.5 \pm 1.5) \times 10^6$	p.r., opt.	Detd. from equil. const. and d.k. of semiquinone in soln. contg. 5 mol L^{-1} 2-PrOH and 2 mol L^{-1} acetone.	730125
225	**Ethylene**					
	$HO_2/O_2^- + H_2C{=}CH_2 \rightarrow$		2×10^5	γ-r., chem.	C.k.; pH not given; rel. to $k(HO_2 + Fe^{2+})$ calcd. from value taken from [730038].	670037
226	**1,1'-Ethylene-2,2'-bipyridinium radical ion (1+)**					
	$O_2^- + BP^{\cdot +} \rightarrow$		$(4.8 \pm 0.5) \times 10^8$	p.r.	Ar-contg. soln. contg. 10^{-3} mol L^{-1} BP^{2+} $2Cl^-$ and 0.1 mol L^{-1} Na formate and ~0.3% O_2; pH not given.	78A321

TABLE 3. Rate constants for reactions of HO_2/O_2^- in aqueous solutions — Continued

No.	Reaction	pH	k (L mol^{-1}s^{-1})	Method	Comment	Ref.
227	**Ethylenediaminetetraacetate ion**					
	$O_2^- + [CH_2N(CH_2CO_2^-)_2]_2 \rightarrow$	9.9	<0.01	*e*-r., s.f., opt.	D.k. at 250 nm in air-satd. soln. contg. 0.2 mol L^{-1} formate and 0.01–0.1 mol L^{-1} EDTA; no reaction obs.	770046
228	**2-Ethyl-1-hydroxy-2,5,5-trimethyl-3-oxazolidine**					
	$HO_2/O_2^- +$ OXANO $\rightarrow$	7.8	6.7×10^3	enz, opt.	C.k. in xanthine oxidase system, rel. to $k(O_2^- +$ cyt C$) = 6 \times 10^5$.	82R165
229	**Ferredoxin (spinach)**					
	HO_2/O_2^- + Ferredoxin $\rightarrow$	7.7	$<10^4$	p.r., opt.	D.k. in soln. contg. 6.5×10^{-2} mol L^{-1} phosphate buffer.	78R208
230	**Flavin adenine dinucleotide semiquinone**					
	O_2^- + FADH· $\rightarrow$	7	$(2.2 \pm 0.2) \times 10^8$	p.r., opt.	D.k. at 540 nm in aerated soln. contg. 0.01 mol L^{-1} formate ion and 8×10^{-5} mol L^{-1} flavin.	81A375
231	**Flavin mononucleotide semiquinone**					
	HO_2 + FMNH· $\rightarrow$	2.5–4.0	6.2×10^8	p.r., opt.	D.k. at 540 nm in aerated soln. contg. 0.01 mol L^{-1} formate and 8×10^{-5} mol L^{-1} flavin. Studied from pH 2–8.	81A375
	O_2^- + FMNH· $\rightarrow$	7	$(3.2 \pm 0.2) \times 10^8$	p.r., opt.	D.k. at 540 nm in aerated soln. contg. 0.01 mol L^{-1} formate ion and 8×10^{-5} mol L^{-1} flavin. Studied as a function of pH 2–8.	81A375
232	**Formate ion**					
	$O_2^- + HCO_2^- \rightarrow$	10.1	<0.01	*e*-r., s.f., opt.	D.k. at 250 nm in air-satd. soln. contg. 5×10^{-4} mol L^{-1} formate and 1×10^{-4} mol L^{-1} EDTA; no reaction obs.	770046
233	**Fumarate ion**					
	O_2^- + *trans*-$^-O_2CCH = CHCO_2^- \rightarrow$	10.1	<0.10	*e*-r., s.f., opt.	D.k. at 250 nm in air-satd. soln. contg. 0.01–0.1 mol L^{-1} fumarate, 0.2 mol L^{-1} formate and 10^{-4} mol L^{-1} EDTA; no reaction obs.	770046
234	**L-Glutamic acid, pK_a = 2.06, 4.26, 9.85**					
	HO_2 + Glu $\rightarrow$	1.6	$<30.0 \pm 6.0$	γ-r., s.f., opt.	D.k. in O_2-satd. soln. contg. formate and 10^{-5} mol L^{-1} EDTA and 0.1 mol L^{-1} glutamic acid; upper limit.	79A358
	O_2^- + Glu $\rightarrow$	8.7	$<0.39 \pm 0.07$	γ-r., s.f., opt.	D.k. in O_2-satd. soln. contg. formate and 5×10^{-5} mol L^{-1} EDTA and 0.025 mol L^{-1} glutamic acid; no reaction obs.	79A358
235	**L-Glutamine, pK_a = 2.17, 9.13**					
	HO_2 + Gln $\rightarrow$	1.5	$<23.0 \pm 6.0$	γ-r., s.f., opt.	D.k. in O_2-satd. soln. contg. formate and 5×10^{-5} mol L^{-1} EDTA and 0.1 mol L^{-1} glutamine, upper limit.	79A358
	O_2^- + Gln $\rightarrow$	10.0	$<0.25 \pm 0.05$	γ-r., s.f., opt.	D.k. in O_2-satd. soln. contg. formate and 5×10^{-5} mol L^{-1} EDTA and 0.1 mol L^{-1} glutamine no reaction obs.	79A358
236	**Glutathione, pK_a = 2, 3.59, 8.75, 9.65**					
	HO_2/O_2^- + GSH $\rightarrow$	7.8	6.7×10^5	enz., opt.	Xanthine-xanthine oxidase system; c.k., rel. to $k(HO_2/O_2^- +$ adrenaline$) = 4 \times 10^4$.	76R183
237	**Glyceraldehyde-3-phosphate dehydrogenase-NADH complex**					
	HO_2 + GPDH-NADH $\rightarrow$	4.8–9.5	2.00×10^7	p.r., opt.	D.k. in soln. contg. 0.05 mol L^{-1} phosphate, 10^{-5} mol L^{-1} EDTA, 10^{-4} mol L^{-1} NADH and 2.5×10^{-4} mol L^{-1} O_2 and 6.48×10^{-5} mol L^{-1} enzyme; estd. from k_{obs} vs pH; O_2^- unreactive.	80A413

TABLE 3. Rate constants for reactions of HO_2/O_2^- in aqueous solutions — Continued

No.	Reaction	pH	k (L mol^{-1}s^{-1})	Method	Comment	Ref.
238	**Glycine, pK_a = 2.35, 9.78**					
	HO_2 + Gly →	1.5	<48.6 ± 4.0	γ-r., s.f., opt.	D.k. in O_2-satd. soln. contg. formate and 10^{-5} mol L^{-1} EDTA and 0.1 mol L^{-1} glycine; upper limit.	79A358
	O_2^- + Gly →	8.8	<0.42 ± 0.12	γ-r., s.f., opt.	D.k. in O_2-satd. soln. contg. formate and 10^{-5} mol L^{-1} EDTA and 0.1 mol L^{-1} glycine no reaction obs.	79A358
239	**Hemocyanin**					
	HO_2/O_2^- + Hemocyanin →	8.0	$<10^6$	p.r., opt.	No reaction obs. at 290 nm in O_2-satd. soln. contg. 2×10^{-2} mol L^{-1} Na formate.	761021
240	**L-Histidine, pK_a = 1.80, 6.04, 9.33**					
	HO_2 + His →	1.8	<95.0 ± 14.0	γ-r., s.f., opt.	D.k. in O_2-satd. soln. contg. formate and 5×10^{-5} mol L^{-1} EDTA and 0.05 mol L^{-1} histidine; upper limit.	79A358
	O_2^- + His →	10.0	<1.00 ± 0.21	γ-r., s.f., opt.	D.k. in O_2-satd. soln. contg. formate and 5×10^{-5} mol L^{-1} EDTA and 0.15 mol L^{-1} histidine no reaction obs.	79A358
241	**Homocysteine**					
	HO_2/O_2^- + Hcy →	7.8	4.6×10^5	enz., opt.	Xanthine-xanthine oxidase system; c.k., rel. to $k(HO_2/O_2^-$ + adrenaline) = 4×10^4.	76R183
242	**1-Hydroperoxy-2-cyclooctene**					
	HO_2 + c-$C_8H_{13}O_2H$ →			s.f., opt.	D.k. at 250–270 nm in 80% EtOH soln. with 5×10^{-2} mol L^{-1} H_2SO_4, 1×10^{-5} mol L^{-1} EDTA, 1.2×10^{-3} mol L^{-1} O_2. Peroxide concn. 4.0×10^{-2} mol L^{-1}. No reaction obs.	84A909
	O_2^- + c-$C_8H_{13}O_2H$ →			s.f., opt.	D.k. at 250–270 nm in 80% EtOH soln. with 10^{-2} mol L^{-1} KOH,, 1×10^{-5} mol L^{-1} EDTA, 1.2×10^{-3} mol L^{-1} O_2. Peroxide concn. 3×10^{-3} mol L^{-1}. No reaction obs.	84A909
243	**Hydroquinone**					
	HO_2 + 1,4-$C_6H_4(OH)_2$ → ·OC_6H_4OH + H_2O_2	0.4–3.5	$(0.85 \pm 0.1) \times 10^4$	f.p., opt.	P.b.k. at 290 nm; value could be twice as fast, see paper for discussion.	79A340
	HO_2/O_2^- + 1,4-$C_6H_4(OH)_2$ → $Q^{\cdot -}$ + H_2O_2	~7	1.7×10^7	p.r.	Soln. cont. 10^{-3} mol L^{-1} QH_2.	751011
		7.0	$(1.6 \pm 0.1) \times 10^7$	p.r., opt.	P.b.k. at 430 nm in soln. contg. 10^{-3} mol L^{-1} QH_2, 1.3×10^{-3} mol L^{-1} O_2 and 1 mol L^{-1} *tert*-BuOH..	730068
244	**1-Hydroxyethyldioxy**					
	HO_2/O_2^- + $CH_3C(\dot{O}_2)HOH$ → CH_3CO_2H + H_2O + O_2	3	~10^7		Calcd. from product distribution and other reaction rates.	83A056
245	**6-Hydroxy-2,5,7,8-tetramethylchroman-2-carboxylic acid**					
	HO_2 + HTC-CO_2H →	acid	$(2.02 \pm 0.18) \times 10^5$	s.f., opt.	D.k. at 254 nm; carried out in 85% EtOH contg. 0.022 mol L^{-1} H_2SO_4.	82Z254
246	**6-Hydroxy-2,5,7,8-tetramethylchroman-2-carboxylate ion**					
	HO_2/O_2^- + HTC-CO_2^- →	7.4	1.7×10^4	enz., opt.	D.k. at 249.6 nm in xanthine-xanthine oxidase system contg. 10^{-4} mol L^{-1} EDTA, 10^{-1} mol L^{-1} phosphate buffer and 2×10^{-4} mol L^{-1} substrate.	75R176
	O_2^- + HTC-CO_2^- →	alk.		s.f., opt.	D.k. at 254 nm; carried out in 85% EtOH contg. 0.01 mol L^{-1} KOH. No reaction obs.	82Z254
247	**3-(6-Hydroxy-2,5,7,8-tetramethylchroman-2-yl)propionate ion**					
	HO_2/O_2^- + HTC-$CH_2CH_2CO_2^-$ →	7.4	5.9×10^3	enz., opt.	D.k. at 248.9 nm, in soln. contg. 4×10^{-4} mol L^{-1} substrate, 1×10^{-4} mol L^{-1} EDTA, 4×10^{-5} mol L^{-1} xanthine, and 0.1 mol L^{-1} phosphate buffer.	78R210

TABLE 3. Rate constants for reactions of HO_2/O_2^- in aqueous solutions — Continued

No.	Reaction	pH	k (L mol^{-1}s^{-1})	Method	Comment	Ref.
248	**Imidazole, pK_a = 6.96**					
	$O_2^- + Im \rightarrow$	10.1	<0.02	*e*-r., s.f., opt.	D.k. at 250 nm in air-satd. soln. contg. 0.2 mol L^{-1} formate and 10^{-4} mol L^{-1} EDTA and 0.01–0.1 mol L^{-1} mol L^{-1} imidazole; no reaction obs.	770046
249	**Indigodisulfonate ion**					
	$HO_2 + IDS^{2-} \rightarrow O_2 + IDS^{\cdot 3-} + H^+$	0.4	2.0×10^4	γ-r., opt.	C.k.; $G(HO_2) = 3.6$; value recalcd. using $k(HO_2 + HO_2) = 8.6 \times 10^5$.	680059
	$O_2^- + IDS^{2-} \rightarrow O_2 + IDS^{\cdot 3-}$	7	9×10^5	p.r., opt.	D.k. of IDS^{2-} in soln. contg. Na formate and oxygen	751090
250	**Indigotetrasulfonate ion**					
	$HO_2 + ITS^{4-} \rightarrow O_2 + ITS^{\cdot 5-}$	0.4	1.8×10^3	γ-r., opt.	C.k.; $G(HO_2) = 3.6$; value recalcd. using $k(HO_2 + HO_2) = 8.6 \times 10^5$.	680059
251	**Indigotrisulfonate ion**					
	$HO_2 + ITS^{3-} \rightarrow O_2 + ITS^{\cdot 4-}$	0.4	1.1×10^4	γ-r., opt.	C.k.; $G(HO_2) = 3.6$; value recalcd. using $k(HO_2 + HO_2) = 8.6 \times 10^5$.	680059
252	**Indomethacin**					
	$HO_2/O_2^- + In \rightarrow$	7.0	$(2.6 \pm 0.1) \times 10^6$	p.r., opt.	D.k. at 250 nm in soln. contg. 10^{-2} mol L^{-1} formate.	80A201
253	**DL-Isoleucine, pK_a = 2.318, 9.758**					
	$HO_2 + Ile \rightarrow$	1.4	$<38.9 \pm 5.0$	γ-r., s.f., opt.	D.k. in O_2-satd. soln. contg. formate and 5×10^{-5} mol L^{-1} EDTA and 0.1 mol L^{-1} isoleucine; upper limit.	79A358
	$O_2^- + Ile \rightarrow$	8.0	$<2.00 \pm 0.40$	γ-r., s.f., opt.	D.k. in O_2-satd. soln. contg. formate and 5×10^{-5} mol L^{-1} EDTA and 0.1 mol L^{-1} mol L^{-1} isoleucine; no reaction.	79A358
254	**Laccase**					
	$HO_2/O_2^- + Laccase \rightarrow$	6.0	$\geq 2 \times 10^6$	p.r., opt.	Transient adduct obs. in soln. contg. 0.01 mol L^{-1} potassium phosphate, 95×10^{-6} mol L^{-1} laccase, and 0.1 mol L^{-1} formate; addn. followed by Cu^{2+} redn.; complex kinetics.	82A422
255	**Lactate ion**					
	$O_2^- + CH_3CHOHCO_2^- \rightarrow$	10.0	<0.50	*e*-r., s.f., opt.	D.k. at 250 nm in air-satd. soln. contg. 0.2 mol L^{-1} formate and 10^{-4} mol L^{-1} EDTA and 0.01–0.1 mol L^{-1} lactate; no reaction.	770046
256	**L-Leucine, pK_a = 2.328, 9.744**					
	$HO_2 + Leu \rightarrow$	1.4	$<23.0 \pm 4.0$	γ-r., s.f., opt.	D.k. in O_2-satd. soln. contg. formate and 5×10^{-5} mol L^{-1} EDTA and 0.1 mol L^{-1} leucine; upper limit.	79A358
	$O_2^- + Leu \rightarrow$	9.9	$<0.21 \pm 0.02$	γ-r., s.f., opt.	D.k. in O_2-satd. soln. contg. formate and 5×10^{-5} mol L^{-1} EDTA and 0.1 mol L^{-1} leucine; no reaction.	79A358
257	**Linoleate hydroperoxide**					
	$HO_2/O_2^- + HO_2L^- \rightarrow$		7.4×10^3	enz, opt.	Rate inferred from ratio of SOD inhibition of linoleate oxidation, HO_2 may be reactive form.	82R039
		8.1	7×10^3	enz, opt.	P.b.k. at 235 nm in soln. contg. 6.3×10^{-8} mol L^{-1} xanthine oxidase, 4.8×10^{-2} mol L^{-1} acetaldehyde, 10^{-3} mol L^{-1} linoleic acid and phosphate.	78R207
	$O_2^- + HO_2L^- \rightarrow$	7		p.r.	No reaction obs. in soln. contg. formate and O_2.	79A295
258	**Linoleate ion**					
	$O_2^- + L^- \rightarrow$		10^{-2}–10^{-1}	s.f., opt.	85% v/v ethanolic soln.; d.k. at 240–270 nm. Strongly alk. conditions (0.001–0.01 mol L^{-1} KOH). Negligible reaction.	83A087

TABLE 3. Rate constants for reactions of HO_2/O_2^- in aqueous solutions — Continued

No.	Reaction	pH	k (L mol^{-1}s^{-1})	Method	Comment	Ref.
259	**Linoleic acid**					
	$HO_2 + LH \rightarrow$		$(1.18 \pm 0.20) \times 10^3$	s.f., opt.	85% v/v ethanolic soln.; d.k. at 240–270 nm; 0.05 mol L^{-1} H_2SO_4.	83A087
260	**Linoleic acid hydroperoxide**					
	$HO_2 + HO_2LH \rightarrow$			s.f., opt.	D.k. at 250–270 nm in 80% EtOH soln. with 5×10^{-2} mol L^{-1} H_2SO_4, 1×10^{-5} mol L^{-1} EDTA, 1.2×10^{-3} mol L^{-1} O_2. Peroxide concn. 2×10^{-3} mol L^{-1}. No reaction obs.	84A909
	$O_2^- + HO_2LH \rightarrow$			s.f., opt.	D.k. at 250–270 nm in 80% EtOH soln. with 10^{-2} mol L^{-1} KOH,, 1×10^{-5} mol L^{-1} EDTA, 1.2×10^{-3} mol L^{-1} O_2. Peroxide concn. 3×10^{-3} mol L^{-1}. No reaction obs.	84A909
261	**Linolenate ion**					
	$O_2^- + L^- \rightarrow$	alk.	10^{-2}–10^{-1}	s.f., opt.	85% v/v EtOH in 0.001–0.01 mol L^{-1} KOH/H_2O, Anaerobic conditions. D.k. at 240–270 nm. Reaction negligible.	83A087
		11	<1	p.r., opt.	D.k. in soln. contg. 0.06 mol L^{-1} formate and 0.01 mol L^{-1} lipid.	78A365
262	**Linolenic acid**					
	$HO_2 + LH \rightarrow$		$(1.70 \pm 0.35) \times 10^3$	s.f., opt.	85% v/v ethanolic soln.; d.k. at 240–270 nm; 0.05 mol L^{-1} H_2SO_4.	83A087
263	**Lipoxidase (soybean)**					
	$HO_2/O_2^- + LOX \rightarrow$	3.98	$(7.0 \pm 1.0) \times 10^6$	p.r., opt.	P.b.k. in O_2-satd. soln. contg. 0.1 mol L^{-1} formate ion and 5×10^{-6} mol L^{-1} lipoxidase, product is Fe(III) yellow enzyme.	80A296
	$O_2^- + LOX \rightarrow$	9.3		p.r., opt.	P.b.k. in O_2-satd. soln. contg. 0.1 mol L^{-1} formate ion. No reaction obs.	80A296
264	**Luminol radical**					
	$O_2^- + lum\cdot \rightarrow lumO_2H$	7.7	1.4×10^9	p.r., opt.	D.k. at 430 nm in soln. contg. 10^{-4} mol L^{-1} luminol and 10^{-1} mol L^{-1} H_2O_2; pK_a for luminol hydroperoxide detd. to be 9.3 ± 0.3; pH range of 7.7–11.0 studied.	80A221
		11	2×10^8			
265	**DL-Lysine, pK_a = 5.05, 10.53, 11.82**					
	$HO_2 + Lys \rightarrow$	1.4	$<13.3 \pm 3.0$	γ-r., s.f., opt.	D.k. in O_2-satd. soln. contg. formate and 5×10^{-5} mol L^{-1} EDTA and 0.1 mol L^{-1} lysine; upper limit.	79A358
	$O_2^- + Lys \rightarrow$	8.5	$<3.30 \pm 0.03$	γ-r., s.f., opt.	D.k. in O_2-satd. soln. contg. formate and 5×10^{-5} mol L^{-1} EDTA and 0.1 mol L^{-1} lysine; no reaction obs.	79A358
266	**L-Malate ion**					
	$O_2^- + {}^-O_2CCH_2CHOHCO_2^- \rightarrow$	10.1	<0.11	*e*-r., s.f., opt.	D.k. at 250 nm in air-satd. soln. contg. 0.2 mol L^{-1} formate and 10^{-4} mol L^{-1} EDTA and 0.01–0.1 mol L^{-1} malate; no reaction obs.	770046
267	**Maleate ion**					
	$O_2^- +$ *cis*-$^-O_2CCH{=}CHCO_2^- \rightarrow$	10.0	<0.06	*e*-r., s.f., opt.	D.k. at 250 nm in air-satd. soln. contg. 0.2 mol L^{-1} formate and 10^{-4} mol L^{-1} EDTA and 10^{-4}–5×10^{-2} mol L^{-1} maleate; no reaction obs.	770046
268	**Methemoglobin**					
	$HO_2/O_2^- + Fe^{3+}Hb \rightarrow Fe^{2+}HbO_2$	7.8	1.4×10^3	γ-r.	Rel. to $k(O_2^- + HO_2) = 8.5 \times 10^7$; soln. contg. 0.16 mol L^{-1} formate and O_2.	78A366
				p.r.	No reaction detected; pH not given.	761137
		7	6×10^3	γ-r., enz.	Rel. to $O_2^- + Fe^{2+}$ HbO_2.	763093

TABLE 3. Rate constants for reactions of HO_2/O_2^- in aqueous solutions — Continued

No.	Reaction	pH	k (L mol^{-1}s^{-1})	Method	Comment	Ref.
269	**Methional**					
	HO_2/O_2^- + $CH_3SCH_2CH_2CHO \rightarrow$	7		p.r., opt.	D.k. at 240–260 nm; first order $k = 5.2 \times 10^3$ s^{-1}. Authors suggest sluggish reaction.	761038
270	**DL-Methionine, pK_a = 2.2, 9.2**					
	HO_2 + Met →	1.5	$<48.8 \pm 15.0$	γ-r., s.f., opt.	D.k. in O_2-satd. soln. contg. formate and 5×10^{-5} mol L^{-1} EDTA and 0.1 mol L^{-1} methionine; upper limit.	79A358
	O_2^- + Met →	8.3	$<0.33 \pm 0.05$	γ-r., s.f., opt.	D.k. in O_2-satd. soln. contg. formate and 5×10^{-5} mol L$^-$ EDTA and 0.1 mol L^{-1} methionone; no reaction obs.	79A358
271	**4-Methoxyphenyl-*N*-*tert*-butylnitrone**					
	HO_2/O_2^- + 4-CH_3O-PBN → OH^- + 4-CH_3O-PBN(OOH)		$<1 \times 10^6$	p.r., opt.	C.k. in O_2-satd. soln. contg. *tert*-BuOH or formate; obs. Q·$^-$ at 420 nm; rel. to $k(O_2^- + Q) = 1.0 \times 10^9$; See [80A176], limit seems high.	82A184
272	**Methyl-1,4-benzoquinone**					
	O_2^- + MeQ → MeQ·$^-$ + O_2	7.0	8.0×10^8	p.r., opt.	P.b.k. at 430 nm in soln. contg. 5×10^{-5} mol L^{-1} quinone.	730068
		7	$(7.6 \pm 1) \times 10^8$	p.r., opt.	P.b.k. (semiquinone)	730125
273	**3-Methylcholanthrene**					
	HO_2/O_2^- + $C_{21}H_{16}$ →		1.1×10^8	p.r.	C.k. in soln. contg. 0.01 mol L^{-1} CTAB; rel. to $k(O_2^- + Q) = 9.5 \times 10^8$; pH not given.	78A367
274	**Methylhydroquinone**					
	O_2^- + $CH_3C_6H_3$-1,4-$(OH)_2$ → MeQ·$^-$ + H_2O_2	7.0	1.7×10^7	p.r.	Soln. cont. 10^{-3} mol L^{-1} QH_2.	751011
275	**1-Methylimidazole, pK_a = 6.95**					
	O_2^- + 1-CH_3Im →	10.1	<0.15	e-r., s.f., opt.	D.k. at 250 nm in air-satd. soln. contg. 0.2 mol L^{-1} formate and 10^{-4} mol L^{-1} EDTA and 0.01–0.1 mol L^{-1} 1-methylimidazole; no reaction obs.	770046
276	**2-Methylimidazole, pK_a = 6.95**					
	O_2^- + 2-CH_3Im →	10.1	<0.18	e-r., s.f., opt.	D.k. at 250 nm in air-satd. soln. contg. 0.2 mol L^{-1} formate and 10^{-4} mol L^{-1} EDTA and 0.01–0.1 mol L^{-1} 2-methylimidazole; no reaction obs.	770046
277	**2-Methyl-1,4-naphthoquinone**					
	O_2^- + 2-CH_3-NQ → O_2 + 2-CH_3-NQ·$^-$	7	3.8×10^7	p.r., opt.	D.k. of semiquinone.	751090
278	**4-Methylphenyl-*N*-*tert*-butylnitrone**					
	HO_2/O_2^- + 4-CH_3-PBN → OH^- + 4-CH_3-PBN(OOH)		$<1 \times 10^6$	p.r., opt.	C.k. in O_2-satd. soln. contg. *tert*-BuOH or formate; obs. Q·$^-$ at 420 nm; rel. to $k(O_2^- + Q) = 1.0 \times 10^9$; See [80A176], limit seems high.	82A184
279	**Metmyoglobin**					
	O_2^- + ferriMb →			p.r.	No reaction detected; pH not given.	761137
280	**NADH-Lactate dehydrogenase complex**					
	HO_2 + NADH-LDH →	4.5–9	$\sim 2 \times 10^6$	p.r.	Rate calcd. from pH study.	763048
	O_2^- + NADH-LDH →	7.5–9.0	$(1.0 \pm 0.2) \times 10^5$	p.r., opt.	D.k. of NADH (varying chain length) at 380 nm in air-satd. soln. contg. 0.1 mol L^{-1} formate and 10^{-4} mol L^{-1} EDTA; pH 4.5–9.0 studied.	763048

TABLE 3. Rate constants for reactions of HO_2/O_2^- in aqueous solutions — Continued

No.	Reaction	pH	k (L mol^{-1}s^{-1})	Method	Comment	Ref.
281	**1,2-Naphthoquinone**					
	$O_2^- + 1,2\text{-NQ} \rightarrow 1,2\text{-NQ}^{\cdot -} + O_2$	7.0	7.2×10^8	p.r., opt.	P.b.k. at 365 nm in soln. contg. 5×10^{-6} mol L^{-1} quinone.	730068
282	**1,2-Naphthoquinone-4-sulfonate ion**					
	$O_2^- + 4\text{-}SO_3NQ^- \rightarrow$	7.0	8.4×10^8	p.r., opt.	P.b.k. at 365 nm in soln. contg. 5×10^{-5} mol L^{-1} quinone.	730068
283	**1,4-Naphthoquinone-2-sulfonate ion**					
	$O_2^- + 2\text{-}SO_3NQ^- \rightarrow$ $2\text{-}SO_3NQ^{\cdot 2-} + O_2$	7.0	6.6×10^8	p.r., opt.	P.b.k. at 400 nm in soln. contg. 5×10^{-5} mol L^{-1} quinone.	730068
		6.8	$(2.5 \pm 0.4) \times 10^8$	p.r., opt.	P.b.k. at 402 nm (semiquinone) in soln. contg. 0.2 mol L^{-1} glycine satd. with N_2O/O_2; same result with formate instead of glycine.	761082
284	**2-Naphthylamine**					
	$HO_2/O_2^- + 2\text{-}NpNH_2 \rightarrow$		1.3×10^7	p.r.	C.k.; rel. to $k(O_2^- + Q) = 9.5 \times 10^8$; pH not given.	78A367
285	**Nicotinamide adenine dinucleotide, reduced**					
	$HO_2 + NADH \rightarrow$ $H_2O_2 + [NAD]\cdot$	4.4–6.3	$(1.8 \pm 0.2) \times 10^5$	f.p., opt.	D.k. at 340 and 366 nm. Value calcd. from k_{obs} vs pH study. Buffered with acetate or phosphate ($I = 0.03$). O_2^- is unreactive.	79A170
	$HO_2/O_2^- + NADH \rightarrow$ $H_2O_2 + [NAD]\cdot$	5.1	$<3.5 \times 10^4$	elec., opt.	Opt. detection at 450 nm in soln. contg. 0.01 mol L^{-1} acetate.	78R209
	$O_2^- + NADH \rightarrow$ $H_2O_2 + [NAD]\cdot$	8.6	≤ 27	X-r., biol.	Estd. in soln. contg. KBr and O_2.	710158
286	**Nitro Blue Tetrazolium**					
	$O_2^- + NBT^{2+} \rightarrow O_2 + NBT^{\cdot +}$	7–11	$(5.88 \pm 0.12) \times 10^4$	phot., s.f., opt.	P.b.k. at 530 nm in soln. contg. 5×10^{-3} mol L^{-1} formate and 0.25–1.25 $\times 10^{-3}$ mol L^{-1} O_2 and 2×10^{-5} mol L^{-1} EDTA, mixed with 0.2 mol L^{-1} phosphate soln. contg. (0.4–1.8) $\times 10^{-3}$ NBT^{2+}.	80A085
		9.8	5.94×10^4	*e*-r., s.f., opt.	P.b.k. at 560 nm in air-satd. soln. contg. 0.2 mol L^{-1} formate and 2×10^{-4} mol L^{-1} EDTA and (0.2–1) $\times 10^{-3}$ mol L^{-1} NBT^{2+}; cor. for O_2^- decay.	770046
287	**4-Nitrophenyl-*N*-*tert*-butylnitrone**					
	$HO_2/O_2^- + 4\text{-}NO_2\text{-}PBN \rightarrow$ $OH^- + 4\text{-}NO_2\text{-}PBN(OOH)$		$<3 \times 10^6$	p.r., opt.	C.k. in O_2-satd. soln. contg. *tert*-BuOH or formate; obs. $Q^{\cdot -}$ at 420 nm; rel. to $k(O_2^- + Q) = 1.0 \times 10^9$; See [80A176], limit seems high.	82A184
288	**9,11-Octadecadienoate ion**					
	$O_2^- + OD^- \rightarrow$	alk.	≤ 0.01	s.f., opt.	85% v/v EtOH in 0.001–0.01 mol L^{-1} KOH/H_2O. Anaerobic conditions. D.k. at 240–270 nm. Reaction negligible. Mixture with 10,12-octadecadienoate ion.	83A087
289	**9,11-Octadecadienoic acid**					
	$HO_2 + ODH \rightarrow$	acid		s.f., opt.	85% v/v EtOH in 0.05 mol L^{-1} H_2SO_4/H_2O. Anaerobic conditions. D.k. at 240–270 nm. Mixture with 10,12-isomer. No reaction obs.	83A087
290	**Oleate ion**					
	$O_2^- + OI^- \rightarrow$	alk.	≤ 0.01	s.f., opt.	85% v/v EtOH in 0.001–0.01 mol L^{-1} KOH/H_2O. Anaerobic conditions. D.k. at 240–270 nm. Reaction negligible.	83A087
291	**Oleic acid**					
	$HO_2 + OIH \rightarrow$	acid		s.f., opt.	No reaction obs.; 85% v/v ethanolic soln.; d.k. at 240–270 nm; 0.05 mol L^{-1} H_2SO_4.	83A087

TABLE 3. Rate constants for reactions of HO_2/O_2^- in aqueous solutions — Continued

No.	Reaction	pH	k (L mol^{-1}s^{-1})	Method	Comment	Ref.
292	**Oleic acid hydroperoxide**					
	HO_2 + HO_2-OlH →	acid		s.f., opt.	D.k. at 250–270 nm in 80% EtOH soln. with 5×10^{-2} mol L^{-1} H_2SO_4, 1×10^{-5} mol L^{-1} EDTA, 1.2×10^{-3} mol L^{-1} O_2. Peroxide concn. 3.8×10^{-2} mol L^{-1}. No reaction obs.	84A909
	O_2^- + HO_2-Ol$^-$ →	alk.		s.f., opt.	D.k. at 250–270 nm in 80% EtOH soln. with 10^{-2} mol L^{-1} KOH„ 1×10^{-5} mol L^{-1} EDTA, 1.2×10^{-3} mol L^{-1} O_2. Peroxide concn. 3×10^{-3} mol L^{-1}. No reaction obs.	84A909
293	**Oxalate ion**					
	O_2^- + $^-O_2CCO_2^-$ →	10.0	<0.20	*e*-r., s.f., opt.	D.k. at 250 nm in air-satd. soln. contg. 0.2 mol L^{-1} formate and 10^{-4} mol L^{-1} EDTA and (5–50) $\times 10^{-3}$ mol L^{-1} oxalate; no reaction obs.	770046
294	**2-Oxoglutarate ion**					
	O_2^- + $^-O_2CCH_2CH_2COCO_2^-$ →	10.1	<0.30	*e*-r., s.f., opt.	D.k. at 250 nm in air-satd. soln. contg. 0.2 mol L^{-1} formate and 10^{-4} mol L^{-1} EDTA and 0.01–0.02 mol L^{-1} 2-oxoglutarate; no reaction obs.	770046
295	**Oxyhemoglobin**					
	HO_2/O_2^- + Fe^{2+} HbO_2 →	7.8	$<5 \times 10^2$	p.r., opt.	Obs. no change at 430 nm in soln. contg. O_2 and 0.16 mol L^{-1} formate; γ-r. showed slight oxidation.	78A366
		7	$(4 \pm 1) \times 10^3$	γ-r., enz.	Obs. inhibition of SOD; rel. to O_2^- + Methemoglobin.	763093
296	**Peroxidase Compound I**					
	HO_2 + HRP Compound I → HRP Compound II	3.8–8.8	2.2×10^8	p.r., opt.	D.k.; calcd. value from pH study and curve fitting; soln cont. 4.7×10^{-6} mol L^{-1} Compound I, 1.5×10^{-5} mol L^{-1} peroxide, 2.5×10^{-4} mol L^{-1} O_2, as well as phosphate and formate.	741148
	O_2^- + HRP Compound I → HRP Compound II	7.2–8.8	1.6×10^6	p.r., opt.	D.k. as well as p.b.k.	741148
297	**Peroxidase (horseradish)**					
	HO_2/O_2^- + HRP →	5.1	1.5×10^5	elec., opt.	Opt. detection at 450 nm, 0.01 mol L^{-1} acetate.	78R209
		5.0	$\sim 3.5 \times 10^8$	enz.,	Obs. formn. of oxyperoxidase at 418 nm in	733173
		5.5	$\sim 2.5 \times 10^8$	opt.	soln. contg. 0.1 mol L^{-1} acetate, 1.5×10^{-6} mol L^{-1} H_2O_2, 10^{-4} mol L^{-1} NADH, 8.4×10^{-6} mol L^{-1} HRP and $0.64–13 \times 10^{-6}$ mol L^{-1} SOD. Rel. to $k(O_2^-$ + SOD).	
298	**Peroxyhydrothymine radical**					
	HO_2/O_2^- + 5-$MeUO_2$· → O_2 + 5-$MeUO_2H$		$\sim 6 \times 10^6$	p.r., opt.	D.k. at 270 nm in oxygenated soln. contg. dihydrothymine; hydroperoxide formn. occurs at about the same rate as the second order decay of the peroxy radical; pH not given.	741151
299	**L-Phenylalanine, pK_a = 2.16, 9.1**					
	HO_2 + Phe →	1.3	$<180.0 \pm 50.0$	γ-r., s.f., opt.	D.k. in O_2—satd. soln. contg. formate and 5×10^{-5} mol L^{-1} EDTA and 0.1 mol L^{-1} phenylalanine; upper limit.	79A358
	O_2^- + Phe →	10.1	$<0.36 \pm 0.05$	phot.	C.k. with NBT^{2+} in soln. contg. 0.043 mol L^{-1} phenylalanine; no reaction obs.	79A358

TABLE 3. Rate constants for reactions of HO_2/O_2^- in aqueous solutions — Continued

No.	Reaction	pH	k (L mol^{-1}s^{-1})	Method	Comment	Ref.
300	**Phenyl-*N*-*tert*-butylnitrone**					
	$HO_2/O_2^- + PBN \rightarrow OH^- +$ PBN(OOH)		$<1 \times 10^6$	p.r., opt.	C.k. in O_2-satd. soln. contg. *tert*-BuOH or formate; obs. $Q\cdot^-$ at 420 nm; rel. to $k(O_2^- + Q) = 1.0 \times 10^9$; See [80A176], limit seems high.	82A184
301	**Phloroglucinol**					
	$HO_2 + C_6H_3(OH)_3 \rightarrow$	0.5–1.5	$(2.3 \pm 0.3) \times 10^3$	s.f., opt.	D.k. at 242 nm; soln. prepd. as in [83G122].	82Z254
302	**Plastocyanin**					
	$HO_2/O_2^- +$ Plastocyanin $\rightarrow$	8.0	$<10^6$	p.r., opt.	No reaction obs. at 290 nm in O_2-satd. soln. contg. 2×10^{-2} mol L^{-1} Na formate.	761021
303	**L-Proline, pK_a = 1.952, 10.640**					
	$HO_2 +$ Pro $\rightarrow$	1.4	$<17.3 \pm 3.0$	γ-r., s.f., opt.	D.k. in O_2-satd. soln. contg. formate ion and 5×10^{-5} mol L^{-1} EDTA and 0.1 mol L^{-1} proline; upper limit.	79A358
	O_2^- + Pro $\rightarrow$	10.0	$<0.16 \pm 0.05$	γ-r., s.f., opt.	D.k. in O_2-satd. soln. contg. formate ion and 5×10^{-5} mol L^{-1} EDTA and 0.1 mol L^{-1} proline; no reaction obs.	79A358
304	**Pyruvate ion**					
	$O_2^- + CH_3COCO_2^- \rightarrow$	10.0	<0.10	*e*-r., s.f., opt.	D.k. at 250 nm in air-satd. soln. contg. 0.2 mol L^{-1} formate and 10^{-4} mol L^{-1} EDTA and (1–10) $\times 10^{-3}$ mol L^{-1} pyruvate; no reaction obs.	770046
305	**Resorcinol**					
	$HO_2 + 1,3\text{-}C_6H_4(OH)_2 \rightarrow$	0.5–1.5	$(4.1 \pm 0.1) \times 10^3$	s.f., opt.	D.k. at 242 nm; soln. prepd. as in [83G122].	82Z254
	$O_2^- + 1,3\text{-}C_6H_4(OH)_2 \rightarrow$	5.0–8.5	2.0 ± 1	s.f., opt.	D.k. at 242 nm; soln. prepd. as in [83G122].	82Z254 83A902
306	**Riboflavin semiquinone**					
	$O_2^- +$ RFH$\cdot \rightarrow$	7	$(7.1 \pm 0.2) \times 10^8$	p.r., opt.	D.k. at 540 nm in aerated soln. contg. 0.01 mol L^{-1} formate ion and 8×10^{-5} mol L^{-1} flavin.	81A375
307	**DL-Serine, pK_a = 2.186, 9.208**					
	$HO_2 +$ Ser $\rightarrow$	1.2	$<54.6 \pm 8.0$	γ-r., s.r., opt.	D.k. in O_2-satd. soln. contg. formate and 5×10^{-5} mol L^{-1} EDTA and 0.1 mol L^{-1} serine; upper limit.	79A358
	O_2^- + Ser $\rightarrow$	9.0	$<0.53 \pm 0.04$	γ-r., s.f., opt.	D.k. in O_2-satd. soln. contg. formate and 5×10^{-5} mol L^{-1} EDTA and 0.1 mol L^{-1} serine; no reaction.	79A358
308	**Succinate ion**					
	$O_2^- + {}^-O_2CCH_2CH_2CO_2^- \rightarrow$	9.9	<0.25	*e*-r., s.f., opt.	D.k. at 250 nm in air-satd. soln. contg. 0.2 mol L^{-1} formate and 0.1 mol L^{-1} EDTA and 0.01–0.1 mol L^{-1} succinate; no reaction obs.	770046
309	**Sulfacetamide**					
	$HO_2/O_2^- +$ SA $\rightarrow$	6.5	7×10^7	p.r., opt.	P.b.k. at 470 nm ($\epsilon_{470} = 155$ L mol^{-1} cm^{-1}) in O_2-satd. soln. contg. 10^{-1} mol L^{-1} Na formate and 10^{-3} mol L^{-1} substrate.	82A138
310	**Superoxide dismutase (Co,Co)**					
	$2\ O_2^- + 2\ H_2O \xrightarrow{SOD} H_2O_2 + O_2 + 2\ OH^-$	7.4 9.4	$(1.9 \pm 0.3) \times 10^8$ $(1.5 \pm 0.2) \times 10^9$	p.r., opt.	(Co,Co) protein. D.k. at 250 nm in presence of phosphate or pyrophosphate buffer and 0.1 mol L^{-1} EtOH and 10^{-4} mol L^{-1} EDTA; also obs. d.k. and p.b.k. at 575 nm (Co). Partial inhibition in presence of phosphate leading to $k \sim 1.9$–2.3×10^8 at pH 9.4.	82R132

TABLE 3. Rate constants for reactions of HO_2/O_2^- in aqueous solutions — Continued

No.	Reaction	pH	k (L mol^{-1}s^{-1})	Method	Comment	Ref.
311	**Superoxide dismutase (Co,Zn)**					
	$2\,O_2^- + 2\,H_2O \xrightarrow{SOD} H_2O_2 + O_2 + 2\,OH^-$	7.4 9.4	$(2.3 \pm 0.3) \times 10^8$ $(1.6 \pm 0.2) \times 10^9$	p.r., opt.	(Co,Zn) protein. D.k. at 250 nm in presence of phosphate or pyrophosphate buffer and 0.1 mol L^{-1} EtOH and 10^{-4} mol L^{-1} EDTA; also obs. d.k. and p.b.k. at 575 nm (Co).	82R132
312	**Superoxide dismutase (Cu,Co)**					
	$2\,O_2^- + 2\,H_2O \xrightarrow{SOD} H_2O_2 + O_2 + 2\,OH^-$	9	$(3.23 \pm 0.14) \times 10^9$	p.r., opt.	(Cu,Co) protein. Soln. cont. 0.01 mol L^{-1} EtOH, 2×10^{-3} mol L^{-1} Na pyrophosphate, 1×10^{-4} mol L^{-1} EDTA.	77R237
		7.4	$(1.3 \pm 0.1) \times 10^9$	p.r., opt.	D.k., Cu,Co enzyme. pH not varied but system shown previously to be independent of pH.	75A243
313	**Superoxide dismutase (Fe)**					
	$2\,O_2^- + 2\,H_2O \xrightarrow{SOD} H_2O_2 + O_2 + 2\,OH^-$	8 6.2–10.1	5.5×10^8 $(6.1 \pm 1.3) \times 10^8$	p.r., opt.	D.k. at 250 nm; SOD from marine bacterium (Fe-contg.); soln. contg. 0.1 mol L^{-1} EtOH. Rate drops as pH increases. Second step as fast as first.	771127
314	**Superoxide dismutase (Mn)**					
	$2\,O_2^- + 2\,H_2O \xrightarrow{SOD} H_2O_2 + O_2 + 2\,OH^-$	6.5 10.2	7.3×10^8 1.2×10^8	p.r., opt.	D.k. at 250 nm; SOD from Bacillus stearothermophilus (Mn-contg.); soln. contg. EtOH and formate. Observed rate.	77A231
		9.5	4×10^8		D.k. at 250 nm; $k = 7.5 \times 10^9$ for human SOD (Cu-Zn contg.); $k = 3 \times 10^9$ for bovine SOD (Cu-Zn contg.). Observed rate.	769352
		7.9	$(1.3 \pm 0.15) \times 10^9$	p.r., opt.	D.k. at 248 nm; E.coli Mn enzyme. Observed rate.	743059
315	**Superoxide dismutase**					
	$2\,O_2^- + 2\,H_2O \xrightarrow{SOD} H_2O_2 + O_2 + 2\,OH^-$	7.3	1.75×10^9	f.p., opt.	Effect of bovine liver SOD on reduction rate constant of cyt C; d.k. in soln. contg. 2×10^{-2} mol L^{-1} tetramethylethylenediamine, 10^{-5} mol L^{-1} EDTA, 6×10^{-5} mol L^{-1} FMN and $\sim 10^{-5}$ mol L^{-1} cyt C and SOD; d.k. without cyt C gave $k = 1.7 \times 10^9$.	82A269
		8.0	$(5.37 \pm 0.42) \times 10^9$	p.r., opt.	D.k. at 245 nm (O_2^-); phosphate buffer.	82A448
		~8	$(1.3 \pm 0.1) \times 10^9$	p.r., opt.	D.k. at 250 nm in soln. contg. 10^{-2} mol L^{-1} formate.	81A430
		7.0	$(2.6 \pm 0.3) \times 10^9$	p.r., opt.	D.k. at 250 nm in oxygenated solution contg. 10^{-2} mol L^{-1} formate. Observed rate.	80A201
		7.8	1.8×10^9	p.r., opt.	D.k. at 250 nm in air-satd. soln. contg. 0.1 mol L^{-1} formate. Observed rate.	80A220
		7.0	3.0×10^9	p.r., opt.	D.k. at 250 nm in oxygenated soln. contg. 3×10^{-2} mol L^{-1} formate and 2–4 $\times 10^{-7}$ mol L^{-1} SOD; cor. for decay in absence of SOD; pH dependent (~4 to 7); reaction is interpreted to be $k(O_2^- + Cu^{II}) = k(O_2^- + Cu^{I}) = k(HO_2 + Cu^{II})$ and pH dependence due to conversion of SOD to inactive form by H^+. Observed rate.	80A391
		7.2	$(1.6 \pm 0.64) \times 10^9$	p.r., opt.	D.k.; protein from E. gracilis gave $k = (8.13 \pm 0.36) \times 10^9$. Observed rate.	79R055
		8.9	5.6×10^8	p.r.	D.k. at 480 nm. Other rates detd. by data fitting with model.	77A194
		8–9	$(3.70 \pm 0.18) \times 10^9$	p.r., opt.	Soln. cont. 1×10^{-4} mol L^{-1} EDTA, 0.1 mol L^{-1} EtOH, 5×10^{-4} mol L^{-1} sodium pyrophosphate; $k = (3.30 \pm 0.16) \times 10^9$ in soln. contg. 2×10^{-3} mol L^{-1} Na pyrophosphate and 0.085 mol L^{-1} EtOH.	77A275

TABLE 3. Rate constants for reactions of HO_2/O_2^- in aqueous solutions — Continued

No.	Reaction	pH	k (L mol^{-1}s^{-1})	Method	Comment	Ref.
		9	$(3.15 \pm 0.14) \times 10^9$	p.r., opt.	Soln. cont. 0.01 mol L^{-1} EtOH, 2×10^{-3} mol L^{-1} Na pyrophosphate, 1×10^{-4} mol L^{-1} EDTA.	77R237
		7.2	$(2.3 \pm 0.2) \times 10^9$	p.r., opt.	Obs. decrease in transmittance at 550 nm (Fe^{3+} cyt C), soln. also contains EDTA, phosphate buffer and formate; observed rate.	761163
		10.1	0.73×10^9	KO_2, s.f., opt.	D.k. at 275 nm in soln. contg. borate and EDTA and bovine SOD contg. Cu. Observed rate.	769257
		7.5–7.7	$(1.3 \pm 0.1) \times 10^9$	p.r., opt.	D.k. at 245 nm in O_2-satd. soln. contg. formate ion 10^{-4} mol L^{-1} EDTA and (1–5) $\times$ 10^{-6} mol L^{-1} Cu,Zn enzyme; k per equivalent of Cu; same result in presence of 0.11 g L^{-1} bovine serum albumin. pH not varied but system shown previously to be independent of pH.	75A243
		9.0–9.9	$(2.37 \pm 0.18) \times 10^9$	p.r., opt.	D.k. at 250 nm; bovine Cu-Zn enzyme; supersedes [723066].	743017
		9–10.2	2.3×10^9	elec., pol.	Obs. increased O_2 formn. with enzyme addn.	743132
		7.5	$(1.2 \pm 0.2) \times 10^9$	p.r., opt.	D.k. at 650 nm; soln. contains Na formate and EDTA; enzyme from bovine blood. Observed rate.	730109
		5.0–9.5	$\sim 2 \times 10^9$	chem., biol., opt.	C.k. (bovine Cu-Zn enzyme); assume $k(O_2^- + \text{cyt C}) = 1.1 \times 10^5$ and $k(O_2^- + \text{TNM}) = 1.9 \times 10^9$; also detd. for Mn and Fe-contg. enzymes.	733052
		5.7–10.5	1.5×10^9	p.r., opt.	D.k. at 690 nm; Cu enzyme from human blood.	733132
		7	$(1.4 \pm 0.2) \times 10^9$	p.r., opt.	D.k. at 245 nm; enzyme from bovine blood	721007
		4.8–9.5	2.3×10^9	p.r., opt.	k studied as a function of pH.	723078
316	**Tartrate ion**					
	$O_2^- + (CHOHCO_2^-)_2 \rightarrow$	10.1	<0.14	e-r., s.f., opt.	D.k. at 250 nm in air-satd. soln. contg. 0.2 mol L^{-1} formate and 10^{-4} mol L^{-1} EDTA and 0.01–0.1 mol L^{-1} tartrate; no reaction.	770046
317	**1,1'-Tetramethylene-2,2'-bipyridinium radical ion (1+)**					
	$O_2^- + BP^{\cdot+} \rightarrow$	6.8	$(13.0 \pm 1) \times 10^8$	p.r.	Ar-satd. soln. cont. 10^{-3} mol L^{-1} BP^{2+} $2Cl^-$, 0.1 mol L^{-1} Na formate and $\sim$0.3% O_2.	78A321
318	**2,2,6,6-Tetramethylpiperidine-*N*-oxyl**					
	$HO_2/O_2^- + \text{TEMPO} \rightarrow$	9.2	730		Calcd. rate. Soln. cont. 0.1 mol L^{-1} borate, 2×10^{-4} mol L^{-1} EDTA, 10^{-7} mol L^{-1} catalase; phosphate adjusted.	79A184
319	**2,2,6,6-Tetramethylpiperidin-1-ol**					
	$HO_2/O_2 + \text{TEMPOH} \rightarrow$	7.8	1.7×10^3	enz., opt.	C.k. in xanthine oxidase system, rel. to $k(O_2^- + \text{cyt C})^- = 6 \times 10^5$.	82R165
320	**Tetranitromethane**					
	$HO_2 + C(NO_2)_4 \rightarrow NO_2 + H^+ + C(NO_2)_3^- + O_2$	0–6	$< 10^5$	p.r., opt.	P.b.k.; calcd. value from rate equation and pH study.	650183
	$O_2^- + C(NO_2)_4 \rightarrow NO_2 + C(NO_2)_3^- + O_2$	5.6–6.2	$(1.9 \pm 0.4) \times 10^9$	p.r., opt.	P.b.k.; pH 0–6.2 studied.	650183
			$(2.0 \pm 0.4) \times 10^9$	p.r., opt.	P.b.k.; pH not given.	640133
321	**DL-Threonine, $pK_a = 2.088, 9.10$**					
	$HO_2 + \text{Thr} \rightarrow$	1.4	$<12.5 \pm 4.0$	γ-r., s.f., opt.	D.k. in O_2-satd. formate soln. contg. 5×10^{-5} mol L^{-1} EDTA and 0.1 mol L^{-1} threonine; upper limit.	79A358
	$O_2^- + \text{Thr} \rightarrow$	10.1	$<0.21 \pm 0.05$	γ-r., s.f., opt.	D.k. in O_2-satd. soln. contg. formate and 5×10^{-5} mol L^{-1} EDTA and 0.15 mol L^{-1} threonine; no reaction.	79A358

TABLE 3. Rate constants for reactions of HO_2/O_2^- in aqueous solutions — Continued

No.	Reaction	pH	k (L mol^{-1}s^{-1})	Method	Comment	Ref.
322	**α-Tocopherol**					
	$HO_2 + C_{29}H_{50}O_2 \rightarrow$	acid	2.0×10^5	s.f., opt.	Soln. cont. 0.022 mol L^{-1} H_2SO_4, 85% EtOH, and 0.025–0.1 mol L^{-1} α-tocopherol.	82A403
	$O_2^- + C_{29}H_{50}O_2 \rightarrow$	alk.		s.f., opt.	Soln. cont. 0.01 mol L^{-1} KOH, 85% EtOH, and 0.025 -0.1 mol L^{-1} α-tocopherol. No reaction obs.	82A403
323	**Tributylammoniobutyldioxy**					
	$O_2^- + (C_4H_9)_3N^+(O_2C_4H_8) \rightarrow O_3^-$	~12–13	6×10^7	p.r., opt.	P.b.k. (O_3^-) in soln. contg. O_2, 0.1 mol L^{-1} KOH and R_4N^+. Concn. of O_2^- and cation varied.	78A095
324	**Triethylammonioethyldioxy**					
	$O_2^- + (C_2H_5)_3N^+(O_2CHCH_3) \rightarrow O_3^-$	~12–13	4×10^8	p.r., opt.	P.b.k. (O_3^-) in soln. contg. O_2, 0.1 mol L^{-1} KOH and R_4N^+. Concn. of O_2^- and cation varied.	78A095
325	**Trimethylammoniomethyldioxy**					
	$O_2^- + (CH_3)_3N^+(O_2CH_2) \rightarrow O_3^-$	~12–13	3×10^8	p.r., opt.	P.b.k. (O_3^-) in soln. contg. O_2, 0.1 mol L^{-1} KOH and R_4N^+. Concn. of O_2^- and cation varied.	78A095
326	**1,1'-Trimethylene-2,2'-bipyridinium radical ion (1+)**					
	$O_2^- + BP^{\cdot+} \rightarrow$	6.8	$(12.0 \pm 1) \times 10^8$	p.r.	Ar-satd. soln. contg. 10^{-3} mol L^{-1} BP^{2+} $2Cl^-$ and 0.1 mol L^{-1} formate and ~0.3% O_2.	78A321
327	**2,5,5-Trimethyl-1-pyrroline *N*-oxide**					
	$HO_2/O_2^- + TMPO \rightarrow$	7.8	7	enz., esr	Spin trapping; c.k. with SOD; rel. to $k(O_2^- + Fe^{3+}$ cyt C) $= 6 \times 10^5$.	80A176
		8.1	1.44	enz., esr	Spin trapping; rel. to $k(O_2^- + O_2^-) = 5.1 \times 10^4$. Xanthine-xanthine oxidase system.	80A176
328	**Tripropylammoniopropyldioxy**					
	$O_2^- + (C_3H_7)_3N^+(O_2C_3H_6) \rightarrow O_3^-$	~12–13	8×10^7	p.r., opt.	P.b.k. (O_3^-) in soln. contg. O_2, 0.1 mol L^{-1} KOH and R_4N^+. Concn. of O_2^- and cation varied.	78A095
329	**Tris(hydroxymethyl)aminomethane**					
	$O_2^- + (HOCH_2)_3CNH_2 \rightarrow$	10.1	<0.001	s.f., opt.	D.k. at 250 nm in air-satd. soln. contg. 0.2 mol L^{-1} formate and 10^{-4} mol L^{-1} EDTA and 0.01–0.1 mol L^{-1} substrate; no reaction.	770046
330	**L-Tryptophan, pK_a = 2.43, 9.44, 11.73**					
	$O_2^- + TrpH \rightarrow$	10.6	$<24.0 \pm 3.00$	phot., opt.	C.k. with NBT^{2+}; obs. at 560 nm in soln. contg. 5×10^{-5} mol L^{-1} EDTA and 0.02 mol L^{-1} tryptophan; no reaction.	79A358
331	**L-Tyrosine, pK_a = 2.2, 9.2, 10.5**					
	$O_2^- + TyrOH \rightarrow$	10.8	$<10.00 \pm 2.00$	phot., opt.	C.k. with NBT^{2+}; obs. at 560 nm in soln. contg. 5×10^{-5} mol L^{-1} EDTA and 0.005 mol L^{-1} tyrosine; no reaction.	79A358
332	**DL-Valine, pK_a = 2.3, 9.7**					
	$HO_2 + Val \rightarrow$	1.5	$<10.5 \pm 1.3$	γ-r., s.f., opt.	D.k. in O_2-satd. soln. contg. formate and 5×10^{-5} mol L^{-1} EDTA and 0.1 mol L^{-1} valine; upper limit.	79A358
	$O_2^- + Val \rightarrow$	10.1	$<0.18 \pm 0.02$	γ-r., s.f., opt.	D.k. in O_2-satd. soln. contg. formate and 5×10^{-5} mol L^{-1} EDTA and 0.15 mol L^{-1} valine; no reaction obs.	79A358
333	**Vitamin K_1**					
	$HO_2/O_2^- + Me(phytyl)NQ \rightarrow Me(phytyl)NQ^{\cdot-} + O_2$	7	$<2 \times 10^5$	p.r., opt.	Detd. from equil. const. and d.k. of semiquinone. Soln. contg. 7 mol L^{-1} 2-PrOH and 1 mol L^{-1} acetone.	730125

9. References to Table 3

530014 The primary radical yield in water. A comparison of the photolysis and radiolysis of solutions of hydrogen peroxide. Dainton, F.S.; Rowbottom, J. Trans. Faraday Soc. **49**: 1160–73 (1953).

570010 Studies in the radiolysis of ferrous sulfate solutions. II. Effect of acid concentration in solutions containing oxygen. Allen, A.O.; Hogan, V.D.; Rothschild, W.G. Radiat. Res. **7**: 603–8 (1957).

580004 Studies in the radiolysis of ferrous sulfate solutions. III. Air-free solutions at higher pH. Rothschild, W.G.; Allen, A.O. Radiat. Res. **8**: 101–110 (1958).

600102 Effect of ferric ion on the γ-ray induced oxidation of ferrous ion. Dobson, G.; Hughes, G. Trans. Faraday Soc. **57**: 1117–22 (1960).

620050 The flash photolysis of water and aqueous solutions. Baxendale, J.H. Radiat. Res. **17**: 312–26 (1962).

630075 The formation and decay of H_2O_3 and HO_2 in electron-irradiated aqueous solutions. Czapski, G.; Bielski, B.H.J. J. Phys. Chem. **67**: 2180–4 (1963).

639017 The kinetics of the oxidation of hydrogen peroxide by cerium(IV). Czapski, G.; Bielski, B.H.J.; Sutin, N. J. Phys. Chem. **67**: 201–3 (1963).

640050 Catalyse d'oxydations radiolytiques en solution aqueuse par le tetroxyde d'osmium. Dran, J.-C.; Haissinsky, M. J. Chim. Phys. **61**. 1421–7 (1964).

640090 Pulse radiolysis of ferrous sulfate solution. Keene, J.P. Radiat. Res. **22**: 14–20 (1964).

640133 Pulsradiolytische Untersuchung schneller Reaktionen von hydratisierten Elektronen, freien Radikalen und Ionen mit Tetranitromethan in waessriger Loesung. Asmus, K.-D.; Henglein, A.; Ebert, M.; Keene, J.P. Ber. Bunsenges. Phys. Chem. **68**: 657–63 (1964).

650007 Spectroscopic studies of reactions of the OH radical in aqueous solutions. Reaction of OH with the ferrocyanide ion. Adams, G.E.; Boag, J.W.; Michael, B.D. Trans. Faraday Soc. **61**: 492–505 (1965).

650046 Photolysis and radiolysis of concentrated aqueous solutions of hydrogen peroxide. Currie, D.J.; Dainton, F.S. Trans. Faraday Soc. **61**: 1156–65 (1965).

650055 Radiolysis of aerated solutions of potassium bromide. Rafi, A.; Sutton, H.C. Trans. Faraday Soc. **61**: 877–90 (1965).

650183 The pulse radiolysis of aqueous tetranitromethane. I. Rate constants and the extinction coefficient of e_{aq}^-. II. Oxygenated solutions. Rabani, J.; Mulac, W.A.; Matheson, M.S. J. Phys. Chem. **69**: 53–70 (1965).

650382 Radical yields and kinetics in the pulse radiolysis of potassium bromide solutions. Sutton, H.C.; Adams, G.E.; Boag, J.W.; Michael, B.D. *Pulse Radiolysis*, p.61–81, Ebert, M.; Keene, J.P.; Swallow, A.J.; Baxendale, J.H. (eds.), Academic Press, New York (1965).

650383 Pulse radiolysis of aerated aqueous potassium bromide solutions. Cercek, B.; Ebert, M.; Gilbert, C.W.; Swallow, A.J. *Pulse Radiolysis*, p.83–98, Ebert, M.; Keene, J.P.; Swallow, A.J.; Baxendale, J.H. (eds.), Academic Press, New York (1965).

650385 Determination of some fast reaction rates using the pulsed radiolysis of permanganate solutions. Baxendale, J.H.; Keene, J.P.; Stott, D.A. *Pulse Radiolysis*, p.107–15, Ebert, M.; Keene, J.P.; Swallow, A.J.; Baxendale, J.H. (eds.), Academic Press, New York (1965).

650386 The pulse radiolysis of aqueous solutions of thiocyanate ion. Adams, G.E.; Boag, J.W.; Currant, J.; Michael, B.D. *Pulse Radiolysis*, p.117–29, Ebert, M.; Keene, J.P.; Swallow, A.J.; Baxendale, J.H. (eds.), Academic Press, New York (1965).

660001 Transient species produced in irradiated water and aqueous solutions containing oxygen. Adams, G.E.; Boag, J.W.; Michael, B.D. Proc. Roy. Soc. (London) Ser. A **289**: 321–41 (1966).

660097 Novel valence states of thallium as studied by pulse radiolysis. Cercek, B.; Ebert, M.; Swallow, A.J. J. Chem. Soc. Pt. A 612–5 (1966).

670037 The influence of ethylene on the radiolytic oxidation of ferrous sulphate. Basson, R.A.; du Plessis, T.A. J. Chem. Soc. Pt. A 778–781 (1967).

670737 Peroxide formation in the radiolysis of aqueous hydrocarbon solutions. Shastri, L.V.; Srinivasan, K.; Rama Rao, K.V.S. *Proc. Nuclear and Radiation Chemistry Symposium*, Poona, India, March 6–9, 1967.

677012 Flash photolysis in the vacuum ultraviolet region of SO_4^{2-}, CO_3^{2-}, and OH^- ions in aqueous solutions. Hayon, E.; McGarvey, J.J. J. Phys. Chem. **71**: 1472–7 (1967).

680014 Rate constants of OH with HO_2, O_2^-, and $H_2O_2^+$ from hydrogen peroxide formation in pulse-irradiated oxygenated water. Sehested, K.; Rasmussen, O.L.; Fricke, H. J. Phys. Chem. **72**: 626–31 (1968).

680059 Geschwindigkeitskonstanten der Reaktion einiger Farbstoffe mit HO_2-Radikalen und hydratisierten Elektronen, gebildet durch ^{60}Co-γ-Radiolyse von waessrigen Loesungen. Rakintzis, N.Th. Z. Phys. Chem. (Frankfurt Am Main) **57**: 99–102 (1968).

680356 Radiolyse de solutions aqueuses du tellure par les rayons γ. III. Solutions acides. Haissinsky, M. J. Chim. Phys. **65**: 1386–92 (1968).

690413 Reactions of H_2O_3 in the pulse-irradiated Fe(II)-O_2 system. Sehested, K.; Bjergbakke, E.; Rasmussen, O.L.; Fricke, H. J. Chem. Phys. **51**: 3159–66 (1969).

690434 Pulse-radiolysis study of some unstable complexes of iron. Jayson, G.G.; Keene, J.P.; Stirling, D.A.; Swallow, A.J. Trans. Faraday Soc. **65**: 2453–64 (1969).

690642 Comportement cinetique des radicaux HO_2 et de leur forme acide vis-a-vis des ions ferreux et ferriques. Pucheault, J.; Ferradini, C.; Buu, A. Int. J. Radiat. Phys. Chem. **1**: 209–18 (1969).

690643 Radiolyse de solutions acides et aerees de peroxyde d'hydrogene. Ferradini, C.; Seide, C. Int. J. Radiat. Phys. Chem. **1**: 219–28 (1969).

697082 The photochemical decomposition of hydrogen peroxide in the presence of bivalent copper ions. Berdnikov, V.M.; Kozlov, Yu.N.; Purmal, A.P. Khim. Vys. Energ. **3**: 321–4 (1969).

699128 Direct demonstration of superoxide anion production during the oxidation of reduced flavin and of its catalytic decomposition by erythrocuprein. Ballou, D.; Palmer, G.; Massey, V. Biochem. Biophys. Res. Commun. **36**: 898–904 (1969).

700247 Carbonate radical in flash photolysis and pulse radiolysis of aqueous carbonate solutions. Behar, D.; Czapski, G.; Duchovny, I. J. Phys. Chem. **74**: 2206–10 (1970).

700882 The radiolysis of oxygenated cysteine solutions at neutral pH. The role of RSSR and O_2^-. Barton, J.P.; Packer, J.E. Int. J. Radiat. Phys. Chem. **2**: 159–66 (1970).

709058 ESR study of a complex formation between HO_2 radical and peroxy-vanadium (V) ion. Samuni, A.; Czapski, G. Isr. J. Chem. **8**: 563–73 (1970).

710158 One-electron reactions in biochemical systems as studied by pulse radiolysis. IV. Oxidation of dihydronicotinamide-adenine dinucleotide. Land, E.J.; Swallow, A.J. Biochim. Biophys. Acta **234**: 34–42 (1971).

710327 One-electron reactions in biochemical systems as studied by pulse radiolysis. V. Cytochrome c. Land, E.J.; Swallow, A.J. Arch. Biochem. Biophys. **145**: 365–72 (1971).

710619 Pulse radiolysis studies of electron transfer in aqueous quinone solutions. Willson, R.L. Trans. Faraday Soc. **67**: 3020–9 (1971).

720308 Reactions of the HO_2 radical in aqueous solution with bromine and related compounds. Sutton, H.C.; Downes, M.T. J. Coated Fabr. **68**: 1498–507 (1972).

720404 Electrical conductivity techniques for studying the kinetics of radiation-induced chemical reactions in aqueous solutions. Schmidt, K.H. Int. J. Radiat. Phys. Chem. **4**: 439–68 (1972).

720431 Pulse radiolysis of the aqueous ferro-ferricyanide system. I. The reactions of OH, HO_2, and O_2^- radicals. Zehavi, D.; Rabani, J. J. Phys. Chem. **76**: 3703–9 (1972).

721007 Decay of the HO_2 and O_2^- radicals catalyzed by superoxide dismutase. A pulse radiolytic investigation. Rabani, J.; Klug, D.; Fridovich, I. Isr. J. Chem. **10**: 1095–1106 (1972).

723066 A pulse radiolysis study of superoxide dismutase. Rotilio, G.; Bray, R.C.; Fielden, E.M. Biochim. Biophys. Acta **268**: 605–9 (1972).

723078 A direct demonstration of the catalytic action of superoxide dismutase through the use of pulse radiolysis. Klug, D.; Rabani, J.; Fridovich, I. J. Biol. Chem. **247**: 4839–42 (1972).

730038 Oxidation of ferrous ions by perhydroxyl radicals. Jayson, G.G.; Parsons, B.J.; Swallow, A.J. J. Chem. Soc., Faraday Trans. 1 **69**: 236–42 (1973).

730049 Comparison between the electron transfer reactions from free radicals and their corresponding peroxy radicals to quinones. Simic, M.; Hayon, E. Biochem. Biophys. Res. Commun. **50**: 364–9 (1973).

730068 Experimental determination of the redox potential of the superoxide radical $\cdot O_2^-$. Rao, P.S.; Hayon, E. Biochem. Biophys. Res. Commun. **51**: 468–73 (1973).

730109 Pulse radiolytic investigations of superoxide catalyzed disproportionation. Mechanism for bovine superoxide dismutase. Klug-Roth, D.; Fridovich, I.; Rabani, J. J. Am. Chem. Soc. **95**: 2786–90 (1973).

730112 Pulse radiolytic investigations of the catalyzed disproportionation of peroxy radicals. Aqueous cupric ions. Rabani, J.; Klug-Roth, D.; Lilie, J. J. Phys. Chem. **77**: 1169–75 (1973).

730116 The reduction of cobalamin. A pulse radiolysis study. Faraggi, M.; Leopold, J.G. Biochem. Biophys. Res. Commun. **50**: 413–20 (1973).

730125 Semiquinone free radicals and oxygen. Pulse radiolysis study of one electron transfer equilibria. Patel, K.B.; Willson, R.L. J. Chem. Soc.. Faraday Trans. 1 **69**: 814–25 (1973).

731074 Bipyridylium quaternary salts and related compounds. V. Pulse radiolysis studies of the reaction of paraquat radical with oxygen. Implications for the mode of action of bipyridyl herbicides. Farrington, J.A.; Ebert, M.; Land, E.J.; Fletcher, K. Biochim. Biophys. Acta **314**: 372–81 (1973).

733052 Superoxide dismutase. A comparison of rate constants. Forman, H.J.; Fridovich, I. Arch. Biochem. Biophys. **158**: 396–400 (1973).

733132 The superoxide dismutase activity of human erythrocuprein. Bannister, J.V.; Bannister, W.H.; Bray, R.C.; Fielden, E.M.; Roberts, P.B.; Rotilio, G. FEBS (Fed. Eur. Biochem. Soc.) Lett. **32**: 303–6 (1973).

733173 One-electron transfer reactions in biochemical systems. VIII. Kinetic study of superoxide dismutase. Sawada, Y.; Yamazaki, I. Biochim. Biophys. Acta **327**: 257–65 (1973).

737514 Photodecomposition of hydrogen peroxide in the presence of copper ions. IV. Determination of rate constants of elementary reactions. Kozlov, Yu.N.; Berdnikov, V.M. Russ. J. Phys. Chem. (Engl. Transl.) **47**: 338–40 (1973) Translated from: Zh. Fiz. Khim. 47(3): 598–602 (1973).

739071 Hydroperoxyl radical reactions. I. Electron paramagnetic resonance study of the complexation of HO_2 with some metal ions. Meisel, D.; Czapski, G.; Samuni, A. J. Am. Chem. Soc. **95**: 4148–53 (1973).

740188 The radiolysis of aqueous solutions of cysteine in the presence of oxygen. Al-Thannon, A.A.; Barton, J.P.; Packer, J.E.; Sims, R.J.; Trumbore, C.N.; Winchester, R.V. Int. J. Radiat. Phys. Chem. **6**: 233–48 (1974).

741107 Hydroperoxyl radical reactions. III. Pulse-radiolytic study of the reaction of the hydroperoxyl radical with some metal ions. Meisel, D.; Ilan, Y.A.; Czapski, G. J. Phys. Chem. **78**: 2330–4 (1974).

741148 Study of peroxidase mechanisms by pulse radiolysis. III. The rate of reaction of O_2^- and HO_2 radicals with horseradish peroxidase compound I. Bielski, B.H.J.; Gebicki, J.M. Biochim. Biophys. Acta **364**: 233–5 (1974).

741151 Formation and decay of peroxy radicals of some pyrimidine derivatives in water. Simic, M.; Hayon, E. FEBS (Fed. Eur. Biochem. Soc.) Lett. **44**: 334–6 (1974).

741163 Superoxide dismutase activity of low molecular weight Cu^{2+}-chelates studied by pulse radiolysis. Brigelius, R.; Spoettl, R.; Bors, W.; Lengfelder, E.; Saran, M.; Weser, U. FEBS (Fed. Eur. Biochem. Soc.) Lett. **47**: 72–5 (1974).

743017 The mechanism of action of superoxide dismutase from pulse radiolysis and electron paramagnetic resonance. Evidence that only half the active sites function in catalysis. Fielden, E.M.; Roberts, P.B.; Bray, R.C.; Lowe, D.J.; Mautner, G.N.; Rotilio, G.; Calabrese, L. Biochem. J. **139**: 49–60 (1974).

743059 The catalytic mechanism of the manganese-containing superoxide dismutase of Escherichia coli studied by pulse radiolysis. Pick, M.; Rabani, J.; Yost, F.; Fridovich, I. J. Am. Chem. Soc. **96**: 7329–33 (1974).

743132 Determination of the superoxide dismutase activity and rate constants by the polarographic catalytic currents method. Rigo, A.; Tomat, R.; Rotilio, G. J. Electroanal. Chem. Interfacial Electrochem. **57**: 291–6 (1974).

750347 Reactions of the hydroperoxyl radical (HO_2) with nitrogen dioxide and tetranitromethane in aqueous solution. Sutton, H.C. J. Chem. Soc., Faraday Trans. 1 **71**: 2142–7 (1975).

750403 Influence des ions NO_2^- dans les radiolyses γ de solutions aqueuses neutres de tetranitromethane et formiate. Julien, R. Int. J. Radiat. Phys. Chem. **7**: 741–8 (1975).

751011 Redox potentials of free radicals. IV. Superoxide and hydroperoxy radicals $\cdot O_2^-$ and $\cdot HO_2$. Rao, P.S.; Hayon, E. J. Phys. Chem. **79**: 397–402 (1975).

751012 Free radical reduction of ferricytochrome-C. Simic, M.G.; Taub, I.A.; Tocci, J.; Hurwitz, P.A. Biochem. Biophys. Res. Commun. **62**: 161–7 (1975).

751031 Oxidation of ascorbic acid with superoxide anion generated by the xanthine-xanthine oxidase system. Nishikimi, M. Biochem. Biophys. Res. Commun. **63**: 463–8 (1975).

751087 The oxidation of tiron by superoxide anion. Kinetics of the reaction in aqueous solution and in chloroplasts. Greenstock, C.L.; Miller, R.W. Biochim. Biophys. Acta **396**: 11–6 (1975).

751090 One-electron transfer equilibria and redox potentials of radicals studied by pulse radiolysis. Meisel, D.; Czapski, G. J. Phys. Chem. **79**: 1503–9 (1975).

751194 Radiation chemical studies of the sensitizer Diamide. Whillans, D.W.; Neta, P. Radiat. Res. **64**: 416–30 (1975).

753093 The reaction between the superoxide anion radical and cytochrome c. Butler, J.; Jayson, G.G.; Swallow, A.J. Biochim. Biophys. Acta **408**: 215–22 (1975).

759347 Electrochemical generation and reactivity of the superoxide ion in aqueous solutions. Divisek, J.; Kastening, B. J. Electroanal. Chem. Interfacial Electrochem. **65**: 603–21 (1975).

75A243 Superoxide dismutase activity of $Cu(Tyr)_2$ and Cu, Co-erythrocuprein. Brigelius, R.; Hartmann, H.-J.; Bors, W.; Saran, M.; Lengfelder, E.; Weser, U. Hoppe-Seyler's Z. Physiol. Chem. **356**: 739–45 (1975).

75R176 Oxidation of α-tocopherol model compound by superoxide anion. Nishikimi, M.; Machlin, L.J. Arch. Biochem. Biophys. **170**: 684–9 (1975).

761021 Pulse radiolytic studies on reactions of aqueous superoxide radicals with copper(II) complexes. Klug-Roth, D.; Rabani, J. J. Phys. Chem. **80**: 588–91 (1976).

761038 Reactions of oxygen radical species with methional: A pulse radiolysis study. Bors, W.; Lengfelder, E.; Saran, M.; Fuchs, C.; Michel, C. Biochem. Biophys. Res. Commun. **70**: 81–7 (1976).

761056 Determination of superoxide (O_2^-) radical anion reaction rates using pulse radiolysis. Greenstock, C.L.; Ruddock, G.W. Int. J. Radiat. Phys. Chem. **8**: 367–9 (1976).

761063 The one-electron transfer redox potentials of free radicals. I. The oxygen/superoxide system. Ilan, Y.A.; Czapski, G.; Meisel, D. Biochim. Biophys. Acta **430**: 209–24 (1976).

761071 One-electron reduction of a ferrihaem. Butler, J.; Jayson, G.G.; Swallow, A.J. J. Chem. Soc., Faraday Trans. 1 **72**: 1391–402 (1976).

761082 Pulse radiolytic investigations of peroxy radicals in aqueous solutions of acetate and glycine. Abramovitch, S.; Rabani, J. J. Phys. Chem. **80**: 1562–5 (1976).

761109 Pulse radiolytic studies of aqueous $Mn(ClO_4)_2$ solutions. Pick-Kaplan, M.; Rabani, J. J. Phys. Chem. **80**: 1840–3 (1976).

761127 Reactions of the ferri-ferrocytochrome-c system with superoxide/oxygen and CO_2^-/CO_2 studied by fast pulse radiolysis. Seki, H.; Ilan, Y.A.; Ilan, Y.; Stein, G. Biochim. Biophys. Acta **440**: 573–86 (1976).

761132 On some fundamental reactions in radiation chemistry: Nanosecond pulse radiolysis. Ilan, Y.; Rabani, J. Int. J. Radiat. Phys. Chem. **8**: 609–11 (1976).

761137 One electron reduction of metmyoglobin and methemoglobin and the reaction of the reduced molecule with oxygen. Ilan, Y.A.; Rabani, J.; Czapski, G. Biochim. Biophys. Acta **446**: 277–86 (1976).

761140 Steady state and pulse radiolysis studies of molybdenum octacyanate in aqueous solution. Faraggi, M. J. Phys. Chem. **80**: 2316–20 (1976).

761163 The kinetics of the reduction of cytochrome c by the superoxide anion radical. Koppenol, W.H.; Van Buuren, K.J.H.; Butler, J.; Braams, R. Biochim. Biophys. Acta **449**: 157–68 (1976).

763048 Re-evaluation of the kinetics of lactate dehydrogenase-catalyzed chain oxidation of nicotinamide adenine dinucleotide by superoxide radicals in the presence of ethylenediaminetetraacetate. Bielski, B.H.J.; Chan, P.C. J. Biol. Chem. **251**: 3841–4 (1976).

763093 The rate of reaction of superoxide radical ion with oxyhaemoglobin and methaemoglobin. Sutton, H.C.; Roberts, P.B.; Winterbourn, C.C. Biochem. J. **155**: 503–10 (1976).

767025 Photoreduction of hydrogen peroxide by hydrogen. Field, R.J.; Noyes, R.M.; Postlethwaite, D. J. Phys. Chem. **80**: 223–9 (1976).

769257 Stopped flow spectrophotometric observation of superoxide dismutation in aqueous solution. McClune, G.J.; Fee, J.A. FEBS (Fed. Eur. Biochem. Soc.) Lett. **67**: 294–8 (1976).

769352 Spectrophotometric study of spontaneous disproportionation of superoxide anion radical and sensitive direct assay for superoxide dismutase. Marklund, S. J. Biol. Chem. **251**: 7504–7 (1976).

76R183 Reactivity of thiols with superoxide radicals. Asada, K.; Kanematsu, S. Agr. Biol. Chem. **40**: 1891–2 (1976).

76R190 Oxidation of manganous pyrophosphate by superoxide radicals and illuminated spinach chloroplasts. Kono, Y.; Takahashi, M.-A.; Asada, K. Arch. Biochem. Biophys. **174**: 454–62 (1976).

770046 A study of the superoxide radical chemistry by stopped-flow radiolysis and radiation induced oxygen consumption. Bielski, B.H.J.; Richter, H.W. J. Am. Chem. Soc. **99**: 3019–23 (1977).

771028 Addition of superoxide radical anion to cobalt(II) macrocyclic complexes in aqueous solution. Simic, M.G.; Hoffman, M.Z. J. Am. Chem. Soc. **99**: 2370–1 (1977).

771088 The reaction of superoxide radical with iron complexes of EDTA studied by pulse radiolysis. Ilan, Y.A.; Czapski, G. Biochim. Biophys. Acta **498**: 386–94 (1977).

771096 $H/^2H$ isotope effect in redox reactions of cytochrome c. Ilan, Y.; Shinar, R.; Stein, G. Biochim. Biophys. Acta **461**: 15–24 (1977).

771127 A pulse-radiolysis study of the catalytic mechanism of the iron-containing superoxide dismutase from Photobacterium leiognathi. Lavelle, F.; McAdam, M.E.; Fielden, E.M.; Roberts, P.B.; Puget, K.; Michelson, M. Biochem. J. **161**: 3–11 (1977).

771130 Use of the method of pulsed radiolysis to investigate the properties of americium(IV) in aqueous solutions. Pikaev, A.K.; Shilov, V.P.; Spitsyn, V.I. Dokl. Phys. Chem. **232**: 70–3 (1977) Translated from: Dokl. Akad. Nauk SSSR **232**: 387–90 (1977).

779154 An attempt to evaluate the rate of the Haber-Weiss reaction by using OH radical scavengers. Rigo, A.; Stevanato, R.; Finazzi-Agro, A.; Rotilio, G. FEBS Lett. **80**: 130–2 (1977).

77A194 A pulse-radiolysis study of the manganese-containing superoxide dismutase from Bacillus stearothermophilus. A kinetic model for the enzyme action. McAdam, M.E.; Fox, R.A.; Lavelle, F.; Fielden, E.M. Biochem. J. **165**: 71–9 (1977).

77A231 A pulse-radiolysis study of the manganese-containing superoxide dismutase from Bacillus stearothermophilus. Further studies on the properties of the enzyme. McAdam, M.E.; Lavelle, F.; Fox, R.A.; Fielden, E.M. Biochem. J. **165**: 81–7 (1977).

77A275 A consideration of the effects of added solutes on the activity of bovine superoxide dismutase. McAdam, M.E. Biochem. J. **161**: 697–9 (1977).

77R237 The involvement of the bridging imidazolate in the catalytic mechanism of action of bovine superoxide dismutase. McAdam, M.E.; Fielden, E.M.; Lavelle, F.; Calabrese, L.; Cocco, D.; Rotilio, G. Biochem. J. **167**: 271–4 (1977).

77R240 Formation of active oxygen and its fate in chloroplasts. Asada, K.; Takahashi, M.; Tanaka, K.; Nakano, Y. *Biochemical and Medical Aspects of Active Oxygen*, p.45–63, O. Hayaishi and K. Asada (eds.), University Park Press, Tokyo (1977).

78A095 Pulse radiolysis of tetraalkylammonium hydroxides in alkaline solution containing oxygen. Bobrowski, K.; Suwalski, J.P.; Zagorski Z.P. Radiat. Phys. Chem. **11**: 71–6 (1978).

78A309 Pulse radiolytically generated superoxide and Cu(II)-salicylates. Younes, M.; Lengfelder, E.; Zienau, S.; Weser, U. Biochem. Biophys. Res. Commun. **81**: 576–80 (1978).

78A321 Bipyridylium quaternary salts and related compounds. Part 6. Pulse radiolysis studies of the reaction of paraquat radical analogues with oxygen. Farrington, J.A.; Ebert, M.; Land, E.J. J. Chem. Soc., Faraday Trans. 1 **74**: 665–75 (1978).

78A361 Reevaluation of the spectral and kinetic properties of HO_2 and O_2^- free radicals. Bielski, B.H.J. Photochem. Photobiol. **28**: 645–9 (1978).

78A362 The Haber-Weiss cycle. Koppenol, W.H.; Butler, J.; van Leeuwen, J.W. Photochem. Photobiol. **28**: 655–60 (1978).

78A364 The reaction between superoxide anion and hydrogen peroxide. Ferradini, C.; Foos, J.; Houee, C.; Pucheault, J. Photochem. Photobiol. **28**: 697–700 (1978).

78A365 Pulse radiolysis studies in model lipid systems: Formation and behavior of peroxy radicals in fatty acids. Hasegawa, K.; Patterson, L.K. Photochem. Photobiol. **28**: 817–23 (1978).

78A366 Gamma and pulse radiolysis studies of the reaction between superoxide ions and oxyhemoglobin-methemoglobin system. Ferradini, C.; Foos, J.; Gilles, L.; Haristoy, D.; Pucheault, J. Photochem. Photobiol. **28**: 851–5 (1978).

78A367 Radiation activation of carcinogens and the role of ·OH and O_2^-. Greenstock, C.L.; Ruddock, G.W. Photochem. Photobiol. **28**: 877–80 (1978).

78A389 Study of the Haber-Weiss reaction using a sensitive method for detection of OH radicals. Melhuish, W.H.; Sutton, H.C. J. Chem. Soc., Chem. Commun. : 970–1 (1978).

78A436 Oxidation of first-row bivalent transition-metal complexes containing ethylenediaminetetra-acetate and nitrilotriacetate ligands by free radicals: A pulse-radiolysis study. Lati, J.; Meyerstein, D. J. Chem. Soc., Dalton Trans. : 1105–18 (1978).

78A483 Kinetic investigations of the autoxidation of adrenalin. Bors, W.; Michel, C.; Saran, M.; Lengfelder, E. Z. Naturforsch., Teil C **33C**: 891–6 (1978).

78R103 The effect of 1,4-diazabicyclo[2.2.2]octane on the radiosensitivity of bacteria. Anderson, R.F.; Patel, K.B. Photochem. Photobiol. **28**: 881–5 (1978).

78R207 The role of the superoxide anion in the xanthine oxidase-induced autoxidation of linoleic acid. Thomas, M.J.; Mehl, K.S.; Pryor, W.A. Biochem. Biophys. Res. Commun. **83**: 927–32 (1978).

78R208 Oxygen activation in isolated chloroplasts. Mechanism of ferredoxin-dependent ethylene formation from methionine. Elstner, E.F.; Saran, M.; Bors, W.; Lengfelder, E. Eur. J. Biochem. **89**: 61–6 (1978).

78R209 The oscillating peroxidase-oxidase reaction in an open system. Analysis of the reaction mechanism. Olsen, L.F. Biochim. Biophys. Acta **527**: 212–20 (1978).

78R210 Oxidation of α-tocopherol with O_2^-. Yagi, K.; Yamada, H.; Nishikimi, M. *Tocopherol, Oxygen and Biomembranes*, p.1–11, C. de Duve and O. Hayaishi (eds.), Elsevier, North Holland Biomedical Press (1978).

79A001 Kinetics of the interaction of HO_2 and O_2^- radicals with hydrogen peroxide. The Haber-Weiss reaction. Weinstein, J.; Bielski, B.H.J. J. Am. Chem. Soc. **101**: 58–62 (1979).

79A014 Pulse-radiolytic investigations of catechols and catecholamines. II. Reactions of Tiron with oxygen radical species. Bors, W.; Saran, M.; Michel, C. Biochim. Biophys. Acta **582**: 537–42 (1979).

79A018 Superoxide dismutase activities of an iron porphyrin and other iron complexes. Pasternack, R.F.; Halliwell, B. J. Am. Chem. Soc. **101**: 1026–31 (1979).

79A036 Electron transfer from pyridinyl radicals, hydrated electrons, $CO_2\cdot^-$ and $O_2\cdot^-$ to bacterial cytochrome P450. Debey, P.; Land, E.J.; Santus, R.; Swallow, A.J. Biochem. Biophys. Res. Commun. **86**: 953–60 (1979).

79A038 Radical oxidation of nickel(II) complexes of tetraazamacrocyclic ligands and the reactions of the resulting nickel(III) complexes: A pulse-radiolysis and flash-photolysis study. Whitburn, K.D.; Laurence, G.S. J. Chem. Soc., Dalton Trans. : 139–48 (1979).

79A072 Functional aspects of the superoxide dismutative action of Cu-penicillamine. Lengfelder, E.; Fuchs, C.; Younes, M.; Weser, U. Biochim. Biophys. Acta **567**: 492–502 (1979).

79A170 Oxidation of nicotinamide adenine dinucleotide by hydroperoxyl radical. A flash photolysis study. Nadezhdin, A.; Dunford, H.B. J. Phys. Chem. **83**: 1957–61 (1979).

79A184 Detection of superoxide ion in aqueous media by N-halopiperidines. Rigo, A.; Argese, E.; Orsega, E.F.; Viglino, P. Inorg. Chim. Acta **35**: 161–4 (1979).

79A240 Pulse-radiolytic investigations of catechols and catecholamines. 3. Adrenalone. Bors, W.; Saran, M.; Michel, C. J. Phys. Chem. **83**: 2447–52 (1979).

79A255 Radiation chemistry of cobalt(II) nitrilotriacetate in aqueous solutions. Bhattacharyya, S.N.; Srisankar, E.V. J. Chem. Soc., Faraday Trans. 1 **75**: 2089–99 (1979).

79A295 Superoxide anions do not react with hydroperoxides. Bors, W.; Michel, C.; Saran, M. FEBS Lett. **107**: 403–6 (1979).

79A303 Pulse-radiolytic investigations of catechols and catecholamines. 4. 3,4-Dihydroxybenzaldehyde and 3,4-dihydroxyacetophenone. Bors, W.; Saran, M.; Michel, C. J. Phys. Chem. **83**: 3084–8 (1979).

79A312 Partitioning of electrostatic and conformational contributions in the redox reactions of modified cytochromes c. Ilan, Y.; Shafferman, A.; Feinberg, B.A.; Lau, Y.-K. Biochim. Biophys. Acta **548**: 565–78 (1979).

79A329 Superoxide and manganese(III). Reactions of Mn-EDTA and Mn-CyDTA complexes with O_2^-. X-ray structure of $KMnEDTA{\cdot}2H_2O$. Stein, J.; Fackler,J.P.,Jr.; McClune, G.J.; Fee, J.A.; Chan, L.T. Inorg. Chem. **18**: 3511–9 (1979).

79A340 The oxidation of ascorbic acid and hydroquinone by perhydroxyl radicals. A flash photolysis study. Nadezhdin, A.D.; Dunford, H.B. Can. J. Chem. **57**: 3017–22 (1979).

79A358 Reaction rates of superoxide radicals with the essential amino acids. Bielski, B.H.J.; Shiue, G.G. *Oxygen Free Radicals and Tissue Damage*, p.43–56, Ciba Foundation Symposium 65 (New Series), Excerpta Medica, New York (1979).

79A455 Reactivity of Cu(indomethacin)$_2$ and Cu-penicillamine with $\cdot O_2^-$. Lengfelder, E.; Sellinger, K.-H.; Weser, U. *Metalloproteins, Structure, Molecular Function and Clinical Aspects*, p.136–41, U. Weser (ed.), Georg Theime Verlag, Stuttgart (1979).

79R055 Cyanide insensitive iron superoxide dismutase in Euglena gracilis. Comparison of the reliabilities of different test systems for superoxide dismutases. Lengfelder, E.; Elstner, E.F. Z. Naturforsch., Teil C **34C**: 374–80 (1979).

79R111 Catalysis of the disproportionation of superoxide by metalloporphyrins. Pasternack, R.F.; Skowronek, W.R.,Jr. J. Inorg. Biochem. **11**: 261–7 (1979).

80A049 Rate of reaction of superoxide radical with chloride-containing species. Long, C.A.; Bielski, B.H.J. J. Phys. Chem. **84**: 555–7 (1980).

80A085 Reduction of nitro blue tetrazolium by CO_2^- and O_2^- radicals. Bielski, B.H.J.; Shiue, G.G.; Bajuk, S. J. Phys. Chem. **84**: 830–3 (1980).

80A139 Reaction between superoxide ion and the superoxide coordinated in a cobalt(III) complex. Natarajan, P.; Raghavan, N.V. J. Am. Chem. Soc. **102**: 4518–9 (1980).

80A175 Reaction of superoxide radicals with copper(II)-histidine complexes. Weinstein, J.; Bielski, B.H.J. J. Am. Chem. Soc. **102**: 4916–9 (1980).

80A176 Spin trapping. Kinetics of the reaction of superoxide and hydroxyl radicals with nitrones. Finkelstein, E.; Rosen, G.M.; Rauckman, E.J. J. Am. Chem. Soc. **102**: 4994–9 (1980).

80A201 Structure of Cu_2(indomethacin)$_4$ and the reaction with superoxide in aprotic systems. Weser, U.; Sellinger, K.-H.; Lengfelder, E.; Werner, W.; Straehle, J. Biochim. Biophys. Acta **631**: 232–45 (1980).

80A220 Does caeruloplasmin dismute superoxide? No. Bannister, J.V.; Bannister, W.H.; Hill, H.A.O.; Mahood, J.F.; Willson, R.L.; Wolfenden, B.S.; FEBS Lett. **118**: 127–9 (1980).

80A221 Role of a peroxide intermediate in the chemiluminescence of luminol. A mechanisttic study. Merenyi, G.; Lind, J.S. J. Am. Chem. Soc. **102**: 5830–05 (1980).

80A296 The oxidation of soybean lipoxygenase-1: A pulse-radiolysis study. Allen, J.C.; Navaratnam, S.; Parsons, B.J.; Phillips, G.O.; Swallow, A.J. Biochem. Soc. Trans. **8**: 121–2 (1980).

80A317 Superoxide reactions with (isonicotinamide)pentaammineruthenium(II) and (III). Stanbury, D. M.; Mulac, W. A.; Sullivan, J. C.; Taube, H. Inorg. Chem. **19**: 3735–40 (1980).

80A378 Some reactions of the dichloride anion radical. Navaratnam, S.; Parsons, B.J.; Swallow, A.J. Radiat. Phys. Chem. **15**: 159–61 (1980).

80A391 Pulse radiolysis investigation of the interaction of bovine superoxide dismutase with organic free radicals. O'Neill, P.; Fielden, E.M. *Chemical and Biochemical Aspects of Superoxide and Superoxide Dismutase*, p.357–63, Proc. Fed. European Biochem. Soc. Sym. No. 62, J.V. Bannister and H.A.O. Hill (eds.), Elsevier, New York, NY (1980).

80A413 Glyceraldehyde-3-phosphate dehydrogenase-catalyzed chain oxidation of reduced nicotinamide adenine dinucleotide by perhydroxyl radicals. Chan, P.C.; Bielski, B.H.J. J. Biol. Chem. **255**: 874–6 (1980).

80R189 Does copper-D-penicillamine catalyze the dismutation of O_2^-? Robertson, P.,Jr.; Fridovich, I. Arch. Biochem. Biophys. **203**: 830–1 (1980).

80Z241 Superoxide dismutation by Cu-penicillamine. Lengfelder, E.; Elstner, E.F.; Younes, M.; Weser, U. *Chemical and Biochemical Aspects of Superoxide and Superoxide Dismutase*, p.347–56, Proc. Fed. European Biochem. Soc. Sym. No. 62, J.V. Bannister and H.A.O. Hill (eds.), Elsevier, New York, NY (1980).

81A207 Superoxide dismuting activity of an iron porphyrin. Ilan, Y.; Rabani, J.; Fridovich, I.; Pasternack, R.F. Inorg. Nucl. Chem. Lett. **17**: 93–6 (1981).

81A216 The reactivity of the azide radical $N_3\cdot$ towards dioxygen species. Eriksen, T.E.; Lind, J.; Merenyi, G. Radiochem. Radioanal. Lett. **48**: 405–10 (1981).

81A227 Reaction between $HO_2\cdot$ and chlorine in aqueous solution. Bjergbakke, E.; Navaratnam, S.; Parsons, B.J. J. Am. Chem. Soc. **103**: 5926–8 (1981).

81A242 Generation of chlorine dioxide from ClO_2^- by pulse radiolysis. Eriksen, T.E.; Lind, J.; Merenyi, G. J. Chem. Soc., Faraday Trans. 1 **77**: 2115–23 (1981).

81A271 Radiolysis study of the alloxan-dialuric acid couple. II. The autoxidation of dialuric acid. Houee-Levin, C.; Gardes-Albert, M.; Ferradini, C.; Pucheault, J. Radiat. Res. **88**: 20–8 (1981).

81A374 Kinetic studies of peroxides and peroxy radicals, and their reactions with biological molecules. Greenstock, C.L.; Wiebe, R.H. *Oxygen and Oxy-Radicals in Chemistry and Biology*, p.119–31, M.A.J. Rodgers and E.L. Powers (eds.), Academic Press, New York, NY (1981).

81A375 The reactions of oxygen and superoxide ions with flavosemiquinone radicals. Anderson, R.F. *Oxygen and Oxy-Radicals in Chemistry and Biology*, p.597–600, M.A.J. Rodgers and E.L. Powers (eds.), Academic Press, New York, NY (1981).

81A430 Imidazole-bridged copper complexes as Cu_2Zn_2-superoxide dismutase models. Weser, U.; Schubotz, L.M.; Lengfelder, E. J. Mol. Catal. **13**: 249–61 (1981).

81G067 A radiolysis study of the role of superoxide ion in the oxidation of sulfite by oxygen. Sadat-Shafai, T.; Pucheault, J.; Ferradini, C. Radiat. Phys. Chem. **17**: 283–8 (1981).

81R125 Catalysis of the disproportionation of superoxide by metalloporphyrins. III. Pasternack, R.F.; Banth, A.; Pasternack, J.M.; Johnson, C.S. J. Inorg. Biochem. **15**: 261–7 (1981).

81R192 Superoxide dismutation by low molecular weight Cu-complexes. Lengfelder, E.; Weser, U. Bull. Europ. Physiopath. Resp. **17**: 73–80 (1981).

82A021 Generation of superoxide radicals by photolysis of oxygenated ethanol solutions. Bielski, B.H.J.; Gebicki, J.M. J. Am. Chem. Soc. **104**: 796–8 (1982).

82A119 Chemical properties of water-soluble porphyrins. 2. The reaction of iron(III) tetrakis(4-N-methylpyridyl)porphyrin with the superoxide radical dioxygen couple. Solomon, D.; Peretz, P.; Faraggi, M. J. Phys. Chem. **86**: 1842–9 (1982).

82A133 Ultraviolet spectrum and decay of the ozonide ion radical, O_3^-, in strong alkaline solution. Sehested, K.; Holcman, J.; Bjergbakke, E.; Hart, E.J. J. Phys. Chem. **86**: 2066–9 (1982).

82A138 Primary processes in the photochemistry of aqueous sulphacetamide: A laser flash photolysis and pulse radiolysis study. Land, E.J.; Navaratnam, S.; Parsons, B.J.; Phillips, G.O. Photochem. Photobiol. **35**: 637–42 (1982).

82A184 Substituent effects in the kinetic analysis of free radical reactions with nitrone spin traps. Greenstock, C.L.; Wiebe, R.H. Can. J. Chem. **60**: 1560–4 (1982).

82A198 The mechanisms of photoredox systems involving $Ru(bpy)_3^{2+}$, O_2 and Fe^{III}. Albery, W.J.; Foulds, A.W.; Darwent, J.R. J. Photochem. **19**: 37–54 (1982).

82A269 A flash-photometric method for determination of reactivity of superoxide: Application of superoxide dismutase assay. Takahashi, M.; Asada, K. J. Biochem. (Tokyo) **91**: 889–96 (1982).

82A281 Kinetics and mechanism of the reduction of ferricytochrome c by the superoxide anion. Butler, J.; Koppenol, W.H.; Margoliash, E. J. Biol. Chem. **257**: 10747–50 (1982).

82A319 Chemical properties of water-soluble porphyrins. 3. The reaction of superoxide radicals with some metalloporphyrins. Peretz, P.; Solomon, D.; Weinraub, D.; Faraggi, M. Int. J. Radiat. Biol. Relat. Stud. Phys., Chem. Med. **42**: 449–56 (1982).

82A403 Reaction of HO_2/O_2^- with α-tocopherol in ethanolic solutions. Arudi, R.L.; Sutherland, M.W.; Bielski, B.H.J. *Oxy Radicals and their Scavenger Systems*, Vol. 1, p. 26–31, Elsevier Biomedical, New York (1983) (3rd International Conference on Superoxide and Superoxide Dismutase, Ellenville, NY, 3 Oct 1982).

82A422 Radical scavenging and electron-transfer reactions in polyporus versicolor laccase. A pulse radiolysis study. Guissani, A.; Henry, Y.; Gilles, L. Biophys. Chem. **15**: 177–90 (1982).

82A446 Iron-ethylenediaminetetraacetic acid (EDTA)-catalyzed superoxide dismutation revisited: An explanation of why the dismutase activity of Fe-EDTA cannot be detected in the cytochrome c/xanthine oxidase assay system. Bull, C.; Fee, J.A.; O'Neill, P.; Fielden, E.M. Arch. Biochem. Biophys. **215**: 551–5 (1982).

82A448 Catalytic activity studies of some copper(II)-histidine-containing dipeptide complexes on aqueous superoxide ion dismutation. Amar, C.; Vilkas, E.; Foos, J. J. Inorg. Biochem. **17**: 313–23 (1982).

82A449 Reaction of iron-EDTA chelates with the superoxide radical. Butler, J.; Halliwell, B. Arch. Biochem. Biophys. **218**: 174–8 (1982).

82A455 On the mechanism of the catalytic scavenging of superoxide radical by manganese pyrophosphate: A pulse radiolysis study. Goetz, F.; Lengfelder, E. *Oxy Radicals and Their Scavenger Systems*, Vol. 1, Molecular Aspects, p.228–33, G. Cohen and R.A. Greenwald (eds.), Elsevier Biomedical, New York, NY (Pub. 1983).

82A456 Mechanistic study of superoxide dismutation by "zinc-free" bovine superoxide dismutase. O'Neill, P.; Fielden, E.M.; Cocco, D.; Calabrese, L.; Rotilio, G. *Oxy Radicals and Their Scavenger Systems*, Vol. 1, Molecular Aspects, p.316–9, G. Cohen and R.A. Greenwald (eds.), Elsevier Biomedical, New York, NY (Pub. 1983).

82N062 The influence of a detergent on the reactivity of cytochrome c towards the superoxide radical as measured by pulse radiolysis. Heijman, M.G.J.; Nauta, H.; Levine, Y.K. Biochim. Biophys. Acta **704**: 560–3 (1982).

82R027 Radical intermediates involved in the bleaching of the carotenoid crocin. Hydroxyl radicals, superoxide anions and hydrated electrons. Bors, W.; Saran, M.; Michel, C. Int. J. Radiat. Biol. Relat. Stud. Phys., Chem. Med. **41**: 493–501 (1982).

82R039 The role of superoxide in xanthine oxidase-induced autoxidation of linoleic acid. Thomas, M.J.; Mehl, K.S.; Pryor, W.A. J. Biol. Chem. **257**: 8343–7 (1982).

82R132 Evidence for catalytic dismutation of superoxide by cobalt(II) derivatives of bovine superoxide dismutase in aqueous solution as studied by pulse radiolysis. O'Neill, P.; Fielden, E.M.; Cocco, D.; Rotilio, G.; Calabrese, L. Biochem. J. **205**: 181–7 (1982).

82R164 A reaction of the superoxide radical with tetrapyrroles. Robertson, P.,Jr.; Fridovich, I. Arch. Biochem. Biophys. **213**: 353–7 (1982).

82R165 A method for the detection of superoxide in biological systems. Rosen, G.M.; Finkelstein, E.; Rauckman, E.J. Arch. Biochem. Biophys. **215**: 367–78 (1982).

82R172 Catalysis of the disproportionation of superoxide by metalloporphyrins. Pasternack, R.F.; Pysnik, D. *Oxy Radicals and Their Scavenger Systems*, Vol. 1, Molecular Aspects, p.151–6, G. Cohen and R.A. Greenwald (eds.), Elsevier Biomedical, New York, NY (Pub. 1983).

82Z254 Evaluation of the reactivities of HO_2/O_2^- with compounds of biological interest. Bielski, B.H.J. *Oxy Radicals and Their Scavenger Systems*, Vol. 1, Molecular Aspects, p.1–7, G. Cohen and R.A. Greenwald (eds.), Elsevier Biomedical, New York, NY (Pub. 1983) (Experimental details deposited at the Radiation Chemistry Data Center).

83A039 Reduction of the naphthazarin molecule as studied by pulse radiolysis. Part 1. Addition of a single electron. Land, E.J.; Mukherjee, T.; Swallow, A.J.; Bruce, J.M. J. Chem. Soc., Faraday Trans. 1 **79**: 391–404 (1983).

83A043 Methyl viologen radical reactions with several oxidizing agents. Levey, G.; Ebbesen, T.W. J. Phys. Chem. **87**: 829–32 (1983).

83A056 Hydroxyl radical-induced oxidation of ethanol in oxygenated aqueous solutions. A pulse radiolysis and product study. Bothe, E.; Schuchmann, M.N.; Schulte-Frohlinde, D.; von Sonntag, C. Z. Naturforsch., Teil B **38B**: 212–9 (1983).

83A087 A study of the reactivity of HO_2/O_2^- with unsaturated fatty acids. Bielski, B.H.J.; Arudi, R.L.; Sutherland, M.W. J. Biol. Chem. **258**: 4759–61 (1983).

83A103 Kinetics and mechanism for the oxidation of ascorbic acid/ascorbate by HO_2/O_2^- radicals. A pulse radiolysis and stopped-flow photolysis study. Cabelli, D.E.; Bielski, B.H.J. J. Phys. Chem. **87**: 1809–12 (1983).

83A117 Rate constants and products of the reactions of e_{aq}^-, O_2^- and H with ozone in aqueous solutions. Sehested, K.; Holcman, J.; Hart, E.J. J. Phys. Chem. **87**: 1951–4 (1983).

83A147 Pulse-radiolysis studies on the interaction of one-electron-reduced species with ascorbate oxidase in aqueous solution. O'Neill, P.; Fielden, E.M.; Finazzi-Agro, A.; Avigliano, L. Biochem. J. **209**: 167–74 (1983).

83A158 The kinetics of the reaction of superoxide radical with Fe(III) complexes of EDTA, DETAPAC [diethylenetriaminepentaacetic acid] and HEDTA [*N*-(2-hydroxyethyl)-ethylenediaminetriacetic acid, trisodium salt hydrate]. Buettner, G.R.; Doherty, T.P.; Patterson, L.K. FEBS Lett. **158**: 143–6 (1983).

83A163 The mechanism of Fe-EDTA catalyzed superoxide dismutation. Bull, C.; McClune, G.J.; Fee, J.A. J. Am. Chem. Soc. **105**: 5290–300 (1983).

83A209 The reaction of superoxide radicals with metal picolinate complexes. Bannister, W.H.; Bannister, J.V.; Searle, A.J.F.; Thornalley, P.J. Inorg. Chim. Acta. **78**: 139–42 (1983).

83A299 The mechanisms of the dismutation of superoxide catalyzed by Cu(II)-phenanthroline complex and of the oxidation of Cu(I)-phenanthroline complex by oxygen in aqueous solution. Goldstein, S.; Czapski, G. J. Am. Chem. Soc. **105**: 7276–80 (1983).

83A304 Kinetics of the superoxide radical oxidation of Co(sepulchrate)$^{2+}$. A flash photolytic study. Bakac, A.; Espenson, J.H.; Creaser, I.I.; Sargeson, A.M. J. Am. Chem. Soc. **105**: 7624–8 (1983).

83A901 Schwarz, H.A., Unpublished data (deposited at the Radiation Chemistry Data Center).

83A902 Spectral and kinetic properties of the products resulting from reactions of HO_2/O_2^- with manganese(II) complexes. Bielski, B.H.J.; Arudi, R.L.; Cabelli, D.E. *Oxygen Radicals Chem. Biol.*, W. Bors, M. Saran and D. Tait, eds., de Gruyter, Berlin, publ. 1984, p. 1–15. (Proc. 3rd Int. Conf. Oxygen Radicals in Chem. and Biol., 10–15 Jul 1983, Munich).

83G122 Preparation and stabilization of aqueous/ethanolic superoxide solutions. Bielski, B.H.J.; Arudi, R.L. Anal. Biochem. **133**: 170–8 (1983).

83R034 Superoxide ion as active intermediate in the autoxidation of ascorbate by molecular oxygen. Effect of superoxide dismutase. Scarpa, M.; Stevanato, R.; Viglino, P.; Rigo, A. J. Biol. Chem. **258**: 6695–7 (1983).

84A908 A reevaluation of the reactivity of hydroxylamine with O_2^-/HO_2. Bielski, B.H.J.; Arudi, R.L.; Cabelli, D.E.; Bors, W. Anal. Biochem. **142**: 207–9 (1984).

84A909 Studies of the reactivity of HO_2/O_2^- with unsaturated hydroperoxides in ethanolic solutions. Thomas, M.J.; Sutherland, M.W.; Arudi, R.L.; Bielski, B.H.J. Arch. Biochem. Biophys. **233**: 772–5 (1984).

84A910 Pulse radiolysis study of the kinetics and mechanisms of the reactions between manganese(II) complexes and HO_2/O_2^- radicals. 1. Sulfate, formate, and pyrophosphate complexes. Cabelli, D.E.; Bielski, B.H.J. J. Phys. Chem., **88**: 3111–5 (1984).

10. Molecular Formula Index

Am^{4+}	Americium(IV) ion **1**
BO_3^{3-}	Borate ion **2**
BrHO	Hypobromous acid **6**
Br_2	Bromine **5**
Br_2^-	Dibromine radical ion **4**
Br_3^-	Tribromine ion **3**
$CHCuO_2^+$	Formatocopper(II) ion **43**
CHO_2^-	Formate ion **232**
CH_2O_3	Carbonic acid **7**
CNS	Thiocyanogen **152**
CN_4O_8	Tetranitromethane **320**
CO_3^-	Carbonate radical ion **8**
$C_2H_2CuO_4$	Copper(II) formate **44**
$C_2H_2MnO_4$	Manganese(II) formate **119**
$C_2H_3O_2^-$	Acetate ion **164**
C_2H_4	Ethylene **225**
$C_2H_4CuNO_2^+$	Glycinatocopper(II) ion **51**
$C_2H_5NO_2$	Glycine **238**
$C_2H_5O_3$	1-Hydroxyethyldioxy **244**
$C_2O_4^{2-}$	Oxalate ion **293**
$C_3H_3CuO_6^-$	Trisformatocuprate(II) ion **45**
$C_3H_3O_3^-$	Pyruvate ion **304**
$C_3H_4N_2$	Imidazole **248**
$C_3H_5O_3^-$	Lactate ion **255**
$C_3H_7CuNO_2^+$	DL-Alaninatocopper(II) ion **48**
$C_3H_7NO_2$	DL-Alanine **169**
$C_3H_7NO_2S$	Cysteine **195**
$C_3H_7NO_3$	DL-Serine **307**
$C_4H_2N_2O_4$	Alloxan **170**
$C_4H_2O_4^{2-}$	Fumarate ion **233** Maleate ion **267**
$C_4H_3N_2O_4$	Alloxan semiquinone **171**
$C_4H_4CuO_8^{2-}$	Tetrakisformatocuprate(II) ion **46**
$C_4H_4N_2O_4$	Dialuric acid **204**
$C_4H_4O_4^{2-}$	Succinate ion **308**
$C_4H_4O_5^{2-}$	L-Malate ion **266**
$C_4H_4O_6^{2-}$	Tartrate ion **316**
$C_4H_6CuN_2O_3^+$	Glycylglycinatocopper(II) ion **52**
$C_4H_6N_2$	1-Methylimidazole **275** 2-Methylimidazole **276**
$C_4H_6O_4$	Acetyl peroxide **166**
$C_4H_7NO_4$	DL-Aspartic acid **179**
$C_4H_8N_2O_3$	DL-Asparagine **178**
C_4H_8OS	Methional **269**
$C_4H_9NO_2S$	Homocysteine **241**
$C_4H_9NO_3$	DL-Threonine **321**
$C_4H_{10}O_2S_2$	Dithiothreitol **223**
$C_4H_{11}NO_3$	Tris(hydroxymethyl)aminomethane **329**
$C_4H_{11}NO_2^+$	Trimethylammoniomethyldioxy **325**
$C_5H_4O_5^{2-}$	2-Oxoglutarate ion **294**
$C_5H_7N_2O_4$	Peroxyhydrothymine radical **298**
$C_5H_9CuNO_2^+$	L-Prolinatocopper(II) ion **64**
$C_5H_9CuNO_3^+$	L-Hydroxyprolinecopper(II) ion **60**
$C_5H_9CuN_2O_3^+$	Glutamatocopper(II) ion **50**
$C_5H_9NO_2$	L-Proline **303**
$C_5H_9NO_4$	L-Glutamic acid **234**
$C_5H_{10}CuNO_2^+$	L-Valinatocopper(II) ion **66**
$C_5H_{10}N_2O_3$	L-Glutamine **235**
$C_5H_{11}CuNO_2S^+$	L-Methioninatocopper(II) ion **62**
$C_5H_{11}NO_2$	DL-Valine **332**
$C_5H_{11}NO_2S$	DL-Methionine **270**
$C_6FeKN_6^{2-}$	Potassium hexacyanoferrate(III) ion **102**
$C_6FeKN_6^{3-}$	Potassium hexacyanoferrate(II) ion **84**
$C_6FeN_6^{3-}$	Ferricyanide ion **101**
$C_6FeN_6^{4-}$	Ferrocyanide ion **83**
$C_6HFeN_6^{3-}$	Hydrogen hexacyanoferrate(II) ion **85**
$C_6H_2Cl_2O_2$	2,5-Dichloro-*p*-benzoquinone **207**
$C_6H_2FeN_6^{2-}$	Dihydrogen hexacyanoferrate(II) ion **86**
$C_6H_4Cl_2O_2$	2,5-Dichlorohydroquinone **208**
$C_6H_4O_2$	1,4-Benzoquinone **182**
$C_6H_4O_8S_2^{2-}$	4,5-Dihydroxy-*m*-benzenedisulfonate ion **212**
$C_6H_5O_7^{3-}$	Citrate ion **191**
$C_6H_6CoNO_6^-$	Nitrilotriacetatocobaltate(II) ion **23**
$C_6H_6MnNO_6^-$	Nitrilotriacetatomanganate(II) ion **120**
$C_6H_6O_2$	Catechol **189** Hydroquinone **243** Resorcinol **305**
$C_6H_6O_3$	Phloroglucinol **301**
$C_6H_6O_6^-$	Ascorbate radical anion **176**
$C_6H_8O_6$	Ascorbic acid **177**
$C_6H_9N_3O_2$	L-Histidine **240**
$C_6H_{11}NO$	5,5-Dimethyl-1-pyrroline-*N*-oxyl **220**
$C_6H_{11}O_2$	Cyclohexylperoxy **194**
$C_6H_{12}N_2$	1,4-Diazabicyclo[2.2.2]octane **206**
$C_6H_{12}N_2O_4S_2$	L-Cystine **196**
$C_6H_{12}N_4O_2$	Diamide **205**
$C_6H_{13}NO_2$	DL-Isoleucine **253** L-Leucine **256**
$C_6H_{14}N_2O_2$	DL-Lysine **265**
$C_6H_{14}N_4O_2$	L-Arginine **174**
$C_6H_{21}N_7ORu^{2+}$	Pentaammine(isonicotinamide)-ruthenium(II) ion **147**
$C_6H_{21}N_7ORu^{3+}$	Pentaammine(isonicotinamide)-ruthenium(III) ion **148**
$C_7H_6O_2$	Methyl-1,4-benzoquinone **272**
$C_7H_6O_3$	3,4-Dihydroxybenzaldehyde **211**
$C_7H_6O_4$	2,5-Dihydroxybenzoic acid **213**
$C_7H_8O_2$	Methylhydroquinone **274**
$C_7H_{13}NO$	2,5,5-Trimethyl-1-pyrroline-*N*-oxyl **327**
$C_7H_{14}O_2$	*tert*-Butyl allyl peroxide **187**
$C_8H_6N_3O_2$	Luminol radical **264**
$C_8H_8O_2$	2,3-Dimethyl-1,4-benzoquinone **215** 2,5-Dimethyl-1,4-benzoquinone **216** 2,6-Dimethylbenzoquinone **217**
$C_8H_8O_3$	3,4-Dihydroxyacetophenone **210**
$C_8H_{10}N_2O_3S$	Sulfacetamide **309**
$C_8H_{11}FeN_2O_7$	*N*-Hydroxyethylenediamine-triacetatoferrate(III) **104**

$C_8H_{19}NO_2^+$ Triethylammonioethyldioxy **324**

$C_8H_{34}Co_2N_9O_2^{4+}$ μ-Amido-μ-superoxidotetrakis-(ethylenediamine)dicobalt(III)] ion **28**

$C_8MoN_8^{3-}$ Octacyanomolybdate(V) ion **129**

$C_8MoN_8^{4-}$ Octacyanomolybdate(IV) ion **128**

$C_9H_{11}NO_2$ L-Phenylalanine **299**

$C_9H_{11}NO_3$ Adrenalone **168**
L-Tyrosine **331**

$C_9H_{13}NO_3$ Adrenaline **167**

$C_9H_{14}CuN_4O_3$ Alanylhistidinatocopper(II) **49**
Histidylalaninatocopper(II) **56**

$C_9H_{18}BrN$ *N*-Bromo-2,2,6,6-tetramethylpiperidine **186**

$C_9H_{18}NO$ 2,2,6,6-Tetramethylpiperidine-*N*-oxyl **318**

$C_9H_{19}NO$ 2,2,6,6-Tetramethylpiperidin-1-ol **319**

$C_{10}Co_2N_{10}O_2^{5-}$ Decakis(cyano)-μ-superoxidodicobaltate(III) ion **29**

$C_{10}H_5O_5S^-$ 1,2-Naphthoquinone-4-sulfonate ion **282**
1,4-Naphthoquinone-2-sulfonate ion **283**

$C_{10}H_6O_2$ 1,2-Naphthoquinone **281**

$C_{10}H_6O_4$ 5,8-Dihydroxy-1,4-naphthoquinone **214**

$C_{10}H_9N$ 2-Naphthylamine **284**

$C_{10}H_{12}CoN_2O_8^{2-}$ Ethylenediaminetetraacetatocobaltate(II) ion **24**

$C_{10}H_{12}CuN_2O_8^{2-}$ Ethylenediaminetetraacetatocuprate(II) ion **68**

$C_{10}H_{12}FeN_2O_8^-$ Ethylenediaminetetraacetatoferrate(III) ion **105**

$C_{10}H_{12}FeN_2O_8^{2-}$ Ethylenediaminetetraacetatoferrate(II) ion **87**

$C_{10}H_{12}MnN_2O_8^-$ Ethylenediaminetetraacetatomanganate(III) ion **125**

$C_{10}H_{12}MnN_2O_8^{2-}$ Ethylenediaminetetraacetatomanganate(II) ion **121**

$C_{10}H_{12}N_2O_8^{4-}$ Ethylenediaminetetraacetate ion **227**

$C_{10}H_{12}O_2$ Duroquinone **224**

$C_{10}H_{14}O_2$ *tert*-Butylhydroquinone **188**

$C_{10}H_{16}FeN_5O_{13}P_3^{2-}$ Adenosine triphosphate-iron(II) complex **89**

$C_{10}H_{16}FeN_5O_{13}P_3^-$ Adenosine triphosphate-iron(III) complex **107**

$C_{10}H_{17}N_3O_6S$ Glutathione **236**

$C_{11}H_8O_2$ 2-Methyl-1,4-naphthoquinone **277**

$C_{11}H_{12}N_2O_2$ L-Tryptophan **330**

$C_{11}H_{14}N_2O_3$ 4-Nitrophenyl-*N*-*tert*-butylnitrone **287**

$C_{11}H_{15}NO$ Phenyl-*N*-*tert*-butylnitrone **300**

$C_{11}H_{18}CuN_4O_3$ Histidylvalinatocopper(II) **59**
Valylhistidinatocopper(II) **67**

$C_{12}H_6Cl_2NO_2^-$ 2,6-Dichloroindophenolate ion **209**

$C_{12}H_8CuN_2O_4$ Bis(2-pyridinecarboxylato)copper(II) **47**

$C_{12}H_8N_2O_4Zn$ Bis(2-pyridinecarboxylato)zinc(II) **163**

$C_{12}H_8O_2$ Diphenoquinone **221**

$C_{12}H_9FeN_2O_5$ Hydroxybis(2-pyridinecarboxylato)-iron(III) **103**

$C_{12}H_{10}O_2$ 2,3-Dimethylnaphthoquinone **219**

$C_{12}H_{12}N_2$ Benzidine **180**

$C_{12}H_{12}N_2^+$ 1,1'-Ethylene-2,2'-bipyridinium radical ion (1+) **226**

$C_{12}H_{14}N_2^+$ 1,1'-Dimethyl-4,4'-bipyridinium radical ion (1+) **218**

$C_{12}H_{14}N_2O$ 4-Cyanophenyl-*N*-*tert*-butylnitrone **193**

$C_{12}H_{17}NO$ 4-Methylphenyl-*N*-*tert*-butylnitrone **278**

$C_{12}H_{17}NO_2$ 4-Methoxyphenyl-*N*-*tert*-butylnitrone **271**

$C_{12}H_{19}CuN_6O_5^+$ Bis(histidinato)copper(II) ion, conjugate monoacid **55**

$C_{12}H_{26}CuN_4O_4$ Bis(lysinato)copper(II) **61**

$C_{12}H_{27}NO_2^+$ Tripropylammoniopropyldioxy **328**

$C_{12}H_{30}CoN_8^{2+}$ 1,3,6,8,10,13,16,19-Octaazabicyclo-[6.6.6]eicosanecobalt(II) ion **22**

$C_{13}H_{14}N_2^+$ 1,1'-Trimethylene-2,2'-bipyridinium radical ion (1+) **326**

$C_{14}H_{10}CuO_6$ Bis(salicylato)copper(II) **69**

$C_{14}H_{12}CuN_2O_6$ Bis(*p*-aminosalicylato)copper(II) **72**

$C_{14}H_{16}N_2^+$ 1,1'-Tetramethylene-2,2'-bipyridinium radical ion (1+) **317**

$C_{14}H_{17}O_4^-$ 6-Hydroxy-2,5,7,8-tetramethylchroman-2-carboxylate ion **246**

$C_{14}H_{18}FeN_3O_{10}^{2-}$ Diethylenetriaminepentaacetatoferrate(III) ion **106**

$C_{14}H_{18}FeN_3O_{10}^{3-}$ Diethylenetriaminepentaacetatoferrate(II) ion **88**

$C_{14}H_{18}MnN_2O_8^-$ 1,2-Cyclohexanediaminetetraacetatomanganate(III) ion **126**

$C_{14}H_{18}N_2O_2^+$ 1,1'-Bis(2-hydroxyethyl)-4,4'-bipyridinium radical ion(1+) **185**

$C_{14}H_{18}O_4$ 6-Hydroxy-2,5,7,8-tetramethylchroman-2-carboxylic acid **245**

$C_{14}H_{28}CoN_4O_2^{2+}$ Diaqua(2,3,9,10-tetramethyl-1,4,8,11-tetraazacyclotetradeca-1,3,8,10-tetraene)cobalt(II) ion **20**

$C_{14}H_{28}CoN_4O_2^{3+}$ Diaqua(2,3,9,10-tetramethyl-1,4,8,11-tetraazacyclotetradeca-1,3,8,10-tetraene)cobalt(III) ion **25**

$C_{15}H_{13}NO$ 2-Acetylaminofluorene **165**

$C_{15}H_{18}CuN_4O_3$ Histidylphenylalaninatocopper(II) **57**
Phenylalanylhistidinatocopper(II) **63**

$C_{15}H_{18}CuN_4O_4$ Histidyltyrosinatocopper(II) **58**

$C_{16}H_6N_2O_{14}S_4^{4-}$ Indigotetrasulfonate ion **250**

$C_{16}H_7N_2O_{11}S_3^{3-}$ Indigotrisulfonate ion **251**

$C_{16}H_8N_2O_8S_2^{2-}$ Indigodisulfonate ion **249**

$C_{16}H_{20}CuN_8O_6^{2-}$ Bis(glycylhistidinato)cuprate(II) ion **53**

$C_{16}H_{22}O_4$ 3-(6-Hydroxy-2,5,7,8-tetramethylchroman-2-yl)propionic acid **247**

$C_{16}H_{28}N_4Ni^{3+}$ 5,7,7,12,12,14-Hexamethyl-1,4,8,11-tetraazacyclotetradeca-1,4,8,11-tetraenenickel(III) ion **140**

$C_{16}H_{32}N_4Ni^{3+}$ 5,7,7,12,12,14-Hexamethyl-1,4,8,11-tetraazacyclotetradeca-4,11-dienenickel(III) ion **139**

$C_{16}H_{35}NO_2^+$ Tributylammoniobutyldioxy **323**

$C_{16}H_{36}CoN_4O_2^{2+}$ Diaqua(5,7,7,12,14,14-hexamethyl-1,4,8,11-tetraazacyclotetradeca-4,11-diene)cobalt(II) ion **21**

$C_{16}H_{36}CuN_4O_2^{2+}$ Diaqua(5,7,7,12,12,14-hexamethyl-1,4,8,11-tetraazacyclotetradeca-4,11-diene)copper(II) ion **38**

$C_{16}H_{36}N_4Ni^{2+}$ 5,7,7,12,12,14-Hexamethyl-1,4,8,11-tetraazacyclotetradecane-nickel(II) ion **134**

$C_{16}H_{36}N_4Ni^{3+}$ 5,7,7,12,12,14-Hexamethyl-1,4,8,11-tetraazacyclotetradecane-nickel(III) ion **138**

$C_{17}H_{21}N_2O_6$ Riboflavin semiquinone **306**

$C_{18}H_{14}CuO_8$ Bis(acetylsalicylato)copper(II) **71**

$C_{18}H_{20}CuN_2O_6$ Bis(tyrosinato)copper(II) **65**

$C_{18}H_{27}O_2^-$ Arachidonate ion **172**

$C_{18}H_{29}O_2^-$ Linolenate ion **261**

$C_{18}H_{30}O_2$ Linolenic acid **262**

$C_{18}H_{31}O_2$ Linoleate ion **258**
9,11-Octadecadienoate ion **288**

$C_{18}H_{32}O_2$ Linoleic acid **259**
9,11-Octadecadienoic acid **289**

$C_{18}H_{33}O_2^-$ Oleate ion **290**

$C_{18}H_{33}O_4^-$ Linoleate hydroperoxide **257**

$C_{18}H_{34}O_2$ Oleic acid **291**

$C_{18}H_{34}O_4$ Linoleic acid hydroperoxide **260**

$C_{18}H_{36}O_4$ Oleic acid hydroperoxide **292**

$C_{19}H_{16}ClNO_4$ Indomethacin **252**

$C_{20}H_{12}$ Benzo[*a*]pyrene **181**

$C_{20}H_{16}CoN_4^{2+}$ Bis(2,2'-bipyridine)cobalt(II) ion **19**

$C_{20}H_{32}O_2$ Arachidonic acid **173**

$C_{21}H_{16}$ 3-Methylcholanthrene **273**

$C_{21}H_{29}N_7O_{14}P$ Nicotinamide adenine dinucleotide, reduced **285**

$C_{22}H_{18}N_2^+$ 1,1'-Diphenyl-4,4'-bipyridinium radical ion (1+) **222**

$C_{24}H_{16}CuN_4^+$ Bis(1,10-phenanthroline)copper(I) ion **32**

$C_{24}H_{16}CuN_4^{2+}$ Bis(1,10-phenanthroline)copper(II) ion **39**

$C_{25}H_{48}N_6O_8$ Desferrioxamine B **108**

$C_{26}H_{34}CuO_6$ Bis(diisopropylsalicylato)copper(II) **70**

$C_{27}H_{33}N_9O_5P_2$ Flavin mononucleotide semiquinone **231**

$C_{28}H_{46}CuN_{10}O_8^{2-}$ Bis(glycylhistidylleucinato)-cuprate(II) ion **54**

$C_{29}H_{34}CuN_8Zn^{3+}$ Copper(2-[2-(pyridyl)ethylimino-methyl]pyridine) zinc(2-[2-(pyridyl)ethyliminomethyl]-pyridine) imidazole bridged complex **74**

$C_{29}H_{34}Cu_2N_8^{3+}$ Bis[copper(2-[2-(pyridyl)ethyl-iminomethyl]pyridine)]imidazole bridged complex **73**

$C_{29}H_{50}O_2$ α-Tocopherol **322**

$C_{30}H_{24}N_6Ru^{3+}$ Tris(2,2'-bipyridine)ruthenium(III) ion **149**

$C_{31}H_{46}O_2$ Vitamin K_1 **333**

$C_{33}H_{34}N_4O_6$ Biliverdin **184**

$C_{33}H_{36}N_4O_6$ Bilirubin **183**

$C_{34}H_{32}ClFeN_4O_4$ Hemin **109**

$C_{36}H_{24}FeN_6^{2+}$ Tris(1,10-phenanthroline)iron(II) ion **78**

$C_{40}H_{30}N_{10}O_6^{2+}$ Nitro Blue Tetrazolium **286**

$C_{40}H_{40}ClFeN_8O_4$ Hemin-diimidazole complex **110**

$C_{44}H_{24}CoN_4O_{12}S_4^{3-}$ Tetrakis(*p*-sulfonatophenyl)-porphinatocobaltate(III) ion **27**

$C_{44}H_{24}CuN_4O_{12}S_4^{4-}$ Tetrakis(*p*-sulfonatophenyl)-porphinatocuprate(II) ion **42**

$C_{44}H_{24}FeN_4O_{12}S_4^{3-}$ Tetrakis(*p*-sulfonatophenyl)-porphineferrate(III) ion **98**

$C_{44}H_{24}MnN_4O_{12}S_4^{3-}$ Tetrakis(*p*-sulfonatophenyl)-porphinatomanganate(III) ion **124**

$C_{44}H_{24}N_4NiO_{12}S_4^{4-}$ Tetrakis(*p*-sulfonatophenyl)-porphinatonickelate(II) ion **137**

$C_{44}H_{24}N_4O_{12}S_4Zn^{4-}$ Tetrakis(*p*-sulfonatophenyl)-porphinatozincate(II) ion **162**

$C_{44}H_{36}CoN_8^{5+}$ Tetrakis(4-*N*-methylpyridyl)-porphinecobalt(III) ion **26**

$C_{44}H_{36}CuN_8^{4+}$ Tetrakis(4-*N*-methylpyridyl)-porphinecopper(II) ion **40**

$C_{44}H_{36}FeN_8^{2+}$ Tetrakis(4-*N*-methylpyridyl)-porphineiron(III) ion **92**

$C_{44}H_{36}FeN_8O_2^{4+}$ Tetrakis(4-*N*-methylpyridyl)-porphineiron(III)-superoxide complex **93**

$C_{44}H_{36}MnN_8^{5+}$ Tetrakis(4-*N*-methylpyridyl)-porphinemanganese(III) ion **122**

$C_{44}H_{36}N_8Ni^{4+}$ Tetrakis(4-*N*-methylpyridyl)-porphinenickel(II) ion **135**

$C_{44}H_{36}N_8Zn^{4+}$ Tetrakis(4-*N*-methylpyridyl)-porphinatezinc(II) ion **160**

$C_{44}H_{64}O_{24}$ Crocin **192**

$C_{46}H_{36}FeN_{10}^{2+}$ Dicyanotetrakis(4-*N*-methyl-pyridyl)porphineiron(II) ion **80**

$C_{46}H_{36}FeN_{10}^{3+}$ Dicyanotetrakis(4-*N*-methyl-pyridyl)porphineiron(III) ion **94**

$C_{48}H_{32}FeN_4^{2+}$ Bis(4,7-diphenyl-1,10-phenanth-roline)iron(II) ion **79**

$C_{48}H_{32}FeN_4^{3+}$ Bis(4,7-diphenyl-1,10-phenanth-roline)iron(III) ion **91**

$C_{50}H_{32}FeN_8O_{12}S_4^{3-}$ Tetrakis(*p*-sulfonatophenyl)-porphineferrate(III)-diimidazole complex **99**

$C_{50}H_{44}FeN_{12}^{4+}$ Tetrakis(4-*N*-methylpyridyl)-porphineiron(II)-diimidazole complex **81**

$C_{50}H_{44}FeN_{12}^{5+}$ Tetrakis(4-*N*-methylpyridyl)-porphineiron(III)-diimidazole complex **95**

$C_{56}H_{54}FeN_{14}O_4^{4+}$ Tetrakis(4-*N*-methylpyridyl)-porphineiron(II)-dihistidine complex **82**

$C_{56}H_{54}FeN_{14}O_4^{5+}$	Tetrakis(4-*N*-methylpyridyl)-porphineiron(III)-dihistidine complex **96**
$C_{56}H_{60}CuN_8^{4+}$	Tetrakis-4-(*N*,*N*,*N*-trimethyl-ammonio)phenylporphine-copper(II) ion **41**
$C_{56}H_{60}FeN_8^{5+}$	Tetrakis-4-(*N*,*N*,*N*-trimethyl-ammonio)phenylporphine-iron(III) ion **97**
$C_{56}H_{60}MnN_8^{5+}$	Tetrakis-4-(*N*,*N*,*N*-trimethyl-ammonio)phenylporphine-manganese(III) ion **123**
$C_{56}H_{60}N_8Ni^{4+}$	Tetrakis-4-(*N*,*N*,*N*-trimethyl-ammonio)phenylporphine-nickel(II) ion **136**
$C_{56}H_{60}N_8Zn^{4+}$	Tetrakis-4-(*N*,*N*,*N*-trimethyl-ammonio)phenylporphinezinc(II) ion **161**
$C_{63}H_{90}CoN_{14}O_{14}P$	Cyanocob(III)alamin **30**
$C_{76}H_{60}Cl_4Cu_2N_4O_{16}$	Copper indomethacin **76**
Ce^{4+}	Cerium(IV) ion **10**
Cl^-	Chloride ion **11**
ClHO	Hypochlorous acid **14**
ClO_2	Chlorine dioxide **16**
ClO_2^-	Chlorite ion **15**
ClO_3^-	Chlorate ion **17**
ClO_4^-	Perchlorate ion **18**
Cl_2	Chlorine **13**
Cl_2^-	Dichlorine radical ion **12**
Cu^+	Copper(I) ion **31**
Cu^{2+}	Copper(II) ion **33**
CuH_3N^{2+}	Amminecopper(II) ion **34**
$CuH_6N_2^{2+}$	Bisamminecopper(II) ion **35**
$CuH_9N_3^{2+}$	Trisamminecopper(II) ion **36**
$CuH_{12}N_4^{2+}$	Tetraamminecopper(II) ion **37**
Fe^{2+}	Iron(II) ion **77**
Fe^{3+}	Iron(III) ion **90**
H^+	Hydrogen ion **113**
HO	Hydroxyl **141**
HO_2^-	Hydroperoxide ion **144**
HO_2Th^{4+}	Thorium(IV)-hydroperoxy complex **155**
HO_4U^{2+}	Dioxouranium(VI)-hydroperoxy complex **158**
H_2	Hydrogen **112**
H_2O_2	Hydrogen peroxide **143**
H_3NO	Hydroxylamine **131**
I_2	Iodine **114**
I_3^-	Triiodine ion **115**
Mn^{2+}	Manganese(II) ion **116**
MnO_4^-	Permanganate ion **127**
MnO_4S	Manganese(II) sulfate **118**
$Mn_2O_7P_2$	Manganese(II) pyrophosphate **117**
NO_2	Nitrogen dioxide **132**
NO_2^-	Nitrite ion **133**
N_3	Azide radical **130**
O^-	Oxygen ion(1−) **142**
O_2U^{2+}	Uranyl(VI) ion **157**
O_3	Ozone **145**
O_3S^{2-}	Sulfite ion **151**
O_3Te^{2-}	Tellurate(IV) ion **153**
O_3V^+	Oxoperoxyvanadium(IV) ion **159**
O_4Os	Osmium tetroxide **146**
S^{2-}	Sulfide ion **150**
Th^{4+}	Thorium(IV) ion **154**
Tl^{2+}	Thallium(II) ion **156**

11. Compound Name Index

Acetate ion **164**
2-Acetylaminofluorene **165**
Acetylcytochrome C **198**
Acetyl peroxide **166**
Adenosine triphosphate-iron(II) complex **89**
Adenosine triphosphate-iron(III) complex **107**
Adrenaline **167**
Adrenalone **168**
DL-Alaninatocopper(II) ion **48**
DL-Alanine **169**
Alanylhistidinatocopper(II) **49**
Alloxan **170**
Alloxan semiquinone **171**
Americium(IV) ion **1**
μ-Amido-μ-superoxidotetrakis(ethylenediamine) dicobalt(III)] ion **28**
2-Amino-2-(hydroxymethyl)-1,3-propanediol **329**
2-Aminonaphthalene **284**
DL-2-Aminosuccinamic acid **178**
DL-Aminosuccinic acid **179**
Amminecopper(II) ion **34**
Arachidonate ion **172**
Arachidonic acid **173**
L-Arginine **174**
Ascorbate oxidase **175**
Ascorbate radical anion **176**
Ascorbate ion **177**
Ascorbic acid **177**
DL-Asparagine **178**
DL-Aspartic acid **179**
Azide radical **130**
1,1'-Azobis(*N*,*N*-dimethylformamide) **205**
Azodicarboxylic acid bis(dimethylamide) **205**
Bathophenanthrolineiron(II) ion **79**
Bathophenanthrolineiron(III) ion **91**
Benzene, 2,5-dichloro-1,4-dihydroxy- **208**
Benzene, 1,2-dihydroxy- **189**
Benzene, 1,3-dihydroxy- **305**
Benzene, 1,4-dihydroxy- **243**
Benzene, 1,4-dihydroxy-2-(1,1-dimethylethyl)- **188**
Benzene, 1,4-dihydroxy-2-methyl- **274**
Benzene, 1,3,5-trihydroxy- **301**
Benzidine **180**
2*H*-1-Benzopyran-2-carboxylic acid, 3,4-dihydro-6-hydroxy-2,5,7,8-tetramethyl- **245**
2*H*-1-Benzopyran-6-ol, 3,4-dihydro-2,5,7,8 tetramethyl-2-(4,8,12-trimethyltridecyl)-, **322**
1,2-Benzopyrene **181**
3,4-Benzopyrene **181**
Benzo[*a*]pyrene **181**
1,4-Benzoquinone **182**
1,4-Benzoquinone, 2,5-dichloro- **207**
1,4-Benzoquinone, 2,3-dimethyl- **215**
1,4-Benzoquinone, 2,5-dimethyl- **216**
1,4-Benzoquinone, 2,6-dimethyl- **217**
1,4-Benzoquinone, methyl- **272**
1,4-Benzoquinone, tetramethyl- **224**
Bilirubin **183**
Biliverdin **184**
1,1'-Biphenyl-4,4'-diamine **180**
Bis(acetylsalicylato)copper(II) **71**
Bis(*p*-aminosalicylato)copper(II) **72**
Bisamminecopper(II) ion **35**
Bis(2,2'-bipyridine)cobalt(II) ion **19**
Bis[copper(2-[2-(pyridyl)ethyliminomethyl]pyridine)]-imidazole bridged complex **73**
Bis(diisopropylsalicylato)copper(II) **70**
Bis(4,7-diphenyl-1,10-phenanthroline)iron(II) ion **79**
Bis(4,7-diphenyl-1,10-phenanthroline)iron(III) ion **91**
Bis(glycylhistidinato)cuprate(II) ion **53**
Bis(glycylhistidylleucinato)cuprate(II) ion **54**
Bis(histidinato)copper(II) ion, conjugate monoacid **55**
1,1'-Bis(2-hydroxyethyl)-4,4'-bipyridinium radical ion(1+) **185**
Bis(lysinato)copper(II) **61**
Bis(1,10-phenanthroline)copper(II) ion **39**
Bis(1,10-phenanthroline)copper(I) ion **32**
Bis(2-pyridinecarboxylato)copper(II) **47**
Bis(2-pyridinecarboxylato)zinc(II) **163**
Bis(salicylato)copper(II) **69**
Bis(tyrosinato)copper(II) **65**
Borate ion **2**
Bromine **5**
N-Bromo-2,2,6,6-tetramethylpiperidine **186**
tert-Butyl allyl peroxide **187**
1,1'-Butylene-2,2'-bipyridinium radical cation **317**
tert-Butylhydroquinone **188**
N-*tert*-Butyl-α-phenylnitrone **300**
Carbonate radical ion **8**
Carbonate ion **7**
Carbonic acid **7**
Carboxymethylcytochrome C **199**
Catechol **189**
Cerium(III) ion **9**
Cerium(IV) ion **10**
Ceruloplasmin **190**
Chlorate ion **17**
Chloride ion **11**
Chlorine **13**
Chlorine dioxide **16**
Chlorite ion **15**
1-(4-Chlorobenzoyl)-5-methoxy-2-methylindoleacetic acid **252**
6-Chromanol, 2-carboxy-2,5,7,8-tetramethyl- **245**
6-Chromanol,
2,5,7,8-tetramethyl-2-(4,8,12-trimethyltridecyl)- **322**
Citrate ion **191**
Cleland's Reagent, **223**
Copper(II) formate **44**
Copper(I) ions **31**
Copper(II) ions **33**
Copper indomethacin **76**
Copper oxidase **254**
Copper(2-[2-(pyridyl)ethyliminomethyl]pyridine) zinc(2-[2-(pyridyl)ethyliminomethyl]pyridine) imidazole bridged complex **74**

Crocin **192**
Cyanocob(III)alamin **30**
4-Cyanophenyl-*N*-*tert*-butylnitrone **193**
1,2-Cyclohexanediaminetetraacetatomanganate(III) ion **126**
Cyclohexylperoxy **194**
Cysteine **195**
L-Cystine **196**
Cytochrome C (ferro) **201**
Cytochrome C (ferri) **197**
Cytochrome C, acetylated **198**
Cytochrome C, carboxymethylated **199**
Cytochrome C, succinylated **200**
Cytochrome P-450 **202**
Cytochrome c_6 **203**
Cytochrome f (Fe^{3+}) **203**
Decakis(cyano)-μ-superoxidodicobaltate(III) ion **29**
Desferal **108**
Desferrioxamine B **108**
Diacetyl peroxide **166**
Dialuric acid **204**
Diamide **205**
4,4'-Diaminobiphenyl **180**
8,8'-Diapo-ψ,ψ-carotendioic acid, bis(6-*O*-β-D-gluco pyranosyl-β-D-glucopyranosyl) ester **192**
1,4-Diazabicyclo[2.2.2]octane **206**
Dibromine radical ion **4**
Dichlorine radical ion **12**
2,5-Dichloro-*p*-benzoquinone **207**
2,5-Dichloro-1,4-dihydroxybenzene **208**
2,5-Dichlorohydroquinone **208**
2,6-Dichloroindophenolate ion **209**
Dicyanotetrakis(4-*N*-methylpyridyl)porphineiron(II) ion **80**
Dicyanotetrakis(4-*N*-methylpyridyl)porphineiron(III) ion **94**
Diethylenetriaminepentaacetatoferrate(II) ion **88**
Diethylenetriaminepentaacetatoferrate(III) ion **106**
Dihydrogen hexacyanoferrate(II) ion **86**
1,2-Dihydro-3-methylbenz[*j*]aceanthrylene **273**
3,4-Dihydroxyacetophenone **210**
3,4-Dihydroxybenzaldehyde **211**
1,2-Dihydroxybenzene **189**
1,3-Dihydroxybenzene **305**
1,4-Dihydroxybenzene **243**
4,5-Dihydroxy-*m*-benzenedisulfonate ion **212**
2,5-Dihydroxybenzoic acid **213**
1,4-Dihydroxy(1,1-dimethylethyl)benzene **188**
3,4-Dihydroxy-α-methylaminoacetophenone **168**
l-3,4-Dihydroxy-α-(methylaminomethyl)benzyl alcohol **167**
1,4-Dihydroxy(methyl)benzene **274**
5,8-Dihydroxy-1,4-naphthoquinone **214**
threo-1,4-Dimercapto-2,3-butanediol, **223**
2,3-Dimethyl-1,4-benzoquinone **215**
2,5-Dimethyl-1,4-benzoquinone **216**
2,6-Dimethylbenzoquinone **217**
1,1'-Dimethyl-4,4'-bipyridinium radical ion (1+) **218**
2,3-Dimethylnaphthoquinone **219**
5,5-Dimethyl-1-pyrroline-*N*-oxide **220**
Dioxouranium(VI)-hydroperoxy complex **158**
Diphenoquinone **221**
1,1'-Diphenyl-4,4'-bipyridinium radical ion (1+) **222**
Dithiothreitol **223**
Duroquinone **224**
5,8,11,14-Eicosatetraenoic acid **173**
Epinephrine **167**
Ethylene **225**
1,1'-Ethylene-2,2'-bipyridinium radical ion (1+) **226**
Ethylenediaminetetraacetatocobaltate(II) ion **24**
Ethylenediaminetetraacetatocuprate(II) ion **68**
Ethylenediaminetetraacetatoferrate(II) ion **87**
Ethylenediaminetetraacetatoferrate(III) ion **105**
Ethylenediaminetetraacetatomanganate(II) ion **121**
Ethylenediaminetetraacetatomanganate(III) ion **125**
Ethylenediaminetetraacetate ion **227**
2-Ethyl-1-hydroxy-2,5,5-trimethyl-3-oxazolidine **228**
Ferredoxin (spinach) **229**
Ferricyanide ion **101**
Ferricytochrome C **197**
Ferriheme chloride **109**
Ferrimyoglobin **279**
Ferriperoxidase **297**
Ferrocyanide ion **83**
Ferrocytochrome C **201**
Ferroxidase **190**
Flavin adenine dinucleotide semiquinone **230**
Flavin mononucleotide semiquinone **231**
N-9*H*-Fluoren-2-ylacetamide **165**
Formate ion **232**
Formatocopper(II) ion **43**
Fumarate ion **233**
Fungal laccase **254**
Gentisic acid **213**
Glutamatocopper(II) ion **50**
L-Glutamic acid **234**
L-Glutamine **235**
γ-L-Glutamyl-L-cysteinylglycine **236**
Glutathione **236**
Glyceraldehyde-3-phosphate dehydrogenase-NADH complex **237**
Glycinatocopper(II) ion **51**
Glycine **238**
Glycylglycinatocopper(II) ion **52**
Hemin **109**
Hemin-diimidazole complex **110**
Hemocyanin **239**
Hexacyanoferrate(III) ion **101**
Hexacyanoferrate(II) ion **83**
(5,7,7,12,14,14-Hexamethyl-1,4,8,11-tetraazacyclotetradeca-4,11-diene)cobalt(II) ion **21**
(5,7,7,12,12,14-Hexamethyl-1,4,8,11-tetraazacyclotetradeca-4,11-diene)copper(II) ion **38**
5,7,7,12,12,14-Hexamethyl-1,4,8,11-tetraazacyclotetradecanenickel(II) ion **134**
5,7,7,12,12,14-Hexamethyl-1,4,8,11-tetraazacyclotetradecanenickel(III) ion **138**

5,7,7,12,12,14-Hexamethyl-1,4,8,11-tetraazacyclotetradeca-4,11-dienenickel(III) ion **139**
5,7,7,12,12,14-Hexamethyl-1,4,8,11-tetraazacyclotetradeca-1,4,8,11-tetraenenickel(III) ion **140**
L-Histidine **240**
Histidylalaninatocopper(II) **56**
Histidylphenylalaninatocopper(II) **57**
Histidyltyrosinatocopper(II) **58**
Histidylvalinatocopper(II) **59**
Homocysteine **241**
Horseradish Peroxidase **297**
Horseradish Peroxidase Compound I **296**
Hydrogen **112**
Hydrogen hexacyanoferrate(II) ion **85**
Hydrogen ion **113**
Hydrogen peroxide **143**
Hydroperoxide ion **144**
1-Hydroperoxy-2-cyclooctene **242**
Hydroperoxylinoleate ion **257**
Hydroquinone **243**
Hydrothymine radical, peroxy- **298**
Hydroxybis(2-pyridinecarboxylato)iron(III) **103**
1-Hydroxyethyldioxy **244**
N-Hydroxyethylenediaminetriacetatoferrate(III) **104**
Hydroxyl radical **141**
Hydroxylamine **131**
3-(*p*-Hydroxyphenyl)-L-alanine **331**
L-Hydroxyprolinecopper(II) ion **60**
2-Hydroxypropionate ion **255**
Hydroxyprotoferrihaem dimer **111**
6-Hydroxy-2,5,7,8-tetramethylchroman-2-carboxylic acid **245**
6-Hydroxy-2,5,7,8-tetramethylchroman-2-carboxylate ion **246**
3-(6-Hydroxy-2,5,7,8-tetramethylchroman-2-yl)propionic acid **247**
5-Hydroxy-2,4,6-trioxopyrimidine **204**
Hypobromous acid **6**
Hypochlorous acid **14**
Imidazole **248**
Indigodisulfonate ion **249**
Indigotetrasulfonate ion **250**
Indigotrisulfonate ion **251**
Indomethacin **252**
Indomethacincopper complex **76**
Iodine **114**
Iron(II) ions **77**
Iron(III) ions **90**
DL-Isoleucine **253**
2-Ketoglutarate ion **294**
Laccase **254**
Lactate ion **255**
L-Leucine **256**
Linoleate hydroperoxide **257**
Linoleate ion **258**
Linoleic acid **259**
Linoleic acid hydroperoxide **260**
Linolenate ion **261**
Linolenic acid **262**
Lipoxidase (soybean) **263**
Luminol radical **264**
DL-Lysine **265**
L-Malate ion **266**
Maleate ion **267**
Manganese(II) formate **119**
Manganese(II) ions **116**
Manganese(II) pyrophosphate complex **117**
Manganese(II) sulfate **118**
Menadione **277**
Methemoglobin **268**
Methional **269**
L-Methioninatocopper(II) ion **62**
DL-Methionine **270**
4-Methoxyphenyl-*N*-*tert*-butylnitrone **271**
Methyl-1,4-benzoquinone **272**
20-Methylcholanthrene **273**
3-Methylcholanthrene **273**
2-Methyl-*N*-[4-cyanophenyl)methylene]-2-propanamine **193**
Methylhydroquinone **274**
1-Methylimidazole **275**
2-Methylimidazole **276**
2-Methyl-*N*-[(4-methoxyphenyl)methylene]-2-propanamine **271**
2-Methyl-*N*-[(4-methylphenyl)methylene]-2-propanamine **278**
2-Methyl-1,4-naphthoquinone **277**
2-Methyl-*N*-[4-nitrophenyl)methylene]-2-propanamine **287**
4-Methylphenyl-*N*-*tert*-butylnitrone **278**
2-Methyl-*N*-phenylmethylene-2-propanamine **300**
2-Methyl-3-phytyl-1,4-naphthoquinone **333**
3-Methylthiopropionaldehyde **269**
Methyl viologen radical cation **218**
Metmyoglobin **279**
NADH-Lactate dehydrogenase **280**
2-Naphthalenamine **284**
Naphthazarin **214**
1,2-Naphthoquinone **281**
1,4-Naphthoquinone, 5,8-dihydroxy- **214**
1,4-Naphthoquinone, 2-methyl- **277**
1,4-Naphthoquinone, 2-methyl-3-(3,7,11,15-tetramethyl-2-hexadecenyl)- **333**
1,2-Naphthoquinone-4-sulfonate ion **282**
1,4-Naphthoquinone-2-sulfonate ion **283**
2-Naphthylamine **284**
Nicotinamide adenine dinucleotide, reduced **285**
Nitrilotriacetatocobaltate(II) ion **23**
Nitrilotriacetatomanganate(II) ion **120**
Nitrite ion **133**
Nitro Blue Tetrazolium **286**
Nitrogen dioxide **132**
4-Nitrophenyl-*N*-*tert*-butylnitrone **287**
1,3,6,8,10,13,16,19-Octaazabicyclo[6.6.6]eicosanecobalt(II) ion **22**
Octacyanomolybdate(IV) ion **128**
Octacyanomolybdate(V) ion **129**
9,11-Octadecadienoate ion **288**

9,11-Octadecadienoic acid **289**
9,12-Octadecadienoate ion **258**
9,12-Octadecadienoic acid **259**
9-Octadecenoate ion **290**
9-Octadecenoic acid **291**
Oleate ion **290**
Oleic acid **291**
Oleic acid hydroperoxide **292**
Osmium tetroxide **146**
Oxalate ion **293**
Oxide radical ion **142**
2-Oxoglutarate ion **294**
Oxoperoxyvanadium(IV) ion **159**
Oxygenase, monophenol mono- **254**
Oxyhemoglobin **295**
Ozone **145**
Penicillaminecopper complex **75**
Pentaammine(isonicotinamide)ruthenium(II) ion **147**
Pentaammine(isonicotinamide)ruthenium(III) ion **148**
Perchlorate ion **18**
Permanganate ion **127**
Peroxidase Compound I **296**
Peroxidase (horseradish) **297**
Peroxyhydrothymine radical **298**
L-Phenylalanine **299**
Phenylalanylhistidinatocopper(II) **63**
Phenyl-*N*-*tert*-butylnitrone **300**
Phloroglucinol **301**
Plastocyanin **302**
Potassium hexacyanoferrate(II) ion **84**
Potassium hexacyanoferrate(III) ion **102**
L-Prolinatocopper(II) ion **64**
L-Proline **303**
1,1'-Propylene-2,2'-bipyridinium radical cation **326**
Protocatechualdehyde **211**
2,4,5,6-Pyrimidinetetrone **170**
2,4,5,6-Pyrimidinetetrone H-adduct **171**
Pyrocatechol **189**
Pyruvate ion **304**
Quinone **182**
Resorcinol **305**
Riboflavin semiquinone **306**
DL-Serine **307**
Succinate ion **308**
Succinylcytochrome C **200**
Sulfacetamide **309**
Sulfide ion **150**
Sulfite ion **151**
Superoxide dismutase **310–315**
Tartrate ion **316**
Tellurate(IV) ion **153**
Tetraakis(4-*N*-methylpyridyl)porphineiron(III)-diimidazole complex **95**
Tetraamminecopper(II) ion **37**
Tetrakisformatocuprate(II) ion **46**
Tetrakis(4-*N*-methylpyridyl)porphinecobalt(III) ion **26**
Tetrakis(4-*N*-methylpyridyl)porphinecopper(II) ion **40**
Tetrakis(4-*N*-methylpyridyl)porphineiron(II)-diimidazole complex **81**
Tetrakis(4-*N*-methylpyridyl)porphineiron(II)-dihistidine complex **82**
Tetrakis(4-*N*-methylpyridyl)porphineiron(III) ion **92**
Tetrakis(4-*N*-methylpyridyl)porphineiron(III)-superoxide complex **93**
Tetrakis(4-*N*-methylpyridyl)porphineiron(III)-dihistidine complex **96**
Tetrakis(4-*N*-methylpyridyl)porphinemanganese(III) ion **122**
Tetrakis(4-*N*-methylpyridyl)porphinenickel(II) ion **135**
Tetrakis(4-*N*-methylpyridyl)porphinatezinc(II) ion **160**
Tetrakis(*p*-sulfonatophenyl)porphinatocobaltate(III) ion **27**
Tetrakis(*p*-sulfonatophenyl)porphinatocuprate(II) ion **42**
Tetrakis(*p*-sulfonatophenyl)porphineferrate(III) ion **98**
Tetrakis(*p*-sulfonatophenyl)porphineferrate(III)-diimidazole complex **99**
Tetrakis(*p*-sulfonatophenyl)porphineferrate(III)-bovine serum albumin complex **100**
Tetrakis(*p*-sulfonatophenyl)porphinatomanganate(III) ion **124**
Tetrakis(*p*-sulfonatophenyl)porphinatonickelate(II) ion **137**
Tetrakis(*p*-sulfonatophenyl)porphinatozincate(II) ion **162**
Tetrakis-4-(*N*,*N*,*N*-trimethylammonio)phenylporphinecopper(II) ion **41**
Tetrakis-4-(*N*,*N*,*N*-trimethylammonio)phenylporphineiron(III) ion **97**
Tetrakis-4-(*N*,*N*,*N*-trimethylammonio)phenylporphinemanganese(III) ion **123**
Tetrakis-4-(*N*,*N*,*N*-trimethylammonio)phenylporphinenickel(II) ion **136**
Tetrakis-4-(*N*,*N*,*N*-trimethylammonio)phenylporphinezinc(II) ion **161**
Tetramethyl-*p*-benzoquinone **224**
N,*N*,*N*',*N*'-Tetramethyl-1,2-diazenedicarboxamide **205**
1,3,5,8-Tetramethyl-2,4-divinylporphine-6,7-dipropionic acid ferrichloride **109**
1,1'-Tetramethylene-2,2'-bipyridinium radical ion (1+) **317**
2,2,6,6-Tetramethylpiperidine-*N*-oxyl **318**
2,2,6,6-Tetramethylpiperidin-1-ol **319**
(2,3,9,10-Tetramethyl-1,4,8,11-tetraazacyclotetradeca-1,3,8,10-tetraene)cobalt(II) ion **20**
(2,3,9,10-Tetramethyl-1,4,8,11-tetraazacyclotetradeca-1,3,8,10-tetraene)cobalt(III) ion **25**
Tetranitromethane **320**
Thallium(II) ion **156**
Thiocyanogen **152**
Thorium(IV)-hydroperoxy complex **155**
Thorium(IV) ion **154**
DL-Threonine **321**
Thymine radical, peroxy- **298**
Tiron dianion **212**
α-Tocopherol **322**
p-Toluquinone **272**
Tribromine ion **3**
Tributylammoniobutyldioxy **323**

Triethylammonioethyldioxy **324**
1,3,5-Trihydroxybenzene **301**
Triiodine ion **115**
Trimethylammoniomethyldioxy **325**
1,1'-Trimethylene-2,2'-bipyridinium radical ion (1+) **326**
2,5,5-Trimethyl-1-pyrroline *N*-oxide **327**
Tripropylammoniopropyldioxy **328**
Trisamminecopper(II) ion **36**
Tris(2,2'-bipyridine)ruthenium(III) ion **149**
Trisformatocuprate(II) ion **45**
Tris(hydroxymethyl)aminomethane **329**
Tris(1,10-phenanthroline)iron(II) ion **78**
Trolox **245**
Trolox anion **246**
L-Tryptophan **330**
L-Tyrosine **331**
Uranyl(VI) ion **157**
L-Valinatocopper(II) ion **66**
DL-Valine **332**
Valylhistidinatocopper(II) **67**
Vitamin B12 **30**
Vitamin K_1 **333**
Zinc(II) 2-picolinate **163**
Zinc(II) tetrakis(4-*N*-methylpyridyl)porphyrin **160**
Zinc(II) tetrakis(*p*-sulfonatophenyl)porphyrin **162**
Zinc(II) tetrakis(4-trimethylammoniophenyl) porphyrin **161**